TECHNISCHE UNIVERSITÄT MÜNCHEN

Lehrstuhl für Experimentelle Genetik

Role of the NFkB subunit p50 in particle induced, aseptic lung inflammation

Renfu Yin

Vollständiger Abdruck der von der Fakultät für Wissenschaftszentrum Weihenstephan für Ernährung, Landnutzung und Umwelt der Technischen Universität München zur Erlangung des akademischen Grades eines

Doktors der Naturwissenschaften

genehmigten Dissertation.

Vorsitzender: Univ.-Prof. Dr. D. Langosch

Prüfer der Dissertation:

1. Univ.-Prof. Dr. M. Hrabé de Angelis
2. Univ.-Prof. Dr. D. H Busch

Die Dissertation wurde am 06.08.2012 bei der Technischen Universität München eingereicht und durch die Fakultät für Wissenschaftszentrum Weihenstephan für Ernährung, Landnutzung und Umwelt am 12.11.2012 angenommen.

I dedicate this work to my family.

Contents

1. Zusammenfassung……..……1

2. Summary……..……3

3. Introduction……5

3.1 Anatomical and physiological basis of lung……..……5

3.1.1 Structural overview of lung……5

3.1.2 Cells of the lung……..……7

3.2 Pulmonary diseases related transcription factors……...…11

3.2.1 The NFkB signalling pathway……..11

3.2.2 The AP-1 signalling pathway……..……..16

3.3 Particle induced aseptic acute lung inflammation model……..……17

3.3.1 Lung inflammation……..……...……17

3.3.2 Carbon nanoparticles……...……...……17

3.3.3 Particle induced aseptic acute lung inflammation……18

3.4 Macrophage polarization and lung inflammation……..……19

3.4.1 Molecular determinants of macrophage polarization……..……...…21

3.4.2 Induction and resolution of inflammation as well as macrophage phenotypic polarization……..……...…21

3.5 Project aims……..……24

4. Materials and methods……..……25

4.1 Materials……...……25

4.1.1 Mice……...……25

4.1.2 Carbon nanoparticles……..……..……25

4.1.3 Commencial available assays…….....…….……25

4.1.4 Equipment……...……26

4.1.5 Chemicals……..……27

4.1.6 Buffers and solutions……27

4.1.7 Recombinant proteins and antibodies……...……29

4.2 Methods……29

4.2.1 Mouse treatment……..…..……29

4.2.2 Preparation of carbon nanoparticles dispersions……...…...…30

4.2.3 Bronchoalveolar lavage (BAL) ……..…...……30

4.2.4 BAL cell differentation……..…...……..……30

4.2.5 Total protein concent and lactate dehydrogenase (LDH) in BAL fliud ……..31

4.2.6 Enzyme-Linked Immunosorbent Assay (ELISA) ……...…31

4.2.7 Extract of nuclear fraction from frozen lung tissue……..……31

4.2.8 TransAM® Transcription Factor (NFkB and AP-1) ELISA ……..…...…31

4.2.9 Electrophoretic Mobility Shift Assay (EMSA) ……..…...…32

4.2.10 Experiments for primary alveolar macrophages (AMs) *in vitro*.……32

4.2.10.1 Isolation of primary alveolar macrophages (AMs) ……...…….32

4.2.10.2 AMs treated with either IL4 or LPS plus IFN gamma……...32

4.2.11 Quantitative real time polymerase chain reaction …..……32

4.2.11.1 Design of qPCR primer…….....……32

4.2.11.2 Isolation of total RNA and cDNA synthesis …….……35

4.2.11.3 PCR reaction……...……36

4.2.11.4 Selection and evaluation of stable housekeeping genes…….……37

4.2.11.5 PCR Data analysis……...……...37

4.2.12 Statistical analysis…….……37

5. Results……38

5.1 Characterization of carbon nanoparticle (CNP)……38

5.2 Characterization of the CNP triggered lung inflammation in mice……38

5.2.1 Pulmonary toxicity upon CNP treatment……39

5.2.1.1 Epithelial-endothelial permeability-barrier integrity……39

5.2.1.2 Cytotoxicity (LDH) ……39

5.2.2 BAL cell analysis……40

5.2.3 BAL cytokines analysis……41

5.2.3.1 Neutrophile chemoattractants in the BALFs……41

5.2.3.2 Other inflammatory cytokines in the BALFs……43

5.2.4 Gene profiles in the lung homogenate……44

5.2.4.1 Profiles of genes for neutrophile chemoattractants…….. 44

5.2.4.2 Profiles of related genes for lung inflammatory response ……..45

5.2.4.3 Profiles of related genes for the transcription factors NFkB and AP-1 ….49

5.3 Compare the acute inflammatory response to CNP from WT and $p50^{-/-}$ mice……50

5.3.1 Analyse inflammatory cell and total protein accumulation in airspace of WT and $p50^{-/-}$ mice in response to CNP exposure…….....51

5.3.1.1 Total cells numbe……51

5.3.1.2 Inflammatory cells ……52

5.3.1.3 Protein concentration in BALFs ……52

5.3.2 Analyse cytokine response in WT and $p50^{-/-}$ mice by BAL..... 53

5.3.3 Analysis of gene expression in lungs..... 56

5.3.3.1 Inflammatory cytokine gene 56

5.3.3.2 Other related genes…….. 57

5.3.4 Analyse transcription factors in lungs of WT and p50$^{-/-}$ mice..... 62

5.3.4.1 Analyse NFkB1 activation in lungs of WT and p50$^{-/-}$ mice 62

5.3.4.2 Analyse NFkB2 and AP-1 activation in lungs of WT and p50$^{-/-}$ mice 64

5.4 Roles of NFkB1 subunit p50 in alveolar macrophage polarization…..…..……...66

5.4.1 Establishment of alveolar macrophage polarization model *in vitro* ……..…...66

5.4.2 Roles of subunit p50 in alveolar macrophages polarization…….....67

5.4.2.1 Genetic ablation of p50 promotes M2 skewed inflammatory response in AMs ……...67

5.4.2.2 Genetic ablation of p50 downregulated M1 skewed inflammatory response in AMs……68

5.4.2.3 NFkB related genes were downregulated, but Ppar-γ was upregulated in p50$^{-/-}$ M1 skewed inflammatory AMs.……...……69

5.5 Impact of alveolar macrophages in particle induced acute lung inflammation in mice……..…….……70

6. Discussion……..……72

6.1 Intratracheal instillation of carbon nanoparticles (CNP) at a single dose of 20µg per mouse causes acute lung inflammation in mice…...…..……..……72

6.2 CNP triggered inflammatory cell influx into the lungs is not altered in p50$^{-/-}$ mice……..……74

6.3 Deletion of NFkB subunit p50 augments lung cytokine expression upon particle induced aseptic acute lung inflammation in mice...……..……75

6.4 No compensatory activation of either NFkB or AP-1 pathways were identified in p50 $^{-/-}$ mice in response to CNP exposure……..……..……76

6.5 Alveolar macrophages from p50$^{-/-}$ mice show M2 skewed polarization profile…….77

6.6 Little impact of alveolar macrophage in particle induced aseptic acute lung inflammation in mice……80

7. References……82

8. Abbreviations……99

9. Appendix……101

10. Acknowledgements……119

11. Curriculum vitae……121

1. Zusammenfassung

Die Inhalation von Kohlenstoff-Nanoteilchen (carbon nanoparticles, CNP), einem wichtigen Bestandteil der Emission aus Verbrennungsprozessen und damit der urbanen Luftverschmutzung, kann sowohl lokal in der Lunge als auch im Herzkreislaufsystem Entzündungsreaktionen bewirken. Denn durch ihre Oberflächenreaktivität können auch sterile Partikel wie CNPs effektiv oxidativen Stress induzieren und somit Entzündungsreaktionen auslösen. Die redoxsensitiven Transkriptionsfaktoren *Nuclear Factor KappaB* (NFkB) und *Activator Protein 1* (AP-1), die einen Großteil der inflammatorischen Genexpression steuern, spielen eine zentrale Rolle für Entstehung und Auflösung von Entzündungsreaktionen in der Lunge. In diesem Zusammenhang scheint der p50-Untereinheit des NFkB1-Komplexes eine zweischneidige Funktion zuzukommen, denn p50 kann die NFkB-abhängige Genexpression sowohl initiieren und fördern oder aber auch hemmen, indem es in Abhängigkeit von den jeweiligen Gegebenheiten wahlweise mit Coactivator- oder Repressor-Molekülen der Transkriptionsmaschinerie des Zellkerns interagiert. Da wie bei den meisten Entzündungsmechanismen der NFkB-Signalweg fast ausschließlich in Modellen der Sepsis untersucht wurde ist die Übertragbarkeit der Mechanismen auf die aseptische Entzündung wie durch CNP-Inhalation hervorgerufen, nicht geprüft. In diesem Projekt soll die Rolle der NFkB1-Untereinheit p50 während der CNP-induzierten, aseptischen Lungenentzündung unter Verwendung von WT und p50-Knock-out-Mäusen ($p50^{-/-}$) untersucht werden.

Die intratracheale Instillation von 20µg CNP in die Mauslunge verursachte eine akute neutrophile Alveolitis, mit höchsten Entzündungszellzahlen 24h nach der Applikation und kompletter Auflösung der Entzündung innerhalb von 7 Tagen. Das Ausmaß der zellulären Entzündungsreaktion zeigte jedoch keinen Genotyp-abhängigen Unterschied obwohl die CNP-induzierte Zytokinfreisetzung in Lungen von p50-Mäusen deutlich höhere Werte erreichte als die in WT-Tieren. Damit scheint p50 zwar der Expression von proinflammatorischen Zytokinen entgegenzuwirken, andererseits aber für die Rekrutierung von Entzündungszellen in den Alveolarbereich der Lunge verzichtbar zu sein. Untersuchungen von Lungen-Zellkernextrakten ergaben, dass die CNP-Behandlung zwar eine Anreicherung der NFkB1 Untereinheiten, p50 und p65 (RelA) in WT, jedoch nicht in p50-Mäusen bewirkte. Damit stellt sich die Frage welcher Transkriptionsfaktor in Abwesenheit von p50 und ohne p65 zu involvieren die inflammatorische Genexpression induziert. Eine kompensatorische Aktivierung von NFkB2 oder AP-1 Faktoren konnte in entsprechenden Lungenextrakten nicht gefunden werden.

1. Zusammenfassung

Eine überproportionale inflammatorische Aktivierbarkeit (Polarisierung) von Alveolarmakrophagen, die für die Lunge als Hauptproduzenten proinflammatorischer Zytokine gelten, könnte die verstärkte Zytokinantwort in p50 Mäusen auf einer anderen Ebene erklären. *In vitro* zeigten Alveolarmakrophagen von p50 Mäusen jedoch eher einen antiinflammatorischen Phänotyp und erklären damit die alveoläre Zytokinfreisetzung nicht. Ausserdem zeigten Alveolarmakrophagen die nach CNP Behandlung der Mäuse isoliert wurden keine inflammatorische Reaktion.

Zusammenfassend kann festgehalten werden, dass im Gegensatz zu Modellen der Sepsis, eine zentrale Rolle der Alveolarmakrophagen für die Initiation der partikelinduzierten Entzündungsreaktion nicht festgestellt werden kann. Ebenso scheint im Gegensatz zur Sepsis für die transkriptionelle Aktivierung der Zytokinexpression der klassische NFkB1 komplex p50/p65 überflüssig, wird aber auch nicht durch NFkB2 oder AP-1 Signalweg kompensiert.

Die Signalwege der septischen Entzündungsreaktion scheinen damit denen der aseptischen nicht unbedingt zu entsprechen und bedürfen genauerer Untersuchung.

2. Summary

Inhalation of carbonaceous nanoparticles (CNP), a main constituent of urban air pollution, is believed to trigger pulmonary and, in some cases, systemic inflammation. Under aseptic conditions, the surface reactivity of pulmonary deposited particles has in this context been shown to trigger inflammatory gene expression via the generation of oxidative stress. Thus the redox-sensitive transcription factors nuclear factor KappaB (NFkB) and activator protein 1 (AP-1), which control a majority of inflammatory genes, are thought to play an important role in the initiation and resolution of pulmonary inflammation. In this context, the NFkB1 subunit p50 seems to work like a double-edged sword; either promoting or suppressing gene expression via interaction with coactivator or corepressor molecules depending on the environmental circumstances. However as for most of the available knowledge about molecular mechanisms of inflammation, also the NFkB pathway has mostly be been investigated in models of sepsis and endotoxin but barely for sterile and aseptic inflammation. This project aims to investigate the role of the NFkB1 subunit p50 in CNP-induced, aseptic lung inflammation in genetically-modified mice lacking p50 ($p50^{-/-}$).

Exposing mice to 20µg CNP by intratracheal instillation caused an aseptic acute neutrophilic alveolitis with the highest inflammatory cells numbers seen around 24 hours after instillation and the resolution of CNP-induced inflammation after 7 days. However, comparing the inflammatory response from wild type (WT) and $p50^{-/-}$ mice upon exposure to 20µg CNP after 24 hours revealed no genotype-related differences in the recruitment of neutrophils into the alveolar space, suggesting a negligible role for p50 in the acute inflammatory response. Surprisingly, however, the CNP exposure related boost of the proinflammatory cytokines IL-1a, IL-1ß, Cxcl1, Cxcl10 and TNF-a observed in $p50^{-/-}$ lungs significantly exceeded that of WT mice at the mRNA and protein level, which suggests an augmentation of inflammatory signalling in the absence of p50. In contrast, CNP-induced nuclear accumulation of both the NFkB subunits p50 and RelA (p65) was seen only in WT mice, and not in $p50^{-/-}$ mice, raising the question of which factor compensates for the defect in p50/p65 nuclearization. No compensatory activation of either NFkB2 (p52, RelB, c-Rel) or AP-1 (c-Jun, Jun-D, c-Fos, FosB) pathways could be identified in $p50^{-/-}$ mice in analysis of nuclear extracts of CNP-exposed lungs. Furthermore, p50, which is also seen as a key component in the control of macrophage activation and polarization *in vitro,* is supposed to assists NFkB-driven M2-polarizing in alveolar macrophage. Investigating the polarization response of alveolar macrophages from $p50^{-/-}$ mice however indicated an M2 skewed phenotype,

therefore making these cells unlikely to explain the increased cytokine release under p50-deficient conditions. Expression analysis of alveolar macrophages, isolated from mice after CNP exposure additionally did not show any inflammatory response at time points where high cytokine expression in CNP treated lungs have been detected.

Taken together, these results show that p50/p65 signalling is dispensable for development of the particle-induced aseptic acute lung inflammation and p50 rather attenuates the acute cytokine storm. Further the acute inflammatory response is unlike that described for models of sepsis not to be driven by cytokine release from alveolar macrophages butte different cells in the lungs of CNP treated mice. Future research may thus be required to clarify the molecular pathway by which particle inhalation induces the acute, aseptic inflammatory response in the lungs.

3. Introduction

3.1 Anatomical and physiological basis of lung

3.1.1 Structural overview of lung

The lung is the essential respiration organ of air-breathing animals, including most tetrapods, a few fish and a few snails [1,2]. Its principal functions are to transport oxygen from the atmosphere into the bloodstream on the one hand, and to release carbon dioxide from the bloodstream into the atmosphere on the other hand, thus maintaining the balance in the systemic pH homeostasis [3,4]. To perform this crucial task the lung can be considered as two distinct zones within which the airway and vascular compartments are situated (Fig.3.1): conducting and respiratory [5].

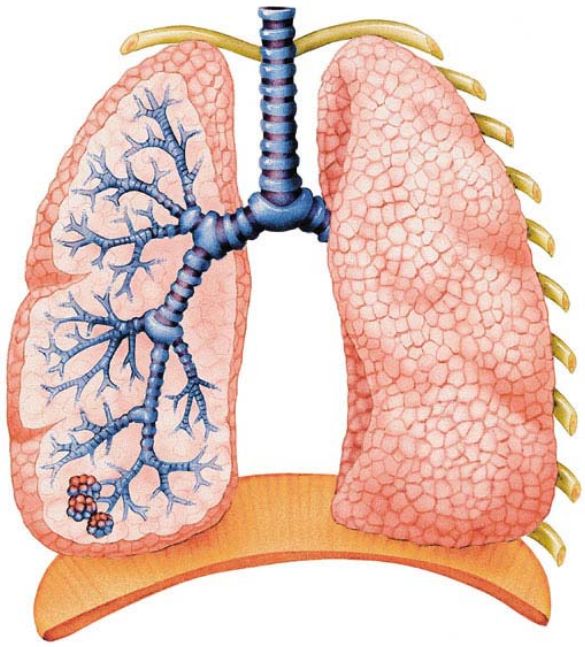

Figure 3.1: A schematic presentation of the lung containing conducting airways (blue) and alveolar gas exchange region (pink) (adapted from [6]).

The conducting zone of the respiratory system is made up of the nose, pharynx and larynx, as well as the first sixteen generations of respiratory tract, consisting of trachea, bronchi, bronchioles and terminal bronchioles. The function of this zone is to filter, warm, and moisten air and to conduct it into the lungs [3,7]. The lower respiratory tract extends from the larynx to the most distal portions of the lung

parenchyma. Of the first sixteen generations of respiratory tract, generation zero represents the trachea, which allow the passage of air which then bifurcates into the two main bronchi and is further subdivided into bronchi that enter the left and right lung lobes. The intrapulmonary bronchi conduct air into the lungs, which continue to subdivide into progressively smaller diameter bronchi and bronchioles where no gas exchange takes place. The conducting zone ends with terminal bronchioles, which are devoid of alveoli (Fig.3.2). In contrast, the respiratory zone is the site where oxygen and carbon dioxide gas exchanges with blood, and is composed of the 16th through to the 23rd division of the respiratory tract, containing respiratory bronchioles, alveolar ducts and alveoli [3].

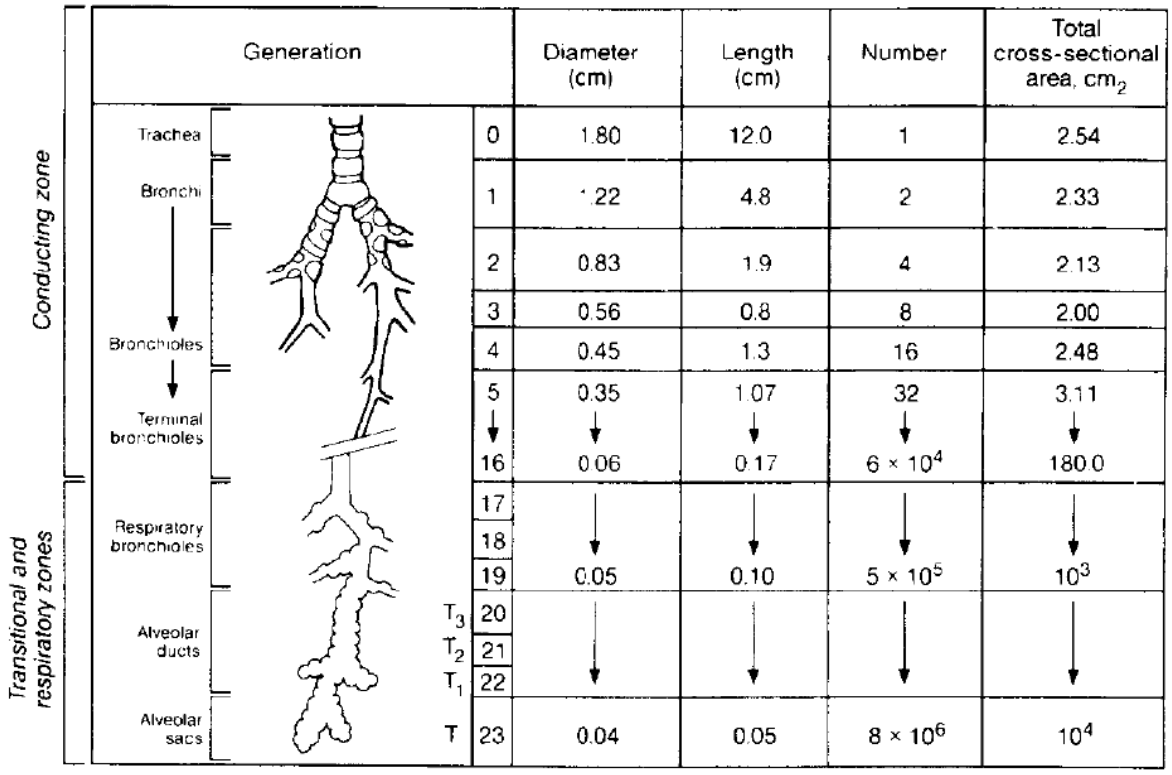

Generation		Diameter (cm)	Length (cm)	Number	Total cross-sectional area, cm_2
	0	1.80	12.0	1	2.54
	1	1.22	4.8	2	2.33
	2	0.83	1.9	4	2.13
	3	0.56	0.8	8	2.00
	4	0.45	1.3	16	2.48
	5 ↓ 16	0.35 ↓ 0.06	1.07 ↓ 0.17	32 ↓ 6×10^4	3.11 ↓ 180.0
	17 18 19	↓ 0.05	↓ 0.10	↓ 5×10^5	↓ 10^3
T_3 T_2 T_1	20 21 22	↓	↓	↓	↓
T	23	0.04	0.05	8×10^6	10^4

Figure 3.2: A schematic of airway branching in the human lung including the upper and lower airways, containing their representative lung structures with their respective diameter (cm), length (cm), number, and total cross-sectional area (cm^2) (Adapted from [3,8]).

The sequence of airway branches containing generation zero bronchi (BR), bronchioles (BL), terminal bronchioles (TBL), and respiratory bronchioles (RBL) are followed by alveolar ducts (AD) and alveolar sacs (AS) in the terminal generation.

Since the first 16 generations of airways contain no alveoli, they are anatomically incapable of gas exchange with the venous blood and constitute the so-called anatomic dead space. In contrast, the respiratory zone consists only of structures that participate in gas exchange, beginning with respiratory bronchioles containing alveoli. Interestingly, the respiratory bronchioles and the alveolar ducts are responsible for 10% of the gas exchange. However, the alveoli are responsible for the other 90% [9]. Human alveolar surface area in subjects 25-79 years varied between 43 and 102 m^2 at tidal inflation which is 22-52% of the surface area of a singles tennis court (195.7 m^2) [10,11].

3.1.2 Cells of the lung

The body relies on an effective inflammatory response for protection. To sustain an armoury of inflammatory cells in a state of permanent activation would be impossible, and so a system whereby such cells can be rapidly activated is employed [12]. Inflammatory cells are a vital part of the armoury against infection, but, when inappropriately or excessively activated, can induce a state of uncontrolled systemic inflammation.

In humans, four major cell types represent the surface of the respiratory epithelium and two main immunocompetent cell types are responsible for the uptake and clearance of foreign materials like bacteria, pollutants or particles, as well as communication with the cell environment (Fig.3.3):

3.1.2.1 Ciliated cells

Ciliated cells are cells covered in tiny hair-like projections known as cilia. Nearly half of the epithelial cells in the normal human airway are ciliated at all airway generations except for the respiratory units distal to the terminal bronchioles.

The surface of the ciliated cell is covered by cilia, about 200 per cell, each normally beating about 1,000 times per minute with its effective stroke generally in the cranial direction and coordinated with those on adjacent cells. The cilia move the overlying mucus layer with their tips up to the airways, away from the alveoli and toward the pharynx. Mucus that reaches the pharynx is usually swallowed or expectorated.

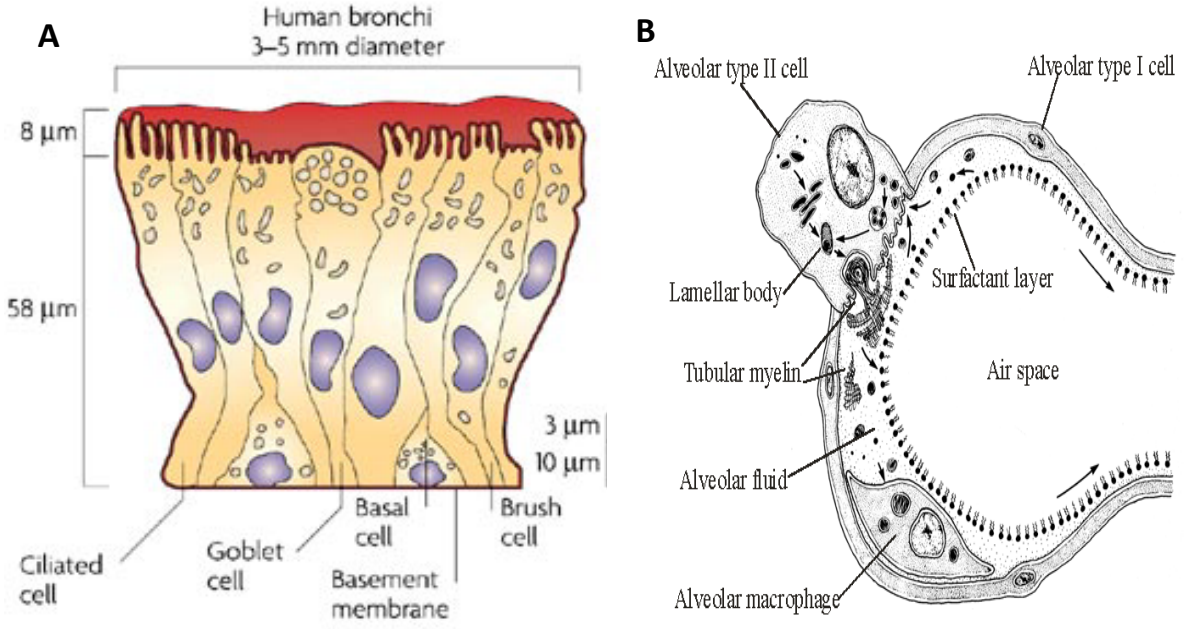

Figure 3.3: In the bronchi there are a variety of cells that make up the epithelium (A, adapted from [13]) and alveolar type I, type II cells as well as alveloar macrophage in the lung (B, adapted from http://www.bio.davidson.edu/people/kabernd/BerndCV/Lab/Online_website2/ROS_background.html).

A: the basal cells, which are the stem or progenitor cells for the epithelium and differentiate to form the other cells in the case of injury or apoptosis; the ciliated cells, which provide the mechanism for moving the mucus blanket; the goblet cells, which secrete the mucus; and the brush cells, which are involved in drug metabolism. These same types of cell persist in the smaller airways, but are not as tall. The basement membrane is not actually a membrane, but an extracellular matrix of different biopolymers to which the epithelial cells attach. B: alveolar type I, type II cells as well as alveloar macrophage in the lung are responsible for the uptake and clearance of foreign materials like bacteria, pollutants or particles, as well as communication to the cell environment.

3.1.2.2 Goblet cell

Goblet cells, so named because they are shaped like a wine goblet, are columnar epithelial cells that contain membrane-bound mucous granules and secrete mucus, which helps maintain epithelial moisture and traps particulate material and pathogens moving through the airway. Goblet cells are glandular

simple columnar epithelial cells whose sole function is to secrete mucin, which dissolves in water to form mucus. They use both apocrine and merocrine methods for secretion. The majority of the goblet cell's cytoplasm is made up by mucinogen granules, except at the bottom.

Goblet cells are situated in the epithelium of the conducting airways, often with their apical surfaces protruding into the lumen, a location which allows them to make a rapid response to inhaled airway insults [14]. Together with the submucosal glands, goblet cells secrete high molecular weight mucus glycoproteins (mucins), which confer upon the airway surface fluid the requisite biochemical and biophysical properties; this determines the efficiency of entrapment and transportation of inhaled irritants, particles and micro-organisms [14].

3.1.2.3 Basal cells

Basal cells are small, nearly cuboidal cells thought to have some ability to differentiate into other cells types found within the epithelium. For example, basal cells respond to injury of the airway epithelium by migrating to cover a site denuded of differentiated epithelial cells and subsequently differentiating to restore a healthy epithelial cell layer.

The basal cell is primarily made up of basal keratinocyte cells, which can be considered the stem cells of the epidermis [15]. Basal cells make up approximately 30% of the pseudostratified mucociliary epithelium of the lung [15].

3.1.2.4 Alveolar type I and type II cells

A lung's constituent alveoli sacs exist deep within it and are the sites responsible for the uptake of oxygen and excretion of carbon dioxide. There are two major alveolar cell types in the alveolar wall (pneumocytes):

(i) Type I (Squamous Alveolar) cells, which form the structure of an alveolar wall and are responsible for gas exchange in the alveolus; they are characterized by a superficial layer consisting of large, thin, scale-like cells. They also cover 95% of the alveolar surface, although they are only half as numerous as type 2 pneumocytes [16,17].

(ii) Type II (Great Alveolar) cells, which secrete pulmonary surfactant (PS) consisting 80-90% of phospholipids (phosophatidylcholine (PC), phosphatidyglycerol (PG), phosphaditylinositol (PI)) and 5-10% of surfactant proteins (SP-A, SP-B, SP-C, AND SP-D). These lower the surface tension of water and allow the membrane to separate, thereby increasing the ability to exchange gases [18]. Surfactant is continuously released by exocytosis. It forms an underlying aqueous protein-containing hypophase and an overlying phospholipid film composed primarily of dipalmitoyl phosphatidylcholine. Meanwhile, type 2 cells are important in that they can proliferate and differentiate into type 1 pneumocytes, which cannot replicate and are susceptible to vast numbers of toxic insults.

3.1.2.5 Alveolar macrophages

An alveolar macrophage (or dust cell) is a type of macrophage found in the pulmonary alveolus, near the pneumocytes, but separated from the wall [19,20]. Alveolar macrophages are phagocytes that play a critical role in homeostasis, host defense, the response to foreign substances, and tissue remodeling [21]. Since alveolar macrophages are pivotal regulators of local immunological homeostasis, their population density is decisive for the many processes of immunity in the lungs. They are highly adaptive components of the innate immune system and can be specifically modified to whatever functions are needed, depending on their state of differentiation and the micro-environmental factors encountered. Alveolar macrophages release numerous secretory products and interact with other cells and molecules through the expression of several surface receptors. Alveolar macrophages are also involved in the phagocytosis of apoptotic and necrotic cells that have undergone cell-death. Besides their phagocytic and mircobicidal functions, alveolar macrophages secrete numerous chemical mediators upon stimulation, mainly cytokines and chemokines, and play an important role in inflammatory regulation in the lung.

3.1.2.6 Dendritic cells

Dendritic cells (DCs) are immune cells that form part of the mammalian immune system. Their main function is to process antigen material and present it on the surface to other cells of the immune system. That means dendritic cells function as antigen-presenting cells and act as messengers connecting the innate and adaptive immunity.

Once activated, dendritic cells migrate to the lymph nodes where they interact with T cells and B cells to initiate and shape the adaptive immune response. Immature dendritic cells are called veiled cells because they possess large cytoplasmic 'veils' rather than dendrites.

In addition, lung DCs express numerous receptors for inflammatory mediators that are released upon damage to tissue by pathogens, trauma, vascular damage, or necrosis. In summary, dendritic cells bridge the innate and the adaptive immune system in humans.

3.2 Pulmonary diseases related transcription factors

The pulmonary diseases chronic obstructive pulmonary disease (COPD) [22,23], pulmonary allergy [24-26], and acute lung injury (ALI) [27,28] are thought to be three of the leading causes of morbidity, mortality and disease-related decreases in the quality of life worldwide [29,30]. The fundamental pathogenesis of these diseases involves the progression of abnormal inflammatory responses to stimuli in the lung [31], leading to the recruitment of immune and inflammatory cells into the lungs as well as their activation. These proinflammatory-activated cells and airway epithelial cells produce cytokines, oxidants and many other mediators which are involved in inflammation [32-35]. It is now believed that there are gene-specific factors which regulate the transcription of particular genes by binding to specific recognition motifs, which are usually located in the upstream (5') promoter region of the target gene. A common mechanism is that these factors are generally located in the cytosol, but can translocate to the cell nucleus upon inflammatory stimuli and there, by binding to specific consensus sites, upregulate or downregulate the rate of transcription of the target gene and thereby increase or decrease the formation of messenger RNA (mRNA) and the protein of an inflammatory mediator [32,36]. The best described transcription factors regarding immune and inflammatory responses are nuclear factor-kappa (κ) B (NFkB) and activator protein 1 (AP-1) [32,37]. This section will focus on recent progress in the understanding of the role of the NFkB and AP-1 which can lead to regulation of specific genes in the pathogenesis of inflammatory lung diseases.

3.2.1 The NFkB signalling pathway

Nuclear factor-kappaB (NFkB) is a transcription factor with a pivotal role in inducing genes involved in physiological processes, such as immune and inflammatory responses, developmental processes, cellular growth, and apoptosis [38]. In addition, NFkB is persistently active in a number of disease states,

including cancer, arthritis, chronic inflammation, asthma, neurodegenerative diseases, and heart disease [39,40]. In most cells, NFkB exists in the cytoplasm in an inactive, latent form associated with regulatory proteins known as inhibitors of κB (IκB), of which the most important appear to be IκBα, IκBβ, and IκBε [41] (Fig.3.4B). IκBα has been associated with transient NFkB activation, while IκBβ seems to be involved in sustained activation [41] (Fig.3.4B). In addition, IκBα is associated with transient NFkB activation, whereas IκBβ is involved in sustained activation [41]. Different IκB molecules might control the regulation of distinct genes in various tissues by inhibiting specific NFkB subsets; therefore, IκB proteins could be an attractive target for specific therapies [35,42].

NFkB subunits

The NFkB/Rel family includes NFkB1 (p50/p105), NFkB2 (p52/p100), p65 (RelA), RelB, and c-Rel [43,44] (Fig.3.4A). Most members of this family (RelB being an exception) can homodimerize, as well as forming heterodimers with each other (Fig.3.4C). Fig. 3.1 shows that all members of the NFkB transcription factor family share a conserved N-terminal 300 amino acid Rel homology domain (RHD) responsible for both dimerization and binding to KB sequence motifs, which also has sequences important for nuclear localization and IKB inhibitor binding [45,46]. RelB has an N-terminal extension, which is known as the leucine zipper (LZ) domain because of the presence of a leucine-rich heptad repeat that is not present in other NFkB family members [47,48]. The C-terminal half of the Rel proteins have transactivation domains (TAD). The most prevalent activated form of NFkB is a heterodimer consisting of subunit p50 and p65, which contains transactivation domains necessary for gene induction [41].

The p50 subunit of NFkB is not synthesized as an active DNA-binding protein, but is generated by proteolytic processing of a 105 kDa precursor of the NFkB 1 gene called p105 that contains p50 in its N-terminal half and IKB-gamma in its C-terminal half [49,50]. For targeted disruption of the NFkB1 gene, a PGK-neo cassette was inserted into exon 6 of the NFkB1 gene, which encodes residues 134-187; these lie within the Rel homology domain that extends from residues 30-330 [51](Fig.3.4D). Therefore, this targeted disruption will produce a truncated polypeptide that has no ability to bind DNA or dimerize with itself and other NFkB family members. On the other hand, this mutant allele is also unable to direct synthesis of the p105 precursor to p50, but cannot affect IKB-gamma synthesis from an internally-promoted mRNA [51]. This means that NFkB1 homozygous knock out ($p50^{-/-}$) mice cannot express either functional p105 or p50 proteins.

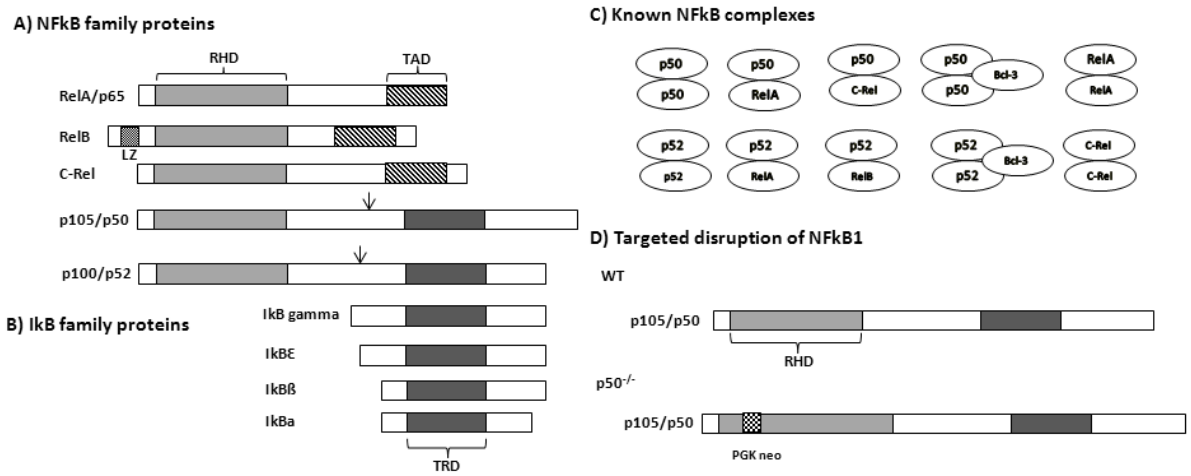

Figure 3.4: Structures of core NFkB signaling proteins, IkB family members and known NFkB dimers, as well as the production of mice lacking the p50 subunit of NFkB. (A) The generalized structures of the two subfamilies (Rel and NFkB) of NFkB transcription factors are shown in the top left. (B) The IkB family members, including p105 and p100, are characterized by ankyrin repeat-containing inhibitory domains (TRD) in the C-termianl halves, which can be removed by proteasome-mediated proteolysis. (C) Known NFkB dimers. (D) The NFkB1 locus and targeting construct. A PGKneo cassette was inserted into the region of the NFkB1 gene encoding the Rel homology domain of p105.

NFkB regulation in the lung inflammation

Under resting conditions, NFkB dimers are bound to inhibitory IκB proteins, which sequester inactive NFkB complexes in the cytoplasm [52]. Stimulus-induced degradation of IκB proteins is initiated through phosphorylation by the IκB kinase (IKK) complex, which consists of two catalytically active kinases, IKKα and IKKβ, and the regulatory subunit IKKγ (NEMO) [52]. The NFkB dimers are activated as a result of the IKK-mediated, phosphorylation-induced degradation of the IkB inhibitor, which enables the NFkB dimers to translocate to the nucleus and activate specific target gene expression [52]. NFkB signaling is often divided into two types of pathway, known as either the canonical and non-canonical pathways or the classical and alternative pathways [53] (Fig.3.5).

The activation and nuclear translocation of classical NFκB dimers (mostly p50/p65) is associated with increased transcription of proinflammatory genes encoding chemokines, cytokines, adhesion molecules such as intercellular adhesion molecule 1 (ICAM-1), vascular cell adhesion molecule-1 (VCAM-1) and endothelial–leukocyte adhesion molecule 1 (ELAM), enzymes that produce secondary inflammatory

mediators and inhibitors of apoptosis [54,55] (Fig.3.5A). These molecules are important components of the innate immune response to invading microorganisms and are required for the migration of inflammatory and phagocytic cells to tissues where NFκB has been activated in response to infection or injury [55]. In contrast, the alternative NFkB activation pathway plays a particular role in lymphoid organ development and adaptive immunity, which responds to blood-borne antigens as well as abnormal splenic microarchitectures that might contribute to several types of immune deficiency [55,56].

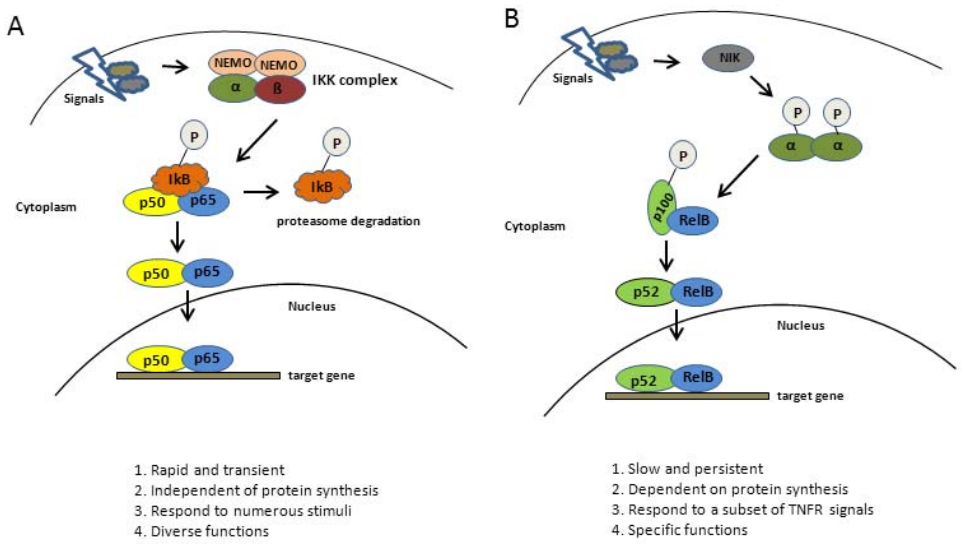

Figure 3.5: Canonical and non-canonical pathways of NFkB activation. The canonical pathway (**A**) is induced by most of the NFkB stimuli. IκB is phosphorylated in an IKKα- (also known as IKK1), β- (also known as IKK2), and NEMO- (NFκB essential modulator, also known as IKKgamma) dependent manner, which results in a rapid ubiquitinization of IkB with subsequent proteasomal degradation and transient nuclear translocation of the prototypical heterodimer p65/p50. In contrast, in the non-canonical pathway, IKKα mediates phosphorylation of p100 associated with RelB, which leads to partial processing of p100 and then a slow and persistent transcriptional activation of p52/RelB heterodimers occurs, as opposed to the p50/p65 heterodimers produced by the canonical pathway (**B**). NIK: NFkB-inducing kinase, a: IkB kinase alpha, ß: IkB kinase belta, p: phosphorylation.

NFkB is clearly one of the most important regulators of proinflammatory gene expression in general and also regulates the expression of many genes involved in inflammatory responses in the lungs (table 3.1). During the inflammatory response, the dynamic regulation of the expression of different adhesion molecules plays an important role in the recruitment of inflammatory cells such as neutrophils,

eosinophils, macrophages, and lymphocytes from the circulation to the site of inflammation [57-59]. NFkB activation increases expression of the adhesion molecules E-selectin, VCAM-1, and ICAM-1, while NFkB inhibition reduces leukocyte adhesion and transmigration [41,60]. These molecules are downregulated in endothelial cells by treatment with antioxidants [61].

Table 3.1: Inflammatory genes regulated by NFkB (adapted from [32])

Cytokines	Tumour necrosis factor α (Tnfα)
	Interleukin 1β
	Interleukin 2
	Interleukin 3
	Interleukin 6
	Interleukin 12
Growth factors	Granulocyte-macrophage colony-stimulating factor (GM-CSF)
	Granulocyte colony-stimulating factor (G-CSF)
	Macrophage colony-stimulating factor (M-CSF)
Chemokines	Interleukin 8
	Macrophage inflammatory protein 1 α (MIP-1α)
	Macrophage chemotactic protein 1 (MCP-1)
Inflammatory mediators	Inducible nitric oxide synthase (iNOS)
	Inducible cyclo-oxygenase 2
	5-lipoxygenase
	Cytosolic phospholipase A_2
	C reactive protein
Adhesion molecules	Intercellular adhesion molecule 1 (ICAM-1)
	Vascular cell adhesion molecule 1 (V-CAM-1)
	E-selectin, P-selectin
Immunoreceptors	Interleukin-2 receptor (α-chain)
	T-cell receptor (β-chain)
	Platelet-activating factor receptor
	CD11b and CD48

As shown in Fig.3.4C, in $p50^{-/-}$ mice the various components and their respective complexes in the NFkB1 pathway are lacking: (1) p50/p50 homodimers, which are known as, (i) signal-specific transcriptional repressors of proinflammatory gene expression, selectively inhibiting transiently activated p65/p50 complexes either by competing with p65 for dimerization [62,63] or by binding to identical NFkB binding sites [64]; and (ii) signal-specific transcriptional activators for antiinflammatory IL-10 [65]. (2) p65/p50, the prevalent, proinflammatory NFkB heterodimer of canonical pathway [53]. (3) p50/C-Rel, which is

critical for proper B-cell development [66]. (4) p50/Bcl-3, which acts as an antiinflammatory regulator in inflammatory responses by attenuating transcription of proinflammatory cytokines and activating IL-10 expression [67]. Meanwhile, according to other previously published observations in mice, p50 deficiency could increase the DNA-binding activity of NFkB in response to cigarette smoke [68] or nuclear accumulation of p65 in the lung tissues of an elastase-induced pulmonary emphysema mouse model [69].

3.2.2 The AP-1 signalling pathway

The transcription factor activator protein 1 (AP-1), which consists of a number of homodimeric and heterodimeric complexes of members of the Jun (c-Jun, Jun-B, and Jun-D) and Fos (Fos, Fos-B, Fra-1, and Fra-2) families of DNA-binding proteins, binds to the 12-O-tetradecanoylphorbol-13-acetate (TPA) response element (TRE, 5'-TGACTCA-3') and regulates the expression of genes involved in various biological processes, including cell proliferation, cell differentiation, cell death, inflammatory response, and cellular defense [70-72]. Activation of AP-1 is associated with increased transcription, leading to increased nuclear accumulation of AP-1 proteins, as well as posttranslational modifications (such as phosphorylation) which, in turn, may either increase or decrease transactivation of the AP-1 complex [73-75].

AP-1 regulation in the lung inflammation

AP-1 activation occurs in response to a number of diverse stimuli, including growth factors, cytokines, chemokines, hormones, ultraviolet irradiation, DNA damage and multiple environmental stresses. For instance, an activation of cascades involving stress-responsive, mitogen-activated protein kinases (MAPK), such as Jun-N-terminal kinases (JNK), leads to activation of AP-1 [76]. Interestingly, the promoter regions of many inflammatory mediators, including TNF-α, IL-1β, IL-6, IL-8, and MCP-1, contain AP-1 binding sites, indicating that AP-1 activation may be necessary for the induction of acute, cytokine-mediated inflammation [75,77,78]. For instance, mice lacking c-Fos exhibit an enhanced production of inflammatory mediators in response to LPS [79] and an enhanced susceptibility to dextran sulfate-induced colitis [80], in part as a result of the activation of NFkB. Meanwhile, the genetic ablation of *c-Jun* and *Jun-B* in the epidermis of adult mice leads to psoriasis, accompanied by the enhanced expression of inflammatory mediators [81], suggesting that Jun proteins control the development of skin disorders

associated with tissue inflammation [82]. However, many inflammatory mediators, such as TNF-a, MMP1 require the simultaneous activation of AP-1 and NFkB that work together cooperatively [77,83].

3.3 Particle-induced aseptic acute lung inflammation model

The increasing use of engineered nanoparticles (NP) such as combustion-derived nanoparticles in industrial and household applications will unavoidably lead to the release of such materials into the environment [84-87]. Numerous epidemiological studies [88-90] have reported a positive association between ambient concentrations of particulate matter (PM) and the incidence of respiratory and cardiovascular morbidity and mortality.

3.3.1 Lung inflammation

Inflammation can in general be divided into (i) acute inflammation, which occurs as an immediate response to trauma such as an injury or surgery which occurs over seconds, minutes, hours and even days, and (ii) chronic inflammation such as arthritis and COPD, which occurs over longer periods. Inflammation is the body's response to insults, including infection, trauma, and hypersensitivity. The inflammatory response is complex and involves a variety of mechanisms to defend against pathogens and to repair tissue [91].

In the lung, inflammation is usually caused by pathogens or by exposure to insults such as toxins, pollutants, irritants, and allergens. Many types of inflammatory cell are activated and recruited into the lumen during inflammation, and then release inflammatory cytokines and mediators to modify the activities of other inflammatory cells. Physiological orchestration of these cells and molecules leads from initiation and progression to the resolution of inflammation [92].

3.3.2 Carbon nanoparticles

In nanotechnology, a particle is defined as a small localized object that behaves as a whole unit in terms of its transport and physical properties, such as volume or mass [93]. Particles are further classified according to size: (i) fine particles are sized between 2,500 and 100 nanometers; (ii) nanoparticles are defined as primary particles with at least one dimension < 100 nm; and (iii) ultrafine particles are defined as particles < 100 nm in all dimensions and are commonly produced by combustion processes [94].

Combustion-derived nanoparticles (CDNP) include welding fume and nanoparticulate carbon black, which are both occupational hazards; coal fly-ash, which is an environmental hazard; and diesel soot,

which is both an environmental and an occupational hazard [94]. Like other nanoparticles, CDNP agglomerate readily moves into the accumulation mode, which decreases the particle number but probably leaves the surface area dose unaffected [94].

3.3.3 Particle induced aseptic acute lung inflammation

Cellular interaction with CDNP has been shown to provoke oxidative stress and inflammatory responses both *in vivo* and *in vitro*, and pathways include MAPK and NFκB activation [95,96]. Induction of these pathways leads to the transcription of a number of proinflammatory mediator genes, such as IL-8, Cxcl1, -2, -5 and Tnfa in epithelial cells treated *in vitro* and in human lungs exposed by inhalation [94] (Fig.3.6). As an important constituent of urban PM in particular, CDNP represent an important factor in the development of particle-related adverse health effects [97].

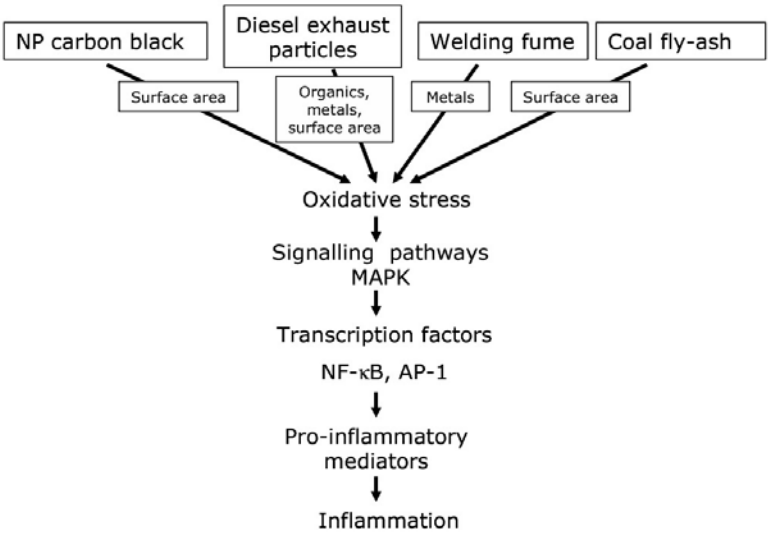

Figure 3.6: Molecular toxicology mechanisms driving the inflammatory effects of CDNP in lung in response to CDNP exposure (adapted from [94]). Different components of different CDNP can cause oxidative stress that acts through well-documented redox-sensitive pathways, such as MAPK and NF-κB, to cause inflammation. Although the components that mediate these effects differ greatly between the different CDNP, there is commonality in their ability to cause oxidative stress and inflammation.

Due to the direct contact of the lung surface with inhaled air pollution and the large surface area of the lungs (approx. 150 m^2), the effects of inhaled and deposited particles to the lung cells are of particular interest. In the alveolar region of the lungs, the type I epithelial cells, which are only approximately 0.1

µm thick, provide the structural lining with a very short diffusion distance for the gas exchange between alveolar air and capillary blood. They cover approximately 93% of the alveolar surface, but account for less than 8% of the number of distal lung cells. In contrast, type II epithelial cells, which are cuboidal in shape and cover only approximately 7% of the alveolar surface, make up 16% of the cells in the distal lung [97]. In addition to the epithelial cells, there is a population of macrophages on the apical side, which are phagocytotic cells, and a population of dendritic cells underneath the airway epithelium, which are the most potent antigen-presenting cells involved in initiating the adaptive immune response [97].

Oxidative stress caused to the lung upon CDNP exposure has, for example, been described by the oxidation of low density lipoprotein (LDL) *in vivo* and of epithelial cells *in vitro* [98,99]. Regarding the components responsible for oxidative stress generation and subsequent proinflammatory signaling, the organic fraction and the transition metals have been described [100], and the oxidative surface reactivity of pure carbon nanoparticles has been related to their proinflammatory potency [101].

3.4 Macrophage polarization and lung inflammation

Macrophages play an essential role in homeostasis and defense, and are characterized by high functional heterogeneity and plasticity [102-104]. The mode of macrophage activation has been suggested to play a central role in disease progression and resolution [105-107].

The growth and differentiation of macrophages depends on lineage-determining cytokines, such as macrophage-colony-stimulating factor (M-CSF) and granulocyte-macrophage-colony-stimulating factor (GM-CSF), as well as interactions with stroma in haematopoietic organs [108,109] (Fig.3.7). Peripheral blood monocytes are attracted from the circulation to the site of damage by chemical substances through chemotaxis, triggered by a range of different stimuli, including damaged cells, pathogens and cytokines, which are often released by activated macrophages at the site of injury [110]. At some sites, such as the testis, macrophages have been shown to populate the organ through proliferation [111-113]. Macrophage populations in different organs have different names: Kupffer cells in the liver, alveolar macrophages in the lung and microglia in the central nervous system (CNS); these have all adapted to their local microenvironment [109].

There are generally two different types of macrophage polarization or activation pathway described, known as M1 macrophages or classically-activated macrophages and M2 macrophages or alternatively-activated macrophages according to the Th1 and Th2 cell paradigm. However, some researchers argue against such a classification, because macrophages might be able to change quickly from one phenotype to another in response to environmental signals, and there might thus be no straightforward correspondence in phenotypes between these T cell subsets and the subpopulations of other immune cells [114]. Furthermore, alternatively-activated macrophages can be divided in three subpopulations: (i) M2a macrophages induced by classical activation with IL-4 and IL-13 [115,116]; (ii) M2b macrophages corresponding to Type II-activated macrophages which are induced with an immune complex and Toll-like receptor (TLR) or IL-1 receptor (IL-1R) ligands via Fc receptor 1 (FcRI), complement receptors and TLR [116-118]; and (iii) M2c macrophages generated stimulated by IL-10 and glucocorticoid hormones [114,115].

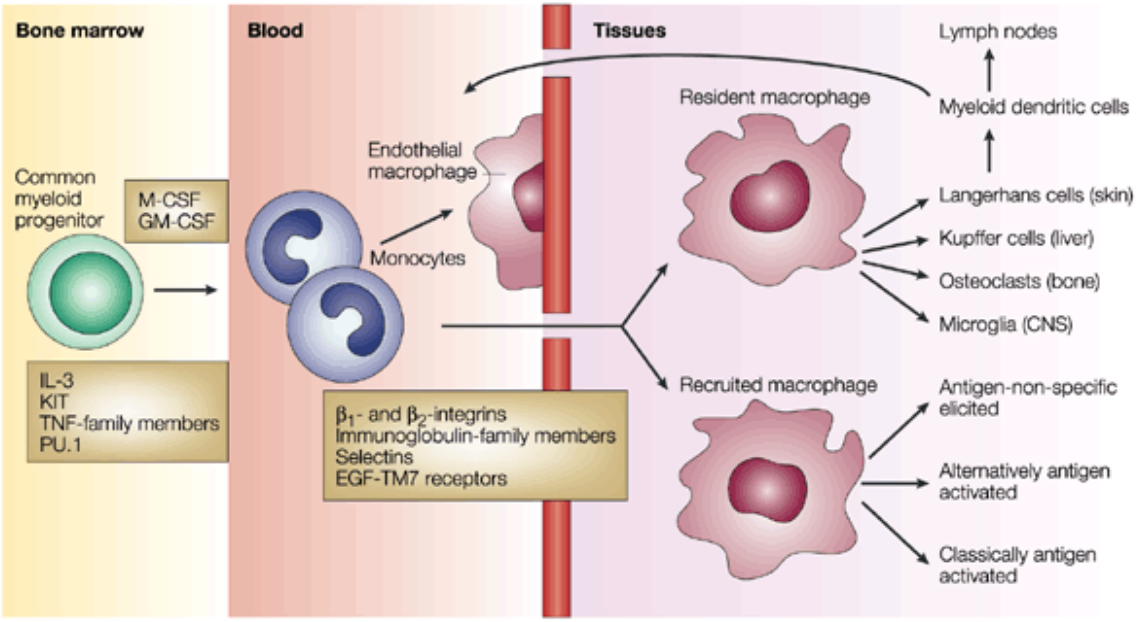

Figure 3.7: Differentiation, distribution and activation of macrophages *in vivo* (adapted from[109]). Macrophages arise from hemopoietic progenitors, which differentiate, either directly or via circulating monocytes, into subpopulations of tissue macrophages and the closely-related myeloid dendritic cells; the latter specialized at presenting antigens to naive T helper lymphocytes [108].

Alveolar macrophages play an important role in host defense and in processes of inflammation in the lung [75]. When faced with an inflammatory response in the lung resulting from large numbers of infectious particles or more virulent microbes, alveolar macrophages synthesize and secrete a wide array of cytokines (including IL-1,IL-6, and TNF-α), chemokines (including IL-8), and arachidonic metabolites [119]. Using these cell-to-cell signals, alveolar macrophages initiate inflammatory responses and recruit activated neutrophils into the alveolar spaces [120].

3.4.1 Molecular determinants of macrophage polarization

A network of signaling molecules, transcription factors, epigenetic mechanisms, and posttranscriptional modification underlies the different forms of macrophage activation [121] (Fig.3.8). The balance between activation of STAT1 and STAT3/STAT6 finely regulates macrophage polarization and activity. A predominance of NFκB and STAT1 activation promotes M1 macrophage polarization, resulting in cytotoxic and inflammatory functions [121]. In contrast, a predominance of STAT3 and STAT6 activation results in M2 macrophage polarization, which is associated with immune suppression and tumour progression and is characterized by the expression of a distinct repertoire of molecules, including arginase I, resistin-like molecule alpha (RELMα), and Ym1/2 [108]. PPAR-γ and PPAR-δ control distinct aspects of M2 macrophage activation and oxidative metabolism [122]. KLF4 and KLF2 participate in the promotion of M2 macrophage functions by cooperating with STAT6 to suppress NFκB/HIF-1α–dependent transcription [123]. IL-4–induced c-Myc activity controls a subset of M2-associated genes [124]. IL-4 also induces the M2-polarizing Jmjd3-IRF4 axis to inhibit IRF5-mediated M1 polarization [107]. IL-10 promotes M2 polarization through the induction of p50 NF-κB homodimer, c-Maf, and STAT3 activities [121,125,126].

3.4.2 Induction and resolution of inflammation as well as macrophage phenotypic polarization

The recruitment of leukocytes from the blood is a key feature of inflammatory responses to tissue damage or infection [111]. Prominent in this cascade is the rapid influx of granulocytes and monocytes that subsequently differentiate into inflammatory macrophages and/or dendritic cells [127,128]. Interestingly, both resident and recruited macrophages can alternatively activate and be driven to proliferate by a TH_2 environment *in vivo* [111].

Converging studies reveal that the phenotypic polarization of macrophages caused by the specific inflammatory microenvironment is critical for both induction and resolution of the inflammatory response [121]. For example, in lean adipose tissue, production of IL-13 or IL-4 can induce the M2 phenotype polarization in ATMs [129]. However, obesity can induce a proinflammatory state that promotes M1 phenotype polarization and initiates a feed-forward circuit that amplifies the inflammatory response and contributes to insulin resistance [130]. Similarly, Th1 cytokines predominate early in the course of an infection and thereby enhance macrophage bactericidal effects, while Th2 cytokines confer an M2 phenotype to help in resolution and repair following an inflammatory insult.

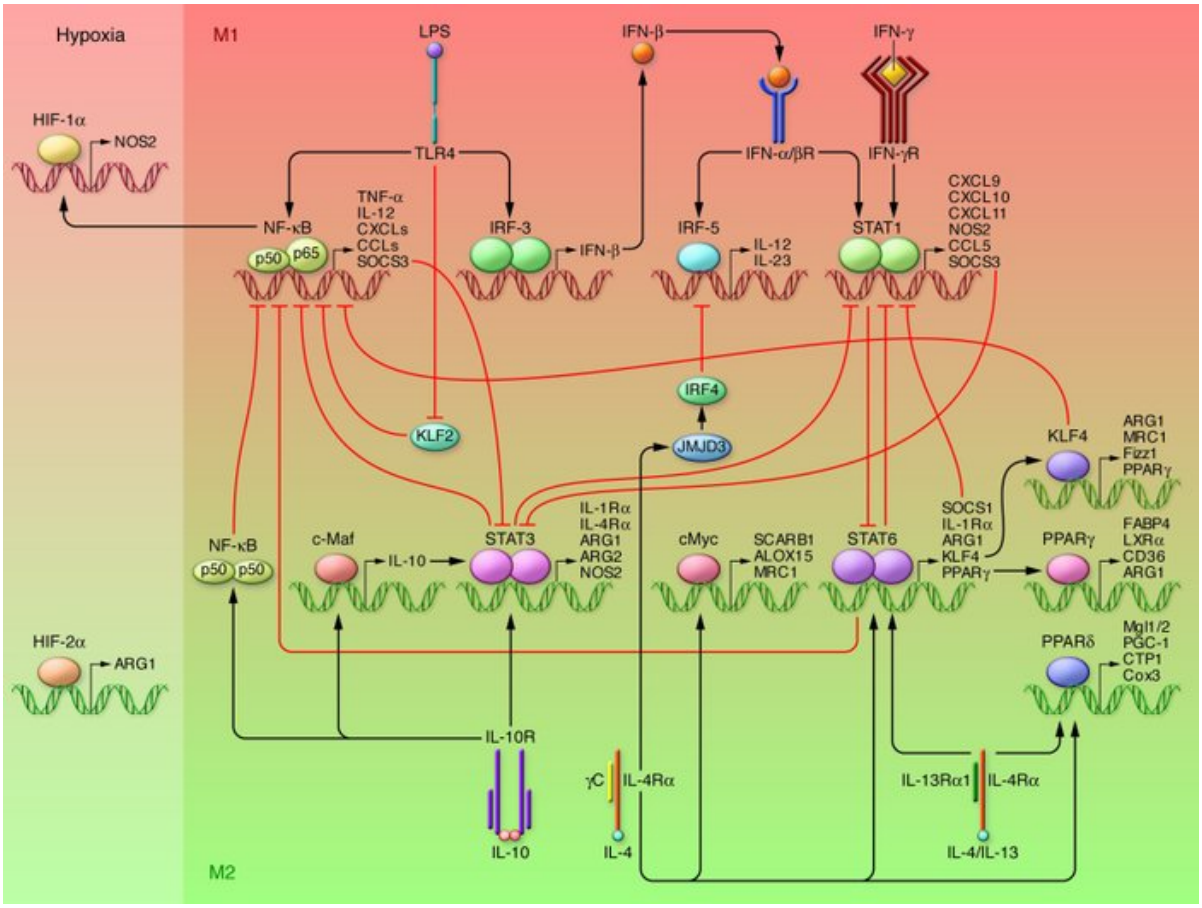

Figure 3.8: Mechanisms of macrophage polarization (adapted from[121]). The major pathways of macrophage polarization are outlined. The crosstalk between the M1-M2 macrophage–polarizing pathways is also indicated. Classical IRF/STAT signaling pathways are activated by IFNs and TLR signaling to skew macrophage function toward the M1 phenotype (via NFkB and STAT1) or by IL-4 and IL-13 to skew toward the M2 phenotype (via STAT3 and STAT6).

Laskin [131] (Fig.3.9) described M1 macrophages as being like soldiers of the Dark Side of The Force in the Star Wars movies on the one hand, releasing a barrage of negative energy (e.g., cytotoxic/proinflammatory mediators) that contributes to tissue injury. The activity of M1 macrophages is opposed by alternatively-activated M2 macrophages that are analogous to the Jedi Order, whose positive protective energy counters the activity of The Dark Side. Alternatively-activated M2 macrophages release mediators that play a tissue protective role by down regulating inflammation and initiating wound repair. The outcome of the response to tissue injury mainly depends on the balance between the two opposing forces of macrophages.

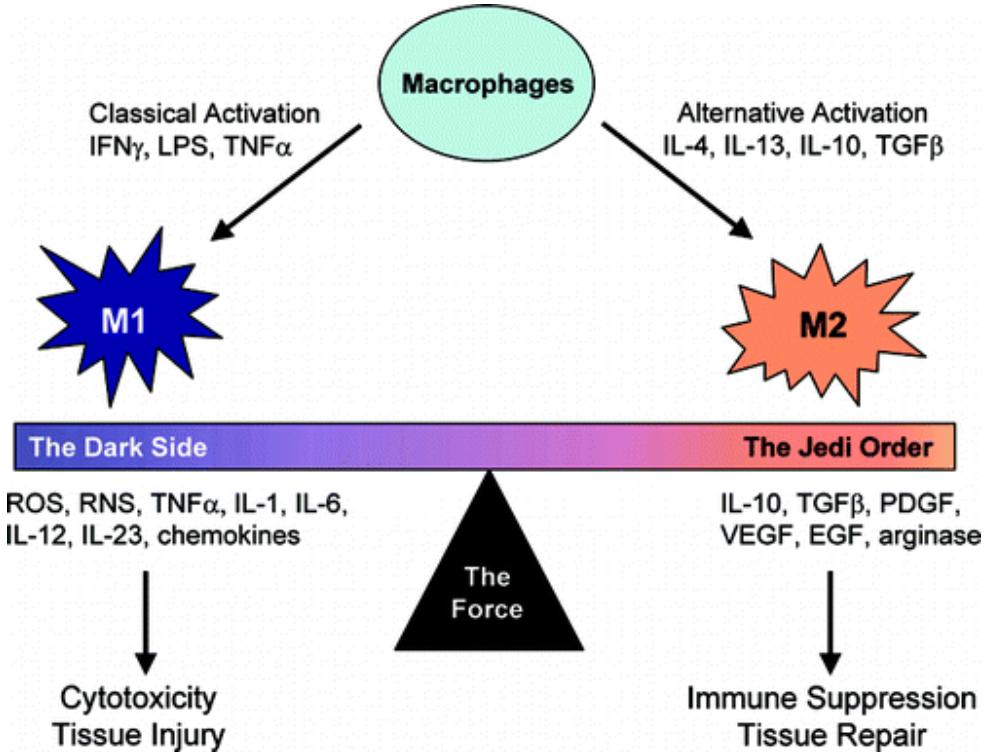

Figure 3.9: In response to inflammatory signals encountered at sites of injury or infection, macrophages develop into either classically-activated M1 cells, which contribute to tissue injury, or alternatively-activated M2 cells, which downregulate inflammation and initiate wound repair (adapted from [131]).

Macrophages are clearly essential in the body for appropriate immunological defense to protect the body from the damaging effects of invading pathogens and toxins and for wound repair; however, an imbalance in macrophage activation and phenotypic polarization may actually contribute to tissue injury.

It is likely that the extent to which macrophages (M1 or M2) contribute to injury or participate in tissue repair depends on the balance of their phenotypic polarization and the timing of their appearance at the target sites. Aberrations in the relative responsiveness of these cells, leading to an imbalance between the production of proinflammatory and antiinflammatory mediators may be important in determining the final outcome of the pathogenic response to toxicants.

3.5 Project aims

The ubiquitous nuclear transcription factor kB (NFkB) is involved in the regulation of numerous genes in various tissues, and activation of NFkB has been shown to be associated with lung disease. The NFkB transcription factor family in mammals consists of five proteins – p65 (RelA), RelB, c-Rel, p105/p50 (NFkB1), and p100/52 (NFkB2) – that associate with each other to form distinct transcriptionally active homo and heterodimeric complexes. It has been reported that NFkB1 p50 plays import roles in NFkB functions via dimerization with other NFkB subunits, including: (i) p50/p65, the prevalent, proinflammatory NFkB heterodimer of classical pathway; (ii) p50/p50, the signal-specific transcriptional repressors of proinflammatory gene expression; (iii) p50/Bcl-3, which acts as an antiinflammatory regulator; and (iv) p50/C-Rel, which is critical for proper B cell development. However, whether the NFkB subunit p50 could impact acute pulmonary inflammation and injury after 24 hours on CNP treatment is not clear. Therefore, we investigated the role of NFkB1 subunit p50 signaling in the regulation of lung inflammation induced by particle exposure.

4. Materials and methods

4.1 Materials

4.1.1 Mice

All mice were kept and bred at institute of Lung Biology and Disease (iLBD), Helmholtz Zentrum München, Neuherberg, according to the national and institutional guidelines.

Wild type (WT) and NFkB1 Knockout ($p50^{-/-}$) mice, all on a C57BL/6J genetic background. Mice were female and 10 -12 weeks of age at the time of study. NFkB1 Knockout ($p50^{-/-}$, NF-kappaB^{tm1Bal}) mouse was established previously [51] via insertion of a PGK-neomycin resistance cassette into exon 6 which encodes the p105 precursor of the p50 subunit of the encoded transcription factor, thus this mutant allele which produces a truncated polypeptide that cannot bind with DNA, or dimerize with itself or other kappaB binding motifs [51]. The $p50^{-/-}$ mouse was gifted from Dr. Falk Weih (Leibniz Institute for Age Research - Fritz Lipmann Institute, Jena, Germany). The WT mouse was obtained from Charles River (Munich, Germany).

The wild type mice with C57BL/6NCrl background were purchased from Charles River (Munich, Germany), and were female with 10 -12 weeks of age during the study.

4.1.2 Carbon nanoparticles

Carbon nanoparticle (CNP) used this project was generated by spark discharge and filter-sampled in our laboratory in a lipopolysaccharide (LPS)-free environment. The methodology of generation and a detailed description of physical particle properties have been described in our study [132-134].

4.1.3 Commencial available assays

Kit Name	Company
TransAM® NFkB Family	Active Motif
Nuclear Extract Kit	Active Motif
TransAM® AP-1 Family	Active Motif
Absolute qPCR SYBR® Green ROX Mix	Applied Biosystems
Superscript™ II Reverse Transcriptase kit	Invitrogen

GoTaq® Polymerase Green Master Mix	Promega
Odyssey Infrared *EMSA Kit*	LI-COR Biosciences
Douset ELISA kit (CXCL1, CXCL2,CXCL5, TNF-a, IL10,OPN,IL1ß)	R&D Systems
Bio-Rad Protein Assay kit	Bio-Rad
RNeasy Mini Kit	Qiagen
High Pure RNA Isolation Kit	Roche
peqGOLD TriFast	Peqlab
Giemsa and May Grünwald solutions kit	Sigma-Aldrich
Quick-RNA™ MicroPrep kit	ZYMO
RNaseOUT TM Recombinant Ribonuclease Inhibitor	Invitrogen
dNTP Mix (10mM each)	Fermentas

4.1.4 Equipment

Equipment Name	Company
NanoDrop® ND-1000 spectrophotometer	Thermo Scientific, Wilmington, USA
Centrifuge: Eppendorf 5415D	Eppendorf, Hamburg, Germany
Centrifuge: Sigma 3K18	Sigma, Osterode am Harz, Germany
ABI PRISM® 7000 detection system	Applied Biosystems, Foster city, CA, USA
Shandon cytospin3 cytocentrifuge	Shandon, PA
4ml, 15 ml and 50 ml Tubes	BD Falcon, Heidelberg, Germany
0.2ml, 0.5ml, 1.5 ml and 2ml Tubes	Eppendorf, Hamburg, Germany
Vortexer	Scientific Industries, Karlsruhe, Germany
PCR- thermal cycler : PTC-225	MJ Research, Hamburg, Biozym, Germany
Pipetman (2µl, 10µl, 20µl, 200µl, 1ml)	Gilson, Limburg-Offheim, Germany

ABsolute ™ QPCR Seal (AB1170)	Thermo Scientific, Wilmington, USA
96 Wells qPCR plate	Thermo Scientific, Wilmington, USA

4.1.5 Chemicals

All chemicals used in this project were purchased from Sigma-Aldrich (Deisenhofen, Germany), Roche (Mannheim, Germany), Bio-rad (Munich, Germany), Fluka (Deisenhofen, Germany), Invitrogen (Karlsruhe, Germany), Merck (Darmstadt, Germany), Roth (Karlsruhe, Germany) unless otherwise specified.

Dulbecco's Modified Eagle Medium (DMEM), Dulbecco's Phosphate buffered saline (DPBS), Fetal Bovine Serum (FBS), Fetal Calf Serum (FCS), RPMI Media 1640 and antibiotics were from either BioChrome (Berlin, Germany) or Invitrogen (Karlsruhe, Germany).

4.1.6 Buffers and solutions

Name	Concentration	Compounds
Wash buffer (PBS-T)	1X	PBS
	0.05%	Tween-20
PBS buffer (10X)	137 mM	NaCl
	2.7 mM	KCl
	10 mM	Na_2HPO_4
	2 mM	KH_2PO_4
TBE buffer (10X)	890 mM	Tris Base
	890 mM	Boric Acid
	20 mM	EDTA (pH 8.0)
RPMI-1640 medium	1X	RPMI-1640 medium
	10%	Fetal bovine serum
	1%	penicillin/streptomycin
	2 mM	glutamine
	50 µM	ß-mercaptoethanol (for macrophage culture)
EMSA binding buffer (10X)	100 mM	Tris
	500 mM	KCl
	10 mM	DTT
Dulbecco's Modified Eagle	1X	Dulbecco's Modified Eagle Medium

Medium (DMEM)	10%	Fetal bovine serum
	1%	penicillin/streptomycin
	2 mM	glutamine
	50 µM	ß-mercaptoethanol (for macrophage culture)
RIPA buffer (1X)	20 mM	Tris-HCl (pH 7.5)
	150 mM	NaCl
	1 mM	Na_2EDTA
	1 mM	EGTA
	1%	NP-40
	1%	sodium deoxycholate
	2.5 mM	sodium pyrophosphate
	1 mM	ß-glycerophosphate
	1 mM	Na_3VO_4
	1 µg/ml	leupeptin
EMSA loading buffer (10X, Orange Loading Dye)	65% (w/v)	Sucrose
	10 mM	Tris-HCl, pH 7.5
	10 mM	EDTA
	0.3% (w/v)	Orange G
Hypotonic buffer (10X)	100mM	Hepes, pH 7.9
	15 mM	$MgCl_2$
	100 mM	KCl
	5 mM	DTT
	2 mM	PMSF
Hypotonic buffer (for tissue homogenization, volume for 3ml/per one gram tissue)	350 µl	10X Hypotonic Buffer
	2.8 ml	Distilled water
	3.5 µl	Protease Inhibitor Cocktail
	350 µl	Phosphatase Inhibitors
	3.5 µl	1 M DTT
	3.5 µl	Detergent (just for tissue homogenization)
Lysis Buffer (200ml volume)	2 ml	1M Hepes
	666.7 µl	3M KCl
	80 µl	0.25M EDTA
	8 ml	10% NP40
	189.3 ml	dd H20
Complete Lysis Buffer (for nuclear fraction extract, 50µl volume)	5 µl	10 mM DTT
	45 µl	Lysis Buffer
	0.5 µl	Protease Inhibitor Cocktail
Block buffer (ELISA)	1g	BSA
	100ml	1X PBS

Stop solution (ELISA)	0.18 M	H_2SO_4

4.1.7 Recombinant proteins and antibodies

Name	Company
Anti-p50, p65	santa cruz biotechnology
Recombinant murine IFN-gamma	Immuno tool
Recombinant murine IL-4	Immuno tool
Lipopolysaccharides (LPS) from *E.coli*	Sigma-Aldrich

4.2 Methods

4.2.1 Mouse treatment

Animals were treated humanely and with regard for alleviation of suffering; all animal experiments were carried out according to the German law of protection of animal life and were approved by the Bavarian Animal Research Authority of Germany (Approval No. 55.2-1-54-2351-115-05 and 55.2-1-54-2351-117-07).

All mice were kept in isolated ventilated cages (IVC-Racks; BioZone, Margate, UK) supplied with filtered air, in a 12 hours light/12 hours dark cycle. Specific pathogen-free (SPF) hygienic status was approved by a health certificate according to the Federation of European Laboratory Animal Science Associations guidelines [135,136]. Food and water were available *ad libitum*.

Each of two genetically modified mice (WT and $p50^{-/-}$ mice) consisted of three groups (each group consisted of 5 animals, at least), and one group was intratracheal instillated with 20 µg CNP, the other two served as control and sham exposed groups.

Mice were anesthetized by intraperitoneal injection of a mixture of Medetomidin (0.5 mg/kg body mass), Midazolam (5.0 mg/kg body mass) and Fentanyl (0.05 mg/kg body mass) prior to intratracheal instillation [133]. The animals were then intubated by a nonsurgical technique [137]. Using a cannula inserted 10 mm into the trachea, a suspension containing 20 µg CNPs, respectively, in 50 µl pyrogene-free distilled water was instilled, followed by 100 µl air. Sham mice were instilled 50 µl pyrogene-free distilled water

only, and control mice were not instilled [133,136]. After instillation mice were antagonized by subcutaneous injection of a mixture of Atipamezol (2.5 mg/kg body mass), Flumazenil (0.5 mg/kg body mass) and Naloxon (1.2 mg/kg body mass) to guarantee their awakening and well-being [133].

After instillation of 3, 6, 12, 18, 24 hours, 3 and 7 days, mice were anesthetized by intraperitoneal injection of a mixture of xylazine (4.1 mg/kg body weight) and ketamine (188.3 mg/kg body weight) and killed by exsanguination [136]. Therefore blood was drawn from the retroorbital plexus by a capillary and collected in either EDTA covered tubes (*Sarstedt*) for haematological analysis (ADVIA Hematology Systems, Bayer Diagnostics) or non EDTA-covered tubes to gain blood serum [133].

4.2.2 Preparation of carbon nanoparticles dispersions

Since the salt content of phosphate-buffered saline (PBS) causes rapid particle aggregation comparable to the "salting-out" effect [138] and thus eliminates consistent instillation conditions [136]. Therefore CNPs were suspensed in pyrogene-free distilled water at concentraction of 20µg per 50µl, was sonicated on ice for 1 min prior to instillation, using a SonoPlus HD70 (Bachofer, Berlin, Germany) at a moderate energy of 20W.

4.2.3 Bronchoalveolar lavage (BAL)

Following by blood sampling, BAL was performed by cannulating the trachea and infusing the lungs 4 times with 1.0 ml PBS (20 drops) without calcium and magnesium, has been described in our previously studies [133,136]. The BAL fluids from lavages 1 and 2 and from lavages 3 and 4 were pooled and centrifuged (425 *g*, 20 min at room temperature). The cell-free supernatant from lavages 1 and 2 were used for biochemical measurements such as lactate dehydrogenase (LDH), the concentrations of total protein and cytokine. The cell pellet was resuspended in 1 ml RPMI 1640 medium (BioChrome, Berlin, Germany) and supplemented with 10% fetal calf serum (Seromed, Berlin, Germany); the number of living cells was determined by the trypan blue exclusion method.

4.2.4 BAL cell differentation

Cell differentials were performed on the cytocentrifuge preparations (May-Grünwald-Giemsa staining; 2 × 200 cells counted). The number of polymorphonuclear leukocytes (PMNs) was used as a marker of inflammation [133,136]. For cell differential analyses, a minimum of 200 cells were counted under microscope. Two slides were made and counted for each sample

4.2.5 Total protein content and lactate dehydrogenase (LDH) in BAL flluid

Total BAL protein content was determined spectrophotometrically with an ELISA reader (Labsystems iEMSReader MF, Helsinki, Finland) at 620 nm, applying the Bio-Rad Protein Assay Dye Reagent (no. 500-0006; BioRad, Munich, Germany), as a potential biological marker for pulmonary capillary leakage and lung injury [139]. Five microliter undilluted BALF per mouse was used for analysis, and bovine serum albumin (BSA) dillution was used for standard.

For detection of the cytosolic enzyme lactate dehydrogenase (LDH) (U/ml), characteristic for membrane damaging effects, the Cytotoxicity Detection Kit (Roche Diagnostics, Germany) was used according to the manufacturer's instructions. LDH concentration in the 30 µl undilluted BALF was spectrophotometrically determined with an ELISA reader (Labsystems iEMS Reader MF, Helsinki, Finland) at a wavelength of 492 nm by monitoring the reduction of NAD^+ in the presence of lactate [133,136].

4.2.6 Enzyme-Linked Immunosorbent Assay (ELISA)

BALF dilutions at volume of 100µl were used for assession of BAL cytokine concentrations. The characteristic CNP induced alveolar macrophage inflammatory markers osteopontin (OPN, SPP1) (mouse Osteopontin; R&D Duo Sets; Catalog Number: DY441) and galectin-3 (mouse Galectin-3; R&D Duo Sets; Catalog Number: DY1197) [140], as well as the known lung mainly epithelial derived inflammatory markers LIX (CXCL5) (mouse LIX; R&D Duo Sets; Catalog Number: DY443), and lipocalin-2 (NGAL), (mouse Lipocalin-2/NGAL; R&D Duo Sets; Catalog Number: DY1857) [134,140] were assayed from BAL samples using the respective ELISA kit (Gotz et al. 2011). Furthermore, other inflammatory mediators such as IL-1a, IL-1ß, CXCL10, CXCL1, IL10 and IFN gamma were also selected to be measured.

.

4.2.7 Extract of nuclear fraction from frozen lung tissue

To determin transcription factors activation in lungs upon CNP exposure, nuclear fraction was extracted from frozen lung tissue following the manufacturer’s instructions (Nuclear Extract Kit, Active Motif). The concentration of protein (dilluted with lysis buffer) was checked by Bio-rad protein assay dye reagent (no. 500-0006, biorad, Germany).

4.2.8 TransAM® Transcription Factor (Nfkb and AP-1) ELISA

TransAM® Transcription Factor (NFkB and AP-1) ELISA kit contain a 96-well plate to which oligonucleotide containing a transcription factor consensus binding site has been immobilized. The

activated transcription factor homodimers and heterodimers contained in nuclear or whole-cell extracts specifically binds to this oligonucleotide. By using an antibody that is directed against subunits of transcription factor, the activated transcription factor subunit bound to the oligonucleotide is detected. Addition of a secondary antibody conjugated to horseradish peroxidase (HRP) provides sensitive colorimetric readout that is easily quantified by spectrophotometry.

4.2.9 Electrophoretic Mobility Shift Assay (EMSA)

EMSA was performed as previously described [141,142]. A densitometrical analysis (Aida Image Analyzer, v3.51) served to quantify transcription factors activity relatively to the positive control Oct 1. The composition of NFκB complexes was analysed by supershift assay using α-p50 (sc-114) and α-p65 (sc-372) antibodies (Santa Cruz Biothechnology). The DNA squence for NFkB activity: 5'-AGT TGA GGG GAC TTT CCC AGG C-3'; AP-1: 5'- CGC TTG ATG ACT CAG CCG GAA -3'; Oct 1: 5' - TGT CGA ATG CAA ATC ACT AGA A-3'.

4.2.10 Experiments for primary alveolar macrophages (AMs) *in vitro*

4.2.10.1 Isolation of primary alveolar macrophages (AMs)

Alveolar macrophages were obtained from WT and $p50^{-/-}$ adult mice with C57BL/6J background. The procudure was same as Bronchoalveolar lavage (BAL), but infusing the lungs 10 times so that received more AMs. Briefly, the lavage fluid was passed through a layer of sterile gauze to remove gross mucus and then centrifuged 425 *g* for 20 min at room temperature to separate cells from fluid. The cell pellet was washed twice in complete RPMI 1640 medium. Then AMs were allowed to adhere during 3 hours and non-adherent cells were removed by two washes in 1X PBS [143].

4.2.10.2 AMs treated with either IL4 or LPS plus IFNgamma

Monolayer of AMs was incubated at 37°C with stimulating agents in the presence or absence of IL-4 or LPS plus IFNgamma for 4 hours. Then the supernants were removed and adhered AMs were isolated for total RNA after washed three times in 1X PBS.

4.2.11 quantitative real time polymerase chain reaction (qPCR)

4.2.11.1 Design of qPCR primer

Primer was designed by online free tool primer 3 (http://frodo.wi.mit.edu/) according to the guideline with (i) PCR product size between 120 to 225bp and (ii) primer size between 18 to 25bp with both 55-60% of GC content and about 55°C of Tm value.

The specificity of primer was tested by online UCSC In-Silico PCR (http://genome.ucsc.edu/cgi-bin/hgPcr?command=start). The specificity of the amplifications was confirmed by the presence of a single band of expected size for each primer pairs in agarose gels following electrophoresis and by the single distinct peak dissociation curves of the amplicon.

Table 4.1: Primer sequences and amplicon characteristics of genes of interest (GOI) in this project

Name	Sequence (5'→3')	Amplicon (bp)
18S rRNA	F: gac tgt ctc gcc ggt gtc R: gga gag ccg gaa cgt cga	98
Actb	F: tcc atc atg aag tgt gac gt R: gag caa ga tct tga tct tca t	154
Arg-1	F:gga acc cag aga gag cat ga R:ttt ttc cag cag acc agc tt	132
B2m	F:ctg acc ggc ctg tat gct a R:cag tct cag tgg ggg tga at	244
Bcl-2	F: tag aga ctc acc agg gtc tg R: ctc ctc tct aca gtg gca ag	101
Casp1	F: cag tag ctc tgc ggt gta g R: gtg cct tgt cca tag cag	194
Ccl2	F:ctt ctg ggc ctg ctg ttc a R:cca gcc tac tca ttg gga tca	127
Ccl22	F: tca tgg cta ccc tgc gtg tc R: cct tca cta aac gtg atg gca gag	156
Cd68	F:cct cca ccc tcg cct agt c R:ttg ggt ata gga ttc gga ttt ga	118
Cox-2	F:caa cac ctg agc ggt tac R:gtt cca gga gga tgg agt	202
Cx3cl1	F:gcg aca aga tga cct cac R:cca ggt gtc aca ttg tcc	230
Cxcl1	F: ccg aag tca tag cca cac R: gtg cca tca gag cag tct	138
Cxcl2	F: tcc aga gct tga gtg tga cg R: tcc agg tca gtt agc ctt gc	161
Cxcl5	F: ccc tac ggt gga agt cat R: ctt cac tgg ggt cag agt	195
Cxcl10	F: agg gct cct taa ctg gag R: gga gta gca gct gat gtg ac	165
C-Jun	F:tga ctg caa aga tgg aaa cg R:cag ggt cat gct ctg ttt ca	98

Cypa	F:ttt gca gac gcc act gtc R:cag tgc tca gag ctc gaa ag	165
Fizz-1	F: tcc cag tga ata ctg atg aga R: cca ctc tgg atc tcc caa ga	214
Fos-B	F:aag tgt gct gtg gag ttc R: atg ttg gaa gtg gtc ga	121
Fra-1	F:tcg ccg gga gct gac a R:gca gct cag caa tct ctt tct g	89
Fra-2	F: tcg ccg gga gct gac a R: gca gct cag caa tct ctt tct g	89
Gal3	F: gag cta cac atc cct agc c R: ctc agg agg atc tga gac tg	169
Gapdh	F: tgc acc acc aac tgc tta gc R: ggc atg gac tgt ggt cat gag	101
Gusb	F:cag ggt caa ctt cag gtt cc R:gct ctt tgt gac agc cac tg	165
Hmbs	F:ggt ccc tgt tca gca aga ag R:aag cca gaa gta ggc agt gg	242
Hmgb1	F: ggc tga caa ggc tcg tta tg R: ggg cgg tac tca gaa cag aa	138
Ho-1	F:agc aca ggg tga cag aag R:gtg tct ggg atg agc tag tg	213
Hprt	F:gtt gga tac agg cca gac ttt gt R: cac agg act aga aca cct gc	224
Icam1	F: ccg cag gtc caa ttc aca ct R: tcc agc cga gga cca tac ag	143
Ifng	F: acg gca cag tca ttg aaa gcc ta R: gtc acc atc ctt ttg cca gtt cc	119
IKBa	F: tac tcc ccc tac cag ctt ac R: gac tcc gtg tca tag tc c	128
IKBß	F:ctg cat cta gca gcc atc R:ggc tct gag tga ggt agg ta	205
IKBz	F:gcc agg cc aga tta ggt R:cct cac cta gag aga ag ca	164
IL-1ß	F:caa cca aca agt gat att ctc cat g R:gat cca cac tct cca gct gca	152
IL-4	F: tcg gca ttt tga acg agg tc R: gaa aag ccc gaa aga gtc tc	216
IL-6	F: gcc aga gtc ctt cag aga g R: cca ctc ctt ctg tga ctc c	138
IL-10	F:tct gtc tag gtc ctg gag tc R:gga gca ggt gaa gag tga	170
IL-12a	F: act aga gag act tct tcc aca aca aga g R: gca cag ggt cat cat caa aga c	75
IL-12ß	F: gga agc acg gca gca gaa ta R: aac ttg agg gag aag tag gaa tgg	180
IL-17f	F: ccc atg gga tta caa cat cac tc	66

	R: cac tgg gcc tca gcg atc	
IL-18	F: aga cag cct gtg ttc gag R: ctt cac aga gag ggt cac ag	126
IL-23r	F: gca tgt ggt gat agc cct tt R: caa ccc aca tgt cac cag ag	86
iNOS	F:cct gtg aga cct ttg atg R:cct ata ttg ctg tgg ctc	92
Mmp7	F: cta tgc agc tca ccc tgt tct g R: gcc tgt tcc cac tga tgt gc	106
Mmp9	F: gaa gtg ggg ttt ctg tcc R: agc cct cga ggt agc tat ac	137
Opn	F: agc tca gag gag aag ctt R: ctt cag agg aca cag cat	115
Ppar-γ	F:gta gaa gcc gtg caa gag R:gag gaa ctc cct ggt cat	192
Rorrt	F: caa gtc atc tgg gat cca cta c R: tgc agg agt agg cca cat tac a	95
Rpl13a	F:ccc tcc acc cta tga caa ga R:ctg cct gtt tcc gta acc tc	221
Vcam1	F: gcc tcg cta ggt tac aca R: gga ctg ccc tcc tct agt at	139
Sdha	F:cag ttc cac ccc aca ggt at R:gat ctt tct cag ggc cac ag	208
Sod2	F: aca aac ctg agc cct aag gg R: gaa cct tgg act ccc aca gac	128
Sod3	F: gcc tga act tca cca gag R: cta ggt cga agc tgg act c	152
Tbp	F:gcc ttc cac ctt atg ctc ag R:gct act gcc tgc tgt tgt tg	202
Tnf-a	F: cac cac gct ctt ctg tct R: ggc tac agg ctt gtc act c	166
Ym1	F:act ttg atg gcc tca acc tg R:aat gat tcc tgc tcc tgt gg	173

4.2.11.2 Isolation of total RNA and cDNA synthesis

4.2.11.2.1 Extract of total RNA

(i) Total RNA from lung tissues (lung tissue after bronchoalveolar lavage (BAL) was stored at −80 °C) was isolated using the RNeasy Mini Kit (Qiagen, Hilden, Germany) following the manufacturer's instructions with an additional peqGOLD TriFast (peqlab, Erlangen, Germany) extraction to improve protein exclusion. But lung tissue were homogenized in 2.5 ml peqGOLD TriFast reagent used IKA Disperser T 10 basic and Disperser toll (S10N).

(ii) Total RNA from cells (cell amount more than 50 000 per sample) was extracted by High Pure RNA Isolation Kit (Roche, Munich, Germany) according to the product's instructions.

(iii) Total RNA from small amount of cells (cell amount less than 50 000 per sample) was purified by Quick-RNA™ MicroPrep kit (ZYMO, Freiburg, Germany) following the product's instructions.

4.2.11.2.2 RNA concentration and purity was determined by A_{260} and A_{280} measurements using a NanoDrop® ND-1000 spectrophotometer. The mean value of A_{260}/A_{280} ratio for all RNA samples extracted by both RNeasy Mini Kit and High Pure RNA Isolation Kit was spanned within between 1.90 and 2.25, reflecting high purity and protein absence. RNA integrity was evaluated by the ratio of 28S/18S ribosomal RNA bands after electrophoresis in denaturing 1% agarose gel. To guarantee the quality necessary for expression analysis all samples used in this project presented a 28S/18S rRNA ratio $\geqslant$ 1.7.

4.2.11.2.3 cDNA synthesis

One microgram total RNA was reverse-transcribed using the Superscript™ II Reverse Transcriptase kit (Invitrogen, Karlsruhe, Germany) for first strand cDNA synthesis with 5 µM Random Nonamer (N9; MWG Biotech, AG, Ebersberg, Germany) primer according to the manufacture's recommendations. In brief, RNA and primers were mixed and incubated at 70 °C for 5 min followed by cooling on ice for 5 min and room temperature for 5–10 min before transcription. The first strand cDNA synthesis was started after adding transcription mixture at 42 °C lasting 1 h for reverse transcription reaction. Finally, the reaction was inactivated by heating to 70 °C for 15 min. All cDNA samples were diluted 1:5 with DNase- and RNase- free H_2O and stored at −20 °C for further studies.

4.2.11.3 PCR reaction

PCR was conducted using the ABI PRISM® 7000 detection system (Applied Biosystems, Foster city, CA, USA), based on ABsolute™ QPCR SYBR® Green ROX Mix (Thermo Scientific, Wilmington, USA). The PCR reaction mixture contained 1 µl cDNA (10 ng), 1 µl (5 µM) of each primer, 12.5 µl ROX mix and PCR-grade H_2O up to a total volume of 25 µl. After initial enzyme activation (one cycle at 50°C for 2min and 95 °C for 15 min), 40 cycles amplification (95 °C for 15 s, 60 °C for 1 min) were performed in 96-well optical reaction plates (Applied Biosystems, Foster city, CA, USA). To verify that the used primer pair produced only a single product, a dissociation protocol was added after thermocycling, determining dissociation of the PCR products from 60 to 95 °C by increasing 0.5 °C per cycle. In all negative control samples no amplification signal was detected.

4.2.11.4 Selection and evaluation of stable housekeeping genes

For the selection and evaluation of stable housekeeping genes (HKGs) for gene expression normalization in qPCR, 11 commonly used HKGs (18S rRNA, Actb, B2m, Cypa, Gapdh, Gusb, Hmbs, Hprt1, Rpl13a, Sdha and Tbp) of varying functional classes were selected [144-146].

The stability of housekeeping genes (HKGs) expression was analysed with geNorm (http://medgen.ugent.be/~jvdesomp/genorm/) [147], NormFinder (http://www.mdl.dk/publicationsnormfinder.htm) [148] and BestKeeper (http://www.gene-quantification.de/bestkeeper.html) [149] software packages.

4.2.11.5 PCR Data analysis

The threshold cycle (C_t) is defined as the number of cycles needed for fluorescence to reach a specific threshold level of detection and is inversely correlated with the amount of RNA or DNA template present in the reaction [150,151]. Relative expression of gene of interest (GOI) was analysed by ΔC_t method was used where $\Delta C_t = (C_t$ target gene, test sample $- C_t$ endogenous control, test sample) [152]. Relative quantities were corrected for efficiency of amplification and fold change in gene expression between groups was calculated as $2^{-\Delta\Delta Ct} \pm$ SEM. Where more than one endogenous control is used, fold change estimates were calculated using the geometric mean of HKGs quantities relative to the calibrator sample which could be the minimum, maximum or a named sample or an average.

4.2.12 Statistical analysis

All values are showed as the mean ± SEM of at least five animals or 3 individual samples *in vitro*. We used analysis of variance (ANOVA), as calculated by GraphPad Prism 5, to establish the statistical significance of differences between the experimental groups. Individual inter-group comparisons were analysed using the two-tailed unpaired t test with Welch's correction. Differences were considered significant at *, $p < 0.05$; **, $p<0.01$ and ***, $p<0.001$.

5. Results

5.1 Characterization of carbon nanoparticle (CNP)

The primary particle size of CNP used in this project was assessed by transmission electron microscopy (TEM) of particles resuspended in water (Fig. 5.1) [132,136]. The specific particle surface area of the applied particles was assessed using the Brunauer, Emmett, and Teller (BET) method, and the organic content (OC) was measured using a thermooptical analysis technique described in our previous publications [132,136]. The results showed that the CNP have diameters of 7-12nm, OC with 17% and surface area with 807 m^2/g [136].

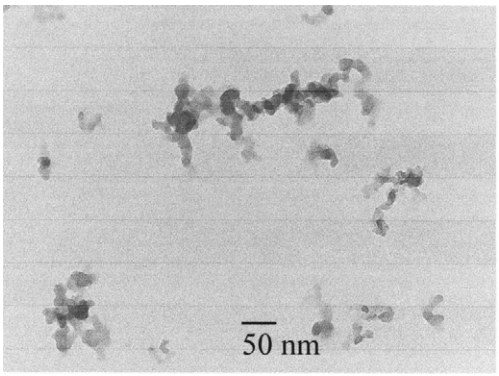

Figure 5.1: CNP used in this project was assessed by transmission electron microscopy (TEM) of particles resuspended in water. The picture has been described in detail in our previous studies [132,136].

5.2 Characterization of the CNP triggered lung inflammation in mice

Inflammation of the airways and lung parenchyma play a major role in the pathogenesis of several pulmonary diseases, such as chronic obstructive pulmonary disease (COPD), pulmonary allergy and acute lung injury (ALI) [153,154]. The primary host defence mechanisms of the lungs against exposure to stimuli such as particles and toxic gases are the innate and adaptive inflammatory immune responses [153]. The progression of acute lung inflammation is strongly associated with infiltration of the small airway walls by inflammatory cells and the accumulation of inflammatory mucous exudates in the lumen [155,156]. Therefore, in this section, a murine model of CNP-induced aseptic acute lung inflammation is used to investigate the time course of pulmonary inflammatory response, with a special emphasis on the mechanisms of acute lung inflammation caused by CNP exposure.

5.2.1 Pulmonary toxicity upon CNP treatment

In order to investigate the effects of CNP exposure on aseptic acute lung inflammation, the two main pulmonary toxicity levels of untreated or CNP-treated mice were studied: the epithelial-endothelial permeability-barrier integrity (total protein level in BALFs) and the cytotoxicity (LDH level in BALFs).

5.2.1.1 Epithelial-endothelial permeability-barrier integrity

To evaluate the integrity of the alveolar blood-air-barrier in mice upon CNP treatment, we measured the levels of total protein in the BALFs from C57BL/6N mice exposed to a single dose of 20 µg CNP per mouse by intratracheal instillation over a period of up to 7 days. Fig. 5.2 shows that at all time points except for 7 days, there was a significant time-dependent increase, up to 24 hours, of total protein levels in mice upon CNP treatment in comparison with untreated mice.

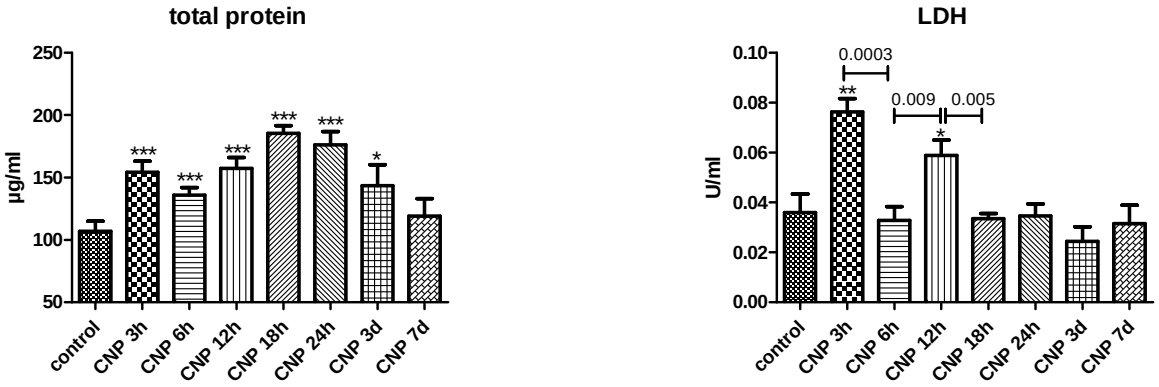

Figure 5.2: Time-course effects of total protein content and LDH concentration in bronchoalveolar lavage fluid (BALF) of mice upon a single dose of 20µg CNP treatment. Total protein concentration was determined using the Braford method. LDH concentraton was checked by Cytotoxicity Detection Kit. Values are given as mean ± SEM, n=5-10, asterisks represent significance compared to the control group with * $p<0.05$, ** $p<0.01$ and *** $p<0.001$.

5.2.1.2 Cytotoxicity (LDH)

To examine the cytotoxicity of the lung upon CNP instillation, we profiled LDH concentration in the BALFs of mice after 3, 6, 12, 18 and 24 hours, and 3 and 7 days of treatment. The results showed that, compared to untreated mice, there was a significant increase in LDH concentration in BALFs after 3 hours

of CNP treatment (2-fold increase, $p<0.01$), while the LDH concentration increased again (1.5-fold, $p<0.05$) at 12 hours (Fig. 5.2).

5.2.2 BAL cell analysis

Pulmonary inflammation was characterized by inflammatory cell recruitment into the airspace [157,158], an assessed by BAL cell differentiation. Fig. 5.3 shows the different cell counts in BALFs obtained from C57BL/6N mice intratracheally instilled with a single dose of CNP over a period of up to 7 days. The total cell numbers in BALFs from 6 hours, 18 hours and 24 hours were significantly different from those in the BALFs of untreated mice ($p<0.05$), while there was no difference among mice treated with CNP at 3 hours, 12 hours, 3 days and 7 days and untreated mice. This increase was mainly due to an accumulation of macrophages and neutrophils in the lumen (Fig. 5.3). The highest relative increase over time was seen for neutrophils and macrophages.

The absolute number of alveloar macrophages (AMs) in BALFs obtained from CNP-treated mice at 12 hours was significantly less than those obtained from untreated or even the flanking time points (6 and 18 hours). In contrast, AM numbers from 24 hours were significantly increased as compared to untreated mice. However, there was no significant change after 3, 6 and 18 hours, and 3 and 7 days CNP compared to the untreated group.

On cytospins, neutrophils were almost absent from the BALFs of untreated mice. However, CNP-exposed mice developed an acute alveolar neutrophilia, as indicated by significantly increased neutrophil numbers over a period of up to 24 hours. The acute lung neutrophilic inflammation phase was followed by drop to the basal levels after 24 hours until day 7. Lymphocyte numbers in BAL were close to the baseline in all groups and did not change significantly over time (data not shown). These results show that exposing mice to 20µg CNP by intratracheal instillation caused an acute neutrophilic alveolitis with the highest inflammatory cell numbers 24 hours after instillation.

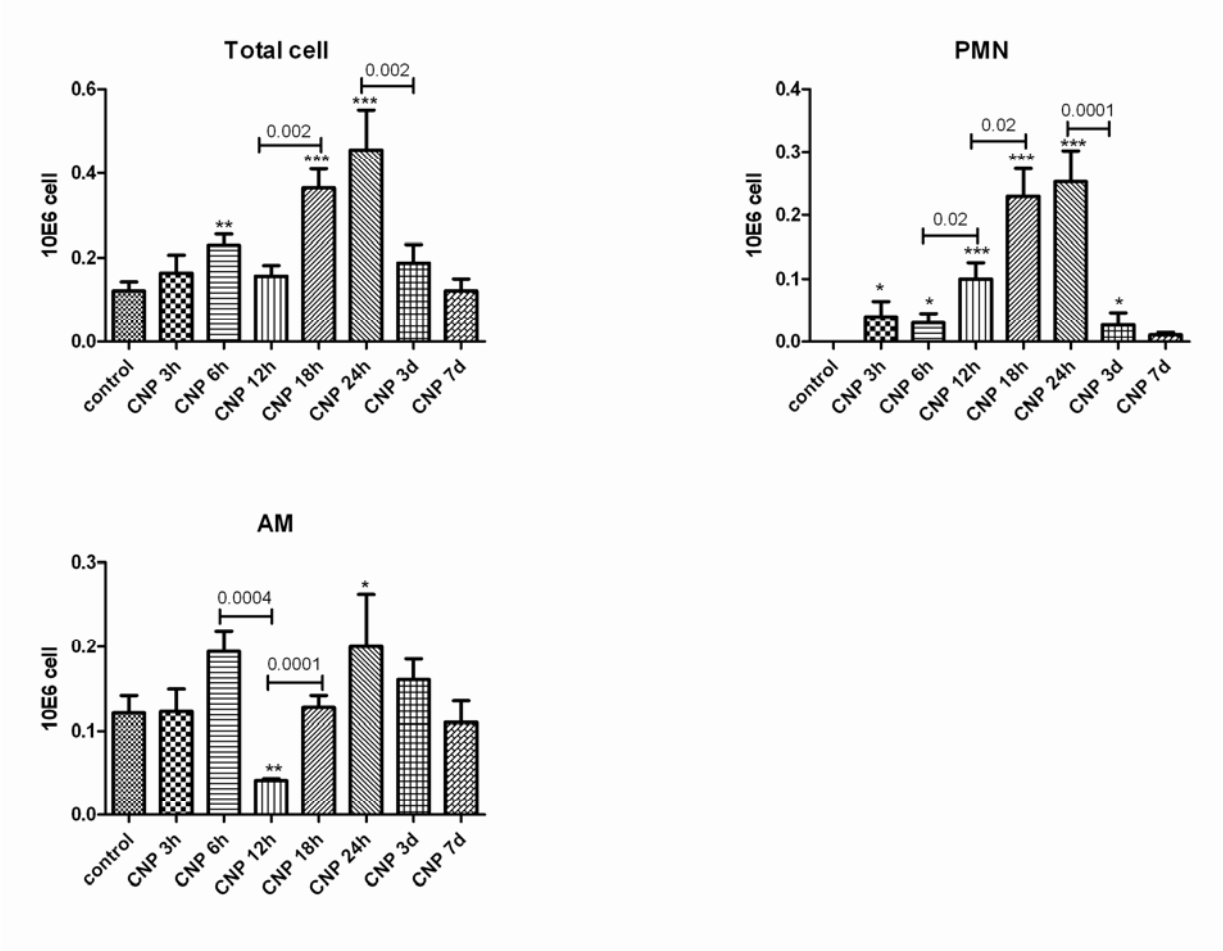

Figure 5.3: Time course of the effect of CNP exposure on total number and cell differentiation in BALF in mice. Bronchoalveolar lavage (BAL) cells were determined after cytospin centrifugation. Dead cells were discriminated by trypanblue staining. Differentitation was performed by May-Grünwald-Giemsa staining. Cell counts are shown in numbers from counts of 2 X 200 cells per cytospin and animal divided by the total cell number. Values are given as mean ± SEM, n=5-10, asterisks represent significance as compared to control group with * $p<0.05$, ** $p<0.01$ and *** $p<0.001$.

5.2.3 BAL cytokines analysis

5.2.3.1 Neutrophile chemoattractants in the BALFs

To further characterize the most obvious, neutrophilic response in the lung after CNP exposure we determined the BALF levels of the neutrophile chemoattractants CXCL1, -2 and -5. All of which are well known NFkB1 targets [159-161]. For all time points from 3 to 24 hours, as compared to control group, CXCL1 levels were significantly, but prior to 12 hours BALF concentrations only yielded in a 4.8-fold

induction that increased to 30-fold induction by 12 hours and 23-fold by 18 hours, followed by a decrease back to 9-fold after 24 hours (Fig. 5.4). In contrast, however, the CXCL1 levels at 3 days and 7 days decreased back to the basal levels. Interestingly, the CXCL5 levels were decreased at 3 hours and 6 hours post instillation, followed by an increase to 8-fold induction at 12 and 18 hours, and 5-fold at 24 hours; they then dropped down to basal levels at 3 days and 7 days. Furthermore, CXCL2 were significantly increased only at 3 hours, 12 hours and 24 hours after CNP exposure by 1.2-fold, 1.3-fold and 1.1-fold the induction respectively in comparison to untreated mice. These results showed that BAL cytokine concentrations of the neutrophile chemoattractants CXCL1, -2 and -5 (well known NFkB1 targets) in mice, increased most rapidly from 6 to 12 hours after CNP treatment.

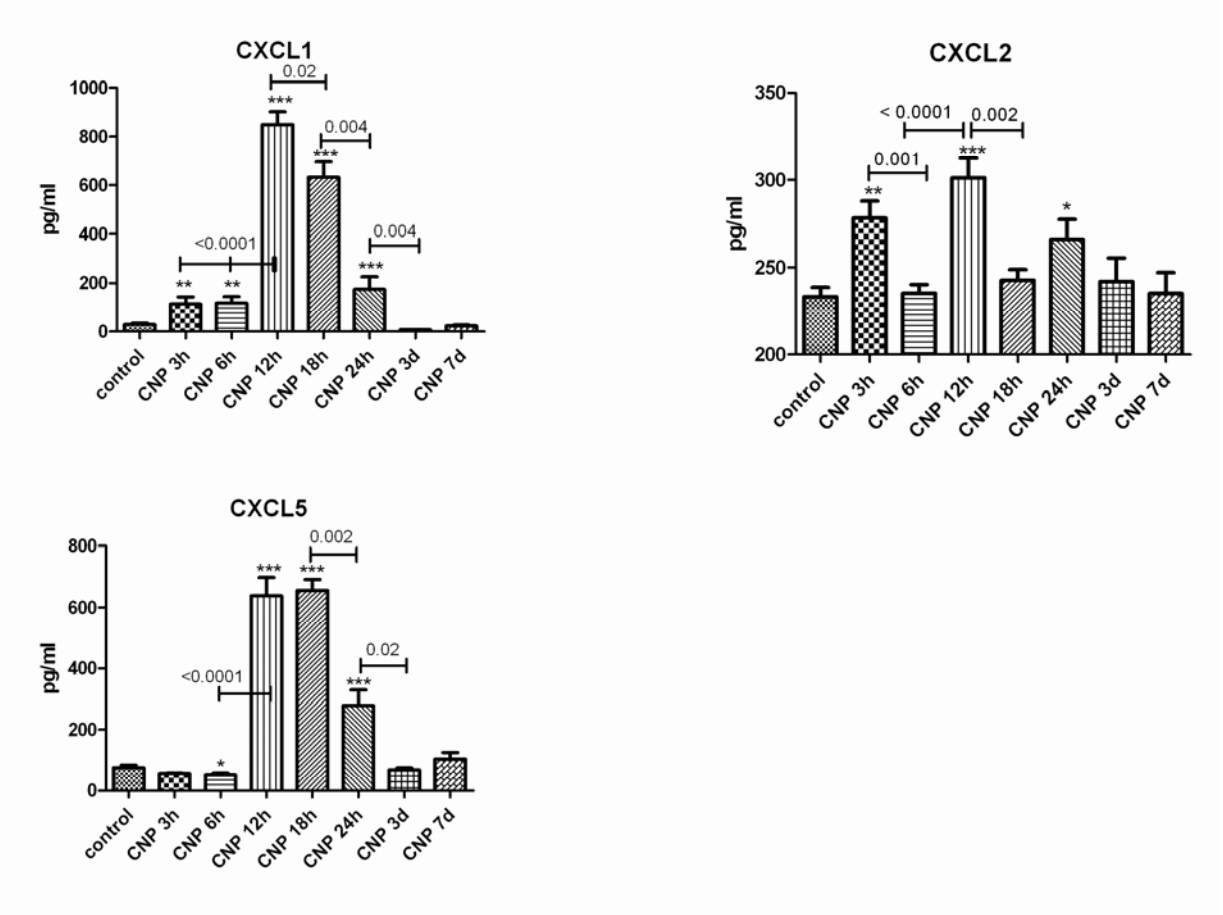

Figure 5.4: Time-course responses of neutrophile chemoattractants released into the alveolar space upon CNP treatment in mice. Cytokine levels were measured by commercial ELISA kits and were determined in BALFs for each animal in each group. Values are given as mean ± SEM, n=5-10, while asterisks represent significance compared to the control group with * $p<0.05$, ** $p<0.01$ and *** $p<0.001$.

5.2.3.2 Other inflammatory cytokines in the BALFs

To be able to localize the response of particular cell populations in the lungs in response to CNP exposure, the concentration of predominantly alveolar macrophage-derived cytokines, such as TNF-a, IL-1ß and OPN [162-164] in BALFs were determined using commercial ELISA kits. As shown in Fig.5.5, the TNF-a concentrations in the BALFs of CNP-exposed mice revealed increased levels prior to 12 hours of exposure, as compared to untreated mice. However, the concentrations of IL-1ß were increased only at 3 hours and 24 hours of CNP exposure followed by a drop down to the basal levels at 3 days and 7 days. In contrast, the opposite was observed for OPN, its concentration decreasing significantly for the first 24 hours, followed by a regress after 24 hours. These results were comfirmed that, in response to a single dose of CNP exposure, the concentrations of alveolar macrophage derived cytokines in the lung fluctuated according to the acute lung inflammation phase, rather than the chronic.

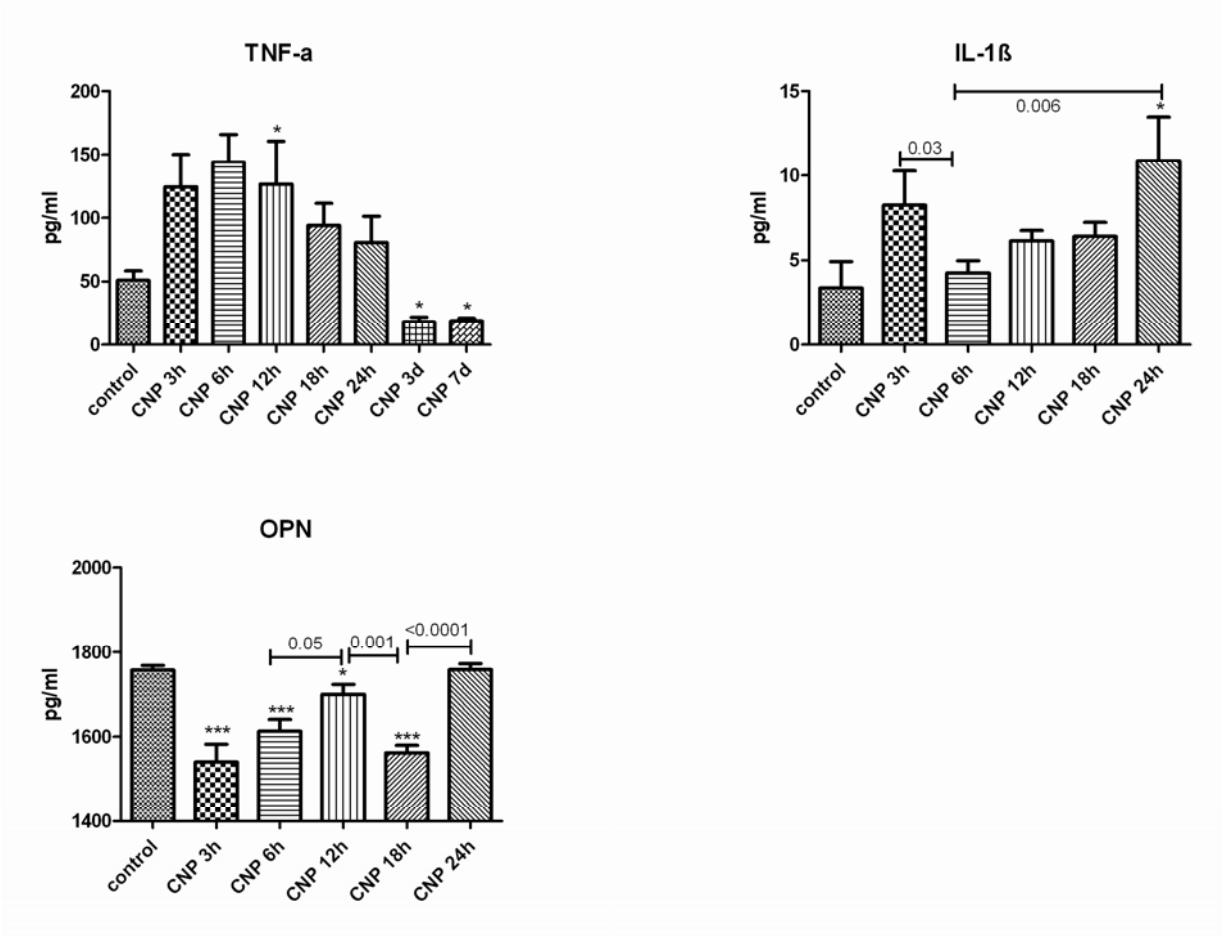

Figure 5.5: Time-course responses of alveolar macrophage derived cytokines release into the lung

lumen in response to CNP exposure. Cytokine levels were determined in BALFs for each animal in each group. Values are given as mean ± SEM, n=5-10, asterisks represent significance compared to the control group with * p<0.05, **p<0.01 and ***p<0.001.

5.2.4 Gene profiles in the lung homogenate

In addition, we isolated total RNA from the lung tissue after lung lavage and measured the mRNA levels of neutrophile chemoattractants such as Cxcl1, -2 and -5 (Fig. 5.6) as well as inflammtory genes (Fig. 5.7).

5.2.4.1 Profiles of genes for neutrophile chemoattractants

The data, as shown above, showed that a single dose of CNP exposure induced acute lung inflammation in mice, which was characterized by an acute influx of neutrophilic granulocytes into the alveolar compartment. Therefore, genes related to these neutrophilic chemoattractants were measured by qPCR. As shown in Fig. 5.6, Cxcl1, -2 and -5 were upregulated significantly over times up to 24 hours upon CNP treatment compared with untreated animals; the peak levels were reached at 12 hours followed by a drop down to basal levels after 24 hours. These results indicated that upon CNP exposure the transcriptional profiles for neutrophile chemoattractants Cxcl1, -2 and -5, detected in lung homogenate, reached their peak levels at 12 hours.

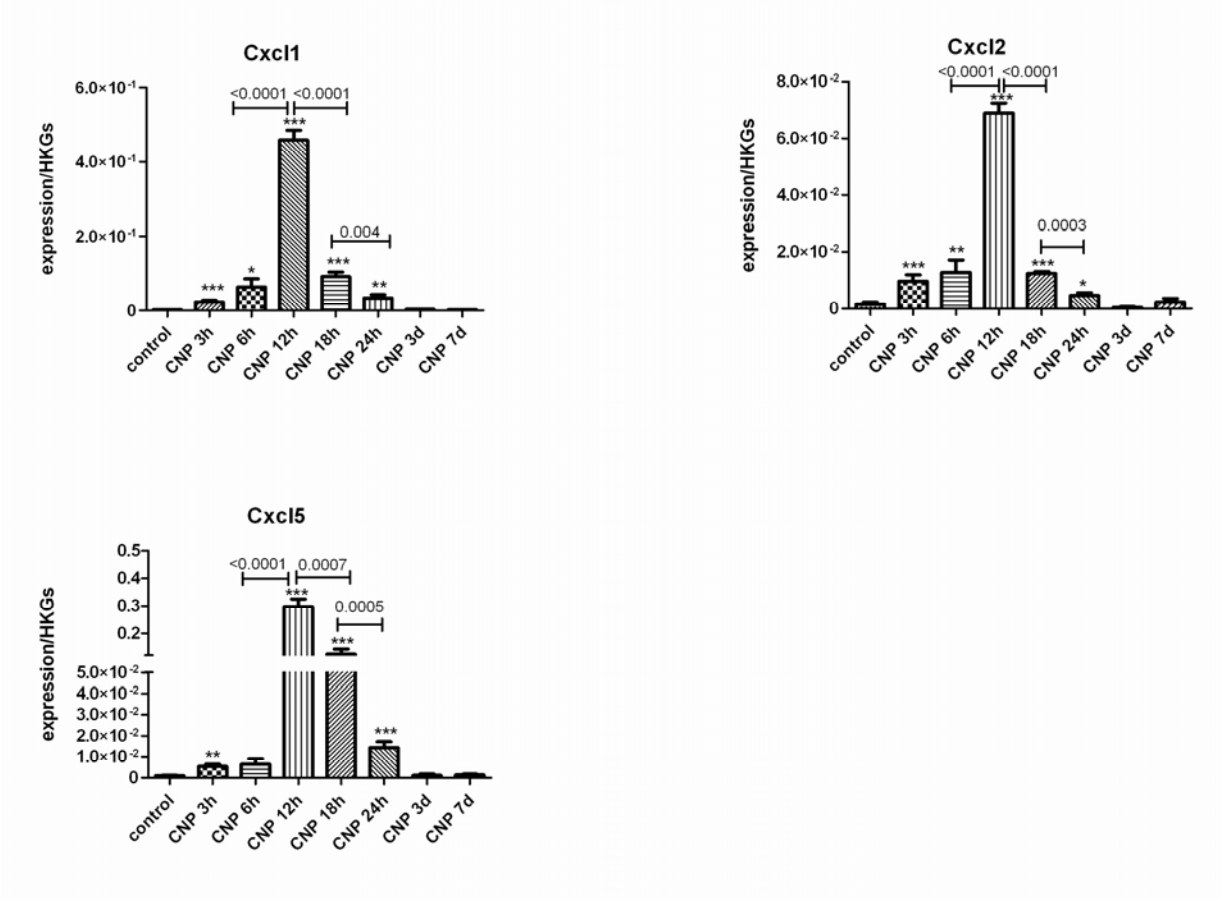

Figure 5.6: Time course of molecular levels of neutrophile chemoattractants Cxcl1, -2 and -5 determined by qPCR in lung homogenate upon CNP treatment in mice. The X-axis corresponds to the time after exposure to CNP instillation. The Y-axis corresponds to the expression level measured for the gene of interest. Measurements were normalized using the Hprt and Actb housekeeping genes and calculated using the $2^{-\Delta Ct}$ method. Values are given as mean ± SEM, n=5-10, asterisks represent significance compared to the control group with * $p<0.05$, ** $p<0.01$ and *** $p<0.001$.

5.2.4.2 Profiles of related genes for lung inflammatory response

To further investegate the aseptic acute lung inflammatory response seen in the lungs of mice exposed to CNP, which were associated with the basal levels of inflammatory cells in the lumen, inflammatory mediators in BALFs and gene expression of neutrophile chemoattractants in lung homogenate at 3 days and 7 days, other related genes profiles for proinflammatory responses (Fig.5.7A), alveolar macrophage polarization (Fig.5.7A and Fig.5.7B), and inflammatory regulator (Fig.5.7C) were determined in the mouse lungs in response to CNP exposure by qPCR method.

Most of these genes for proinflammatory responses in the lungs of CNP-treated mice reached a peak between 12 and 24 hours, rather than prior to 12 hours or after 24 hours (Fig.5.7A): (i) Mcp-1, Tnf-a, IL-1ß, Opn and Ifn gamma reached a peak at 12 hours; (ii) IL-12p40, iNOS and Ccl22 reached a peak at 18 hours; and (iii) IL-12p35 and Lcn2 reached a peak at 24 hours, all in comparison to untreated mice.

However, the profiles of genes related to alveolar macrophage polarization indicated that, in the lungs of mice treated with CNP exposure: (i) M2 classical macrophage markers such as Arg-1 and Fizz-1 were significantly increased between 18 and 24 hours after CNP exposure; (ii) Gal3 was significant increase prior to 12 hours; (iii) in contrast to the gene expression of Gal3, IL-4 was increased only after 12 hours, but not after 3 or 7 days; (iv) furthermore, Ppar-γ and IL-10 were moderately changed across all periods, but PPAR-γ was significantly decrease between 18 and 24 hours and IL-10 reached a peak at 3 hours.

Heme oxygenase 1 (HO-1), an essential enzyme in heme catabolism; it cleaves heme to form biliverdin, which is subsequently converted to bilirubin by biliverdin reductase, and carbon monoxide, a putative neurotransmitter [165,166]. In CNP-induced acute lung inflammation in the mice model we studied, Ho-1 gene expression was significantly increased only at 3 hours and 12 hours, followed by a decrease from 18 hours and 24 hours that recovered to basal levels at 3 and 7 days.

Caspase 1 is an enzyme that proteolytically cleaves other proteins, such as the precursor forms of the inflammatory cytokines IL-1β and IL-18, into active mature peptides [167,168]. Expression of caspase 1 was significantly decreased prior to 6 hours followed by a peak at 12 hours after CNP exposure in comparision to untreated mice. This finding is corelated with caspase 1 dependent induced IL-1ß gene expression, which also reached a peak at 12 hours, but not with the IL-18 gene (Fig.5.7A).

Soluble CX3CL1 potently chemoattracts T cells and monocytes, while the cell-bound chemokine promotes the strong adhesion of leukocytes to activated endothelial cells, where it is primarily expressed [169]. In our acute lung inflammation mouse model, Cx3cl1 were upregulated at 18 and 24 hours; this finding is corroborated by higher levels of inflammatory cells being attracted into the lung space from lung tissue and blood at the same time points (Fig.5.3 total cell number).

CD68 is a particular marker gene for the various cells of the macrophage/monocytes lineage [170]. Our data showed that Cd68 in lung tissue was significantly upregulated between 12 and 24 hours, while alveolar macrophage amounts in the lung increased by the highest rate at the same time compared to all other time intervals (Fig.5.3 AM number).

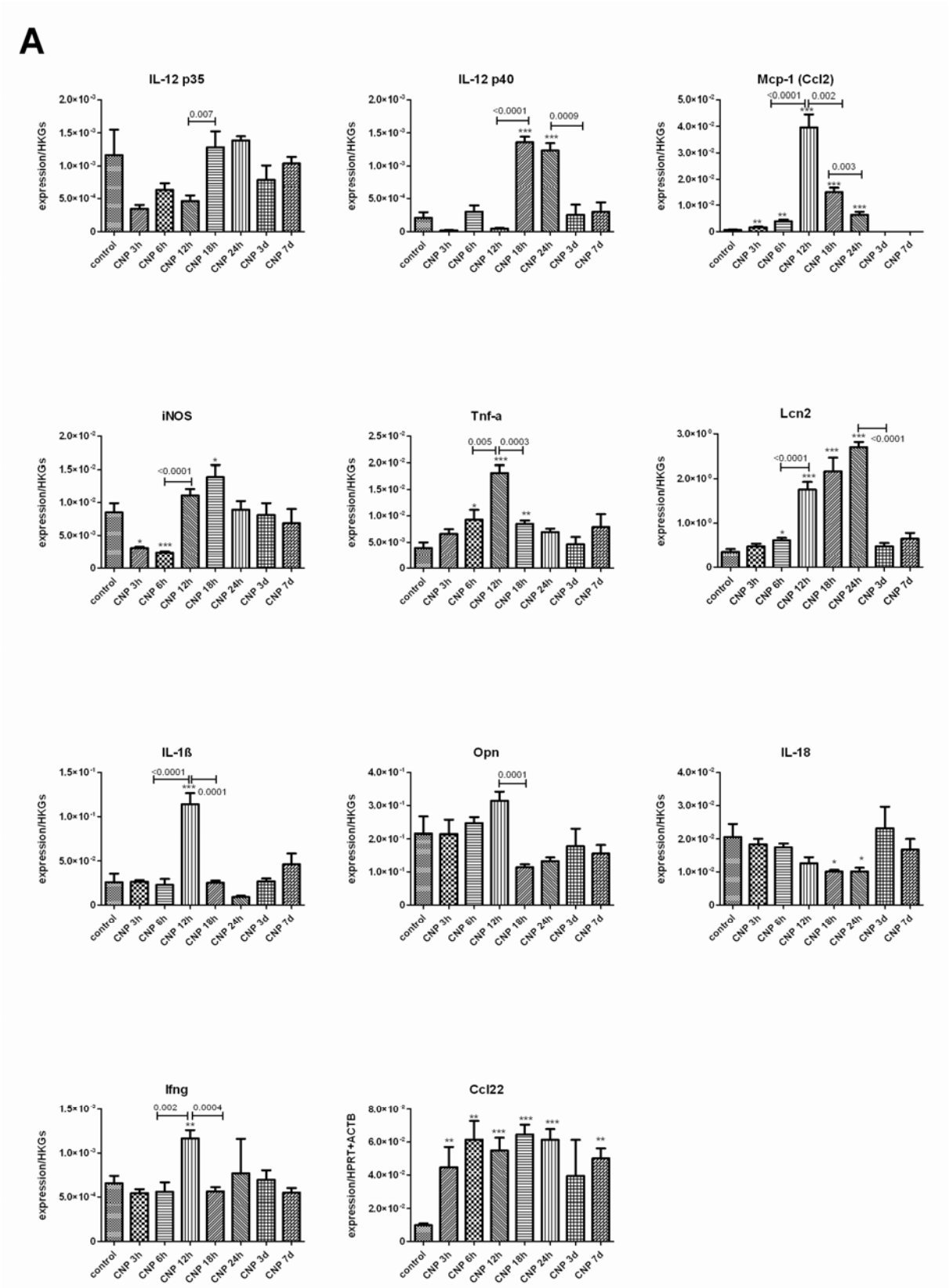
A
IL-12 p35
IL-12 p40
Mcp-1 (Ccl2)
iNOS
Tnf-a
Lcn2
IL-1ß
Opn
IL-18
Ifng
Ccl22
expression/HKGs
expression/HPRT+ACTB
control
CNP 3h
CNP 6h
CNP 12h
CNP 18h
CNP 24h
CNP 3d
CNP 7d

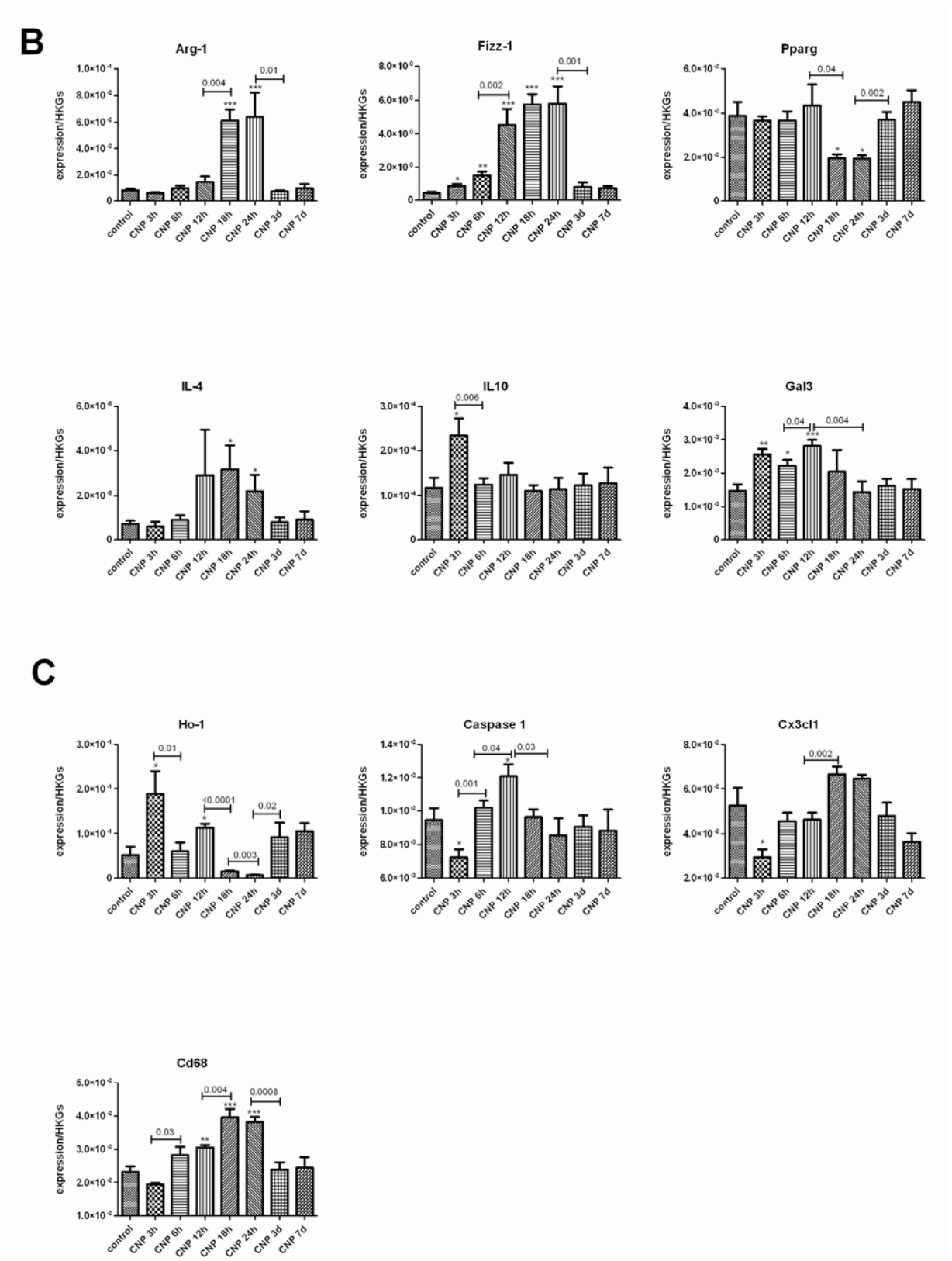
B
Arg-1
Fizz-1
Pparg
IL-4
IL10
Gal3
C
Ho-1
Caspase 1
Cx3cl1
Cd68
expression/HKGs
control
CNP 3h
CNP 6h
CNP 12h
CNP 18h
CNP 24h
CNP 3d
CNP 7d

Figure 5.7: Time course of molecular levels of inflammatory genes determined by qPCR in lung homogenate upon CNP treatment in mice. Proinflammatory genes (A), M2 macrophage marker genes (B) and other genes related inflammatory reponse (C) were measured by qPCR which normalized with the Hprt and Actb housekeeping genes and calculated using the $2^{-\Delta Ct}$ method. The X-axis corresponds to the time after exposure to CNP instillation. The Y-axis corresponds to the expression level measured for the gene of interest. Values are given as mean ± SEM, n=5-10, asterisks represent significance compared to the control group with * $p<0.05$, ** $p<0.01$ and *** $p<0.001$.

5.2.4.3 Profiles of related genes for the transcription factors NFkB and AP-1

To get insight into the regulate mechanism of proinflammatory gene expression, which is known to be regulated to a major extend by NFkB and AP-1 factors, the transcriptional signatures of the lung tissue from these mice have been analysed by qPCR.

Our data showed that (Fig.5.8): upon CNP exposure in mice, (i) as compared to untreated mice, IKBß was significant upregulated during early time (3, 6 and 12 hours) following by drop down to basal levels after 18 hours; (ii) IKBz was reach a peak at 12 hours of CNP exposure over a time up to 7 days; (iii) IKBa, c-Jun, Fos-B and Fra-2 were not affected during all time points. These results described that CNP exposure only induced IKBß and IKBz expression in early time, however, other subunit genes such as IKBa, c-Jun, Fos-B and Fra-2 are not affected by CNP exposure.

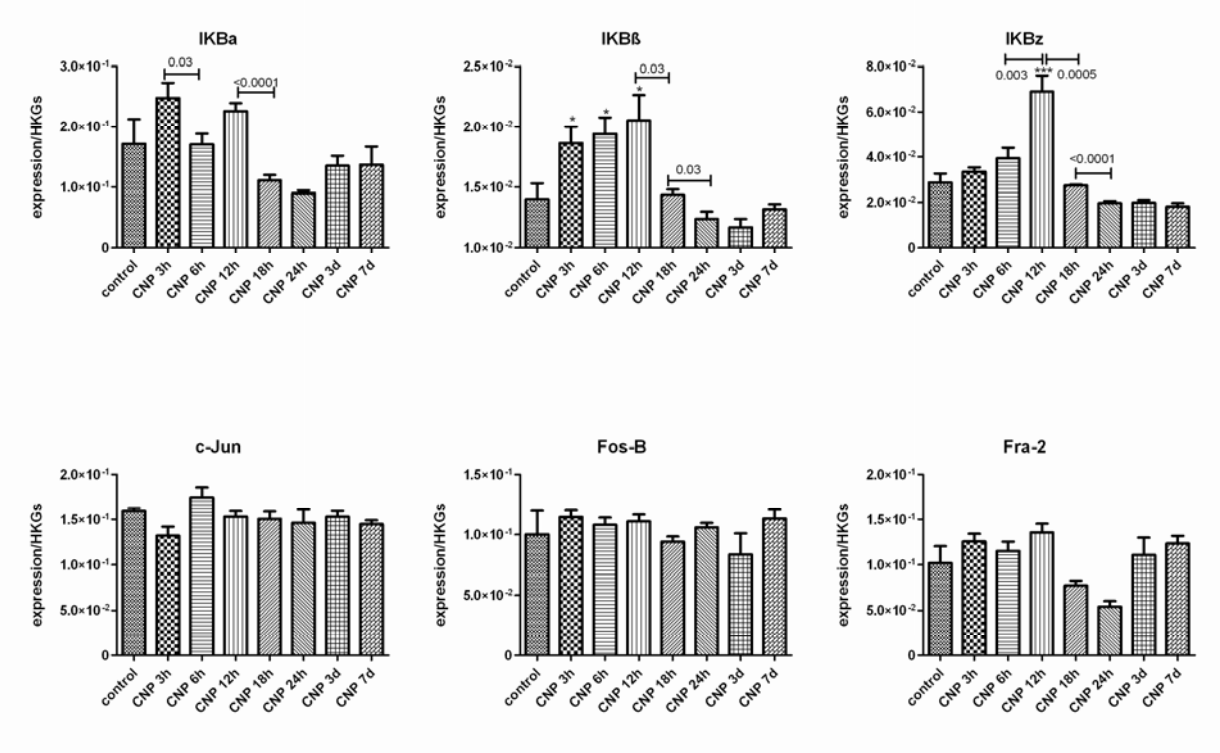

Figure 5.8: NFkB and AP-1 related genes expression levels were determined by qPCR in mouse lung homogenates upon CNP treatment. The X-axis corresponds to the exposure time after CNP instillation. The Y-axis corresponds to the expression level of the target gene. Measurements were normalized using the Hprt and Actb housekeeping genes and calculated by the $2^{-\Delta Ct}$ method. Values are given as mean ± SEM, n=5-10, asterisks represent significance compared to the control group with * p<0.05, **p<0.01 and ***p<0.001.

5.3 Compare the acute inflammatory response to CNP from WT and p50$^{-/-}$ mice

Inhalation of CNP, a main constituent of urban air pollution, is believed to trigger pulmonary or even systemic inflammation via the generation of oxidative stress [171,172]. The redox-sensitive transcription factor NFkB, which controls a majority of inflammatory genes, is thought to play an important role in the onset of pulmonary inflammation [173,174]. In mammalian cells, the NFkB family is composed of five members: NFkB1 (p50, precursor p105), NFkB2 (p52, precursor p100), RelA, RelB and c-Rel, which function as either hetero- or homo-dimmers [175]. It has been reported that Nfkb1 p50 plays an import role in NFkB functions [176-178]; however, whether the NFkB subunit p50 could impact acute pulmonary inflammation and injury 24 hours after CNP treatment is not clear.

5.3.1 Analyse inflammatory cell and total protein accumulation in the airspace of WT and p50$^{-/-}$ mice in response to CNP exposure

Exposure of mice to CNP has previously been shown to result in a dose-dependent lung inflammatory response [136,179-181]. To assess the acute lung inflammatory responses in p50$^{-/-}$ and WT mice after a single dose of intratracheal delivered 20µg CNP, inflammatory cells in the alveolar space as well as total protein levels in the BALFs were investigated after 24 hours, the time point at which the most significant inflammatory changes had been observed in the WT lung (Fig. 5.3). 20µg CNP but not sham (vehicle) exposure caused a significant neutrophilic, acute lung inflammation in WT C57BL/6J mice (Fig.5.9 and Fig.5.10); however, no p50-genotype-related difference could be detected in the recruitment of inflammatory cells into the alveolar space in mutants.

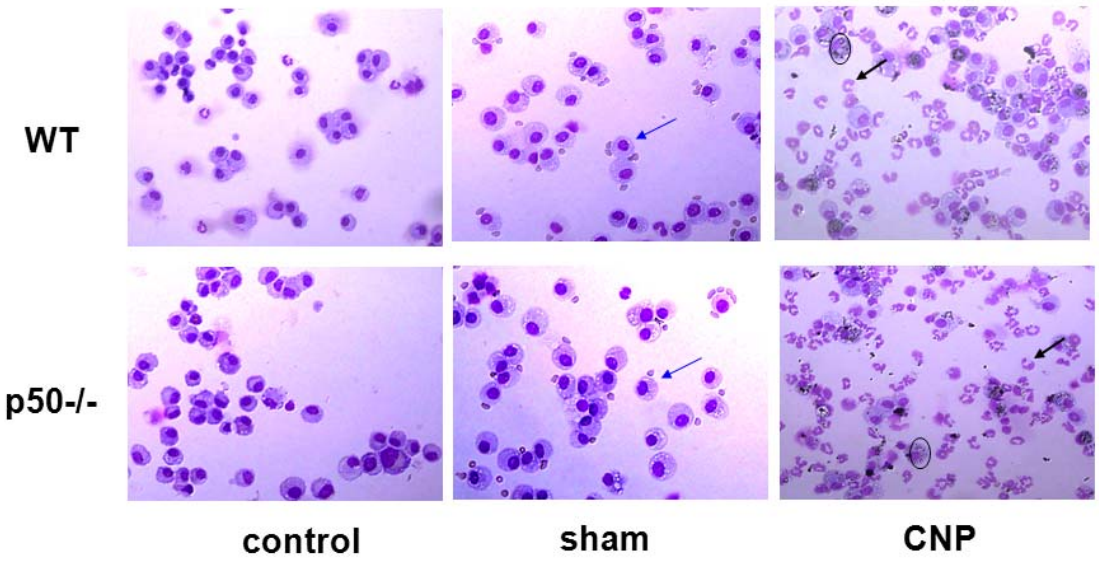

Figure 5.9: CNP exposure induced a significant neutrophilic aseptic acute lung inflammation in mice. Either no or fewer neutrophils (black arrow) were detected in the lungs of untreated and sham-treated mice. In addition, particle-laden macrophages (open circle) were seen in CNP-exposed lungs from all mice, regardless of genotype. These pictures were displayed from cytospins using a microscope at 100X.

5.3.1.1 Total cell numbers

After instillation of 20µg CNP per mouse in both genotypes of mice, the total cell number was reduced in comparison with untreated and H_2O-treated mice after 24 hours. Furthermore, no p50 genotype-related

difference in total cell number could be detected in the alveolar space in the individual treatment groups.

5.3.1.2 Inflammatory cells

Absolute cell number: After treatment with 20µg CNP per mouse, the absolute number of neutrophils in BALF was elevated 47.3-fold in WT mice and 56-fold in $p50^{-/-}$ mice, as compared to untreated genotype-matched mice; in contrast, however, the absolute amount of alveolar macrophage (AM) decreased 1.8-fold in WT mice, and 2-fold in $p50^{-/-}$ mice (Fig.5.10A). Lymphocyte numbers were generally very low and were not changed by the treatment (data not shown).

Percentage of inflammatory cells: After instillation of 20µg CNP per mouse, the percentage of neutrophils of all cells in the BALF was about 34% in WT mice and 43% in $p50^{-/-}$ mice; whereas the percentage of alveolar macrophages dropped to 56% in WT mice and 49% in $p50^{-/-}$ mice (Fig.5.10B). The lymphocyte percentage was below 5% and was not changed by the treatment (data not shown).

5.3.1.3 Protein concentration in BALFs

After 24 hours of treatment with 20µg CNP per mouse, the protein concentration was significant increased in WT mice, but not in $p50^{-/-}$ mice. Furthermore, no p50 genotype difference was detected in H_2O-treated and CNP-treated mice; however, this genotype effect was only significant in $p50^{-/-}$ untreated mice when compared to WT untreated mice (Fig.5.10C).

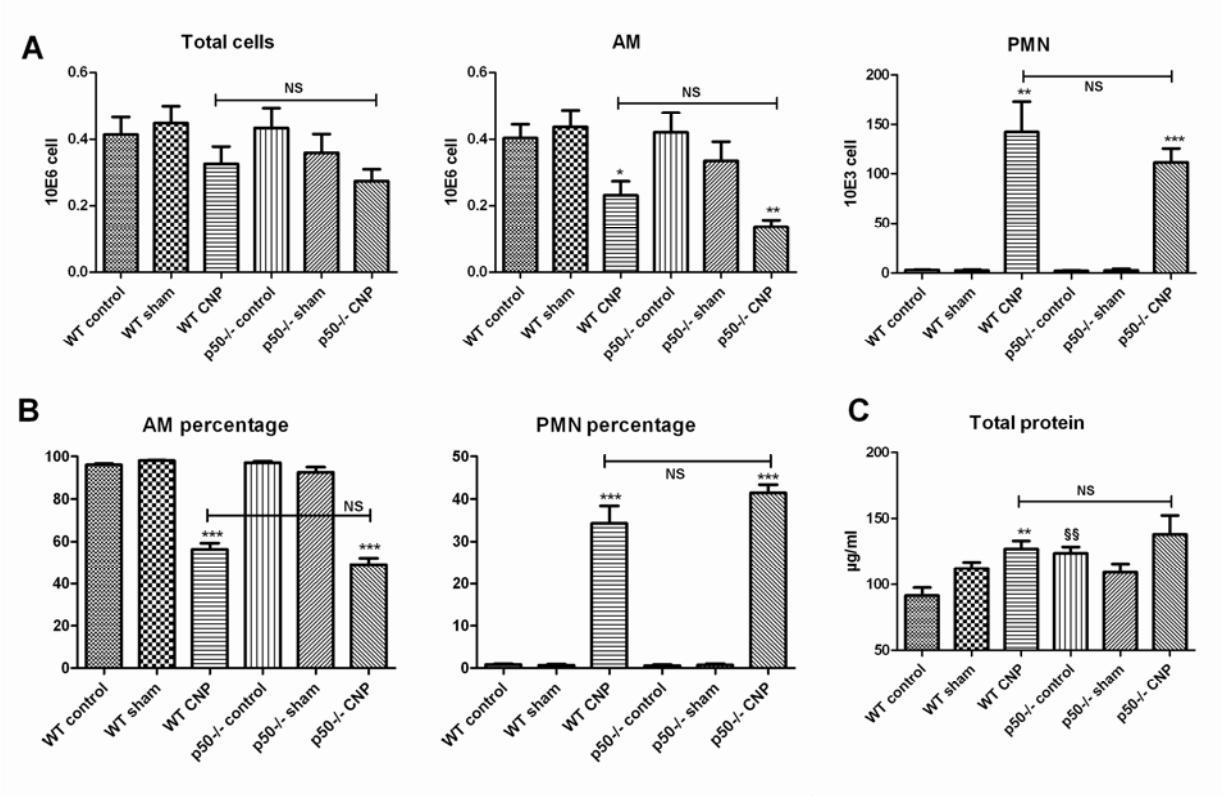

Figure 5.10: CNP induced acute lung inflammatory responses in p50$^{-/-}$ and WT mice. The absolute number of inflammatory cells (A) and the percentage of inflammatory cells (B) in BALFs were counted in cytospins; total protein levels in BALFs were measured by the Braford method. Values are plotted with means ± SEM. Significant differences versus respective untreated genotype mice were calculated using an unpaired t test on data. A value of $P < 0.05$ was considered significant ($P <$ *0.05, ** 0.01, *** 0.001 compared with respective control mice); ($P <$ § 0.05, §§ 0.01, §§§ 0.001) indicate statistical significant changes with respective WT mice. n=7 to 12.

5.3.2 Analyse cytokine response in WT and p50$^{-/-}$ mice by BAL

Recent mouse studies provide strong and direct genetic evidence that the NFkB activation pathway, which was proposed as the molecular hub for the proinflammatory response several years ago, is a crucial mediator in the pathogenesis of pulmonary inflammatory diseases [182-184]. Indeed, several proinflammatory cytokines and chemokines such as TNF-a, IL-1ß, IL-6 and CXCL8, which drive the recruitment of inflammatory cells, are encoded by target genes of the NFkB activation pathway and thus are associated with the initiation and progression of inflammation in humans and mice [173,185,186].

The heterodimer p65/p50, which is the most prominent subunit of NFkB1, is mainly involved in the transactivation of NFkB-dependent proinflammatory gene expression. Unlike p65, the p50 subunit lacks a transactivation domain [187,188]; however, p50-homodimers are known to drive IL-10 expression in macrophages during LPS tolerance [102,189]. The role of the p50 subunit during sterile (aseptic) lung inflammation, as induced by particle exposure, has not yet been described. Therefore, p50 knock-out ($p50^{-/-}$) and wild-type (WT) mice were exposed to 20µg CNP for 24 hours, and their inflammatory responses and related transcription factors were investigated.

CNP-mediated release of proinflammatory mediators recruits macrophages and neutrophils into the lung tissue [142,190-192]. Therefore, in order to compare the pulmonary inflammatory response between $p50^{-/-}$ and WT mice exposed to 20µg CNP, the levels of proinflammatory mediators in the BALFs were measured using commercially-available ELISA kits. To potentially associate the response of particular cell populations in the lungs, we measured TNF-a, IL-6, CCL2, CXCL2 and osteopontin (OPN/SPP1), IL-1ß, as predominatly alveolar macrophage derived cytokines [193-197]. In addition, to determine the inflammatory status of the epithelium in response to CNP instillation we investigated the BAL concentrations of anti-bacterial lipocalin-2 (LCN2/NGAL) and neutrophil-recruiting cytokine CXCL5 [198,199]. Furthermore, other inflammatory mediators, such as IL-1a, CXCL10, CXCL1, IL10 and IFN gamma were also selected to be measured.

CNP exposure significantly ($P < 0.05$) increased the levels of all proinflammatory mediators, including CXCL1, CXCL2, CXCL5, IL-1ß, LCN2, SPP1, CCL2, TNF-a, IL-6 and CXCL10, in both WT mice and $p50^{-/-}$ mice at 24 hours (Table 5.1 and Fig.5.11), but did not alter these levels in H_2O-treated mice compared with untreated mice. Interestingly, however, $p50^{-/-}$ mice showed statistical significantly increased levels of CXCL1, TNF-a, IL-6, SPP1 and CXCL10 in response to 24 hours of CNP exposure compared with WT mice (Fig.5.11), but not of IL-1a, IL-1ß, CCL2, NGAL and MMP9. In contrast, the levels of IL-10, IFN gamma and IL-1ß were not changed in either set of mice in response to CNP exposure and, furthermore, CXCL2 was undetectable in all groups (Table 5.1).

These results indicate that the lungs of $p50^{-/-}$ mice are more susceptible than those of WT mice to specific CNP-induced proinflammatory mediators released in an acute lung inflammation phase.

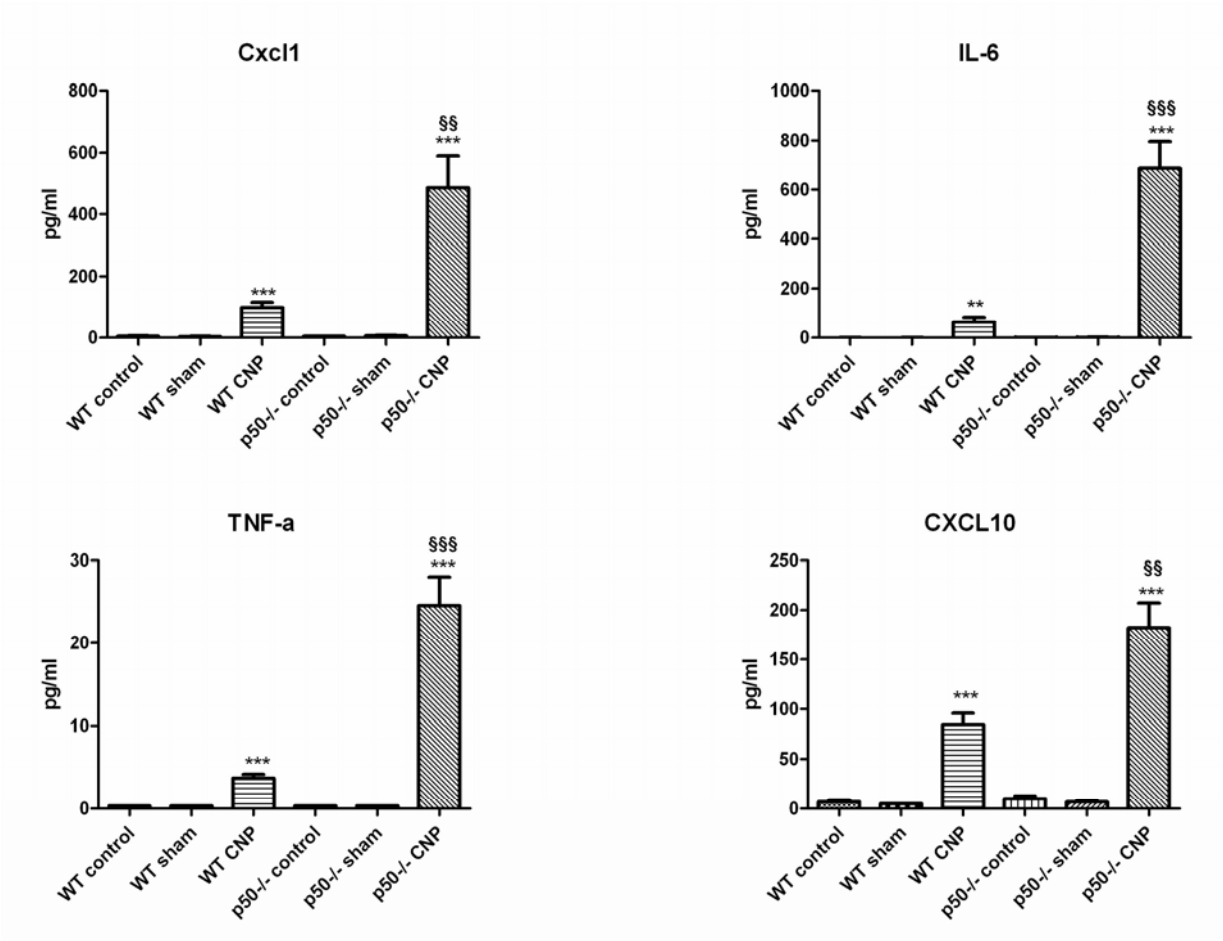

Figure 5.11: Increased levels of proinflammatory mediators in lungs of p50$^{-/-}$ mouse in response to CNP exposure. The level of proinflammatory mediators such as CXCL1, TNF-a, IL-6 and CXCL10 (also known as interferon-inducible protein-10, IP-10) were measured by ELISA in the BALFs of 24 hours untreated, H_2O-treated and CNP-exposed WT and p50$^{-/-}$ mice. (P < *0.05, ** 0.01, *** 0.001) indicates statistically significant changes with WT and p50$^{-/-}$ either untreated or H_2O-treated mice. In addition (P < § 0.05, §§ 0.01, §§§ 0.001) indicates statistically significant changes with respective treated WT mice. Data are shown as means ± SEM (n=7 to 12 per group).

Table 5.1: Summary of the NFkB subunit p50 impact on inflammatory mediators' release into lungs of mice in response to CNP exposure

	WT CNP	$p50^{-/-}$ CNP	$p50^{-/-}$ CNP
	(vs WT sham)	(vs $p50^{-/-}$ sham)	(vs WT CNP)
TNF-a	+++	+++	+++
IL-6	++	+++	+++
CXCL1	+++	+++	++
CXCL10	+++	+++	++
OPN	+	+++	++
IL-1ß	+++	+++	(+)
CCL-2	+++	+++	(+)
LCN2	+++	+++	(+)
MMP9	++	+++	(+)
IL-1a	~	~	(+)
IL-10	(-)	(-)	~
IFN gamma	~	(-)	~
CXCL5	+++	+++	(-)
CXCL2	ND	ND	

Differences in release of inflammatory mediators into lungs between WT and $p50^{-/-}$ mice are shown after 24 hours of intratracheal instillation with a single dose of 20µg CNP per mouse. + $p<0.05$, ++ $p<0.01$ and +++ $p<0.001$ indicate statistically significant differences to H_2O treated mice; (+) indicates increases which are not of statistical significance; (-) indicates decreases which are not of statistical significance; ~ indicates no change; ND indicates not detectable.

5.3.3 Analysis of gene expression in lungs

Furthermore, we isolated total RNA from lung tissue after lavage and measured the expression levels of genes of interest related to inflammatory responses in the lungs of WT and $p50^{-/-}$ mice upon CNP exposure.

5.3.3.1 Inflammatory cytokine gene

Our results indicate that WT mice showed significant upreguration of Cxcl1, Cxcl2, Cxcl5 and Cxcl10 in lung tissue, but not of IL-6 and Tnf-a, after CNP exposure, whereas $p50^{-/-}$ mice showed significantly higher expression levels of these proinflammatory mediator genes except with Tnf-a compared with WT mice at 24 hours after CNP exposure (Fig.5.11 and Table 5.2). These finding are corroborated by the

previous obervations that $p50^{-/-}$ mice showed an augumented proinflammatory response to LPS [200-202], TNF-a [203,204], *E-coli* pneumonia [205] and cigarette smoke [68], which was associated with increased NFkB1-dependent specific proinflammatory gene expression.

In contrast, however, inflammatory cytokine genes such as Gal-3, IL-12ß, Hmgb1, Ppar-γ, Lcn2 and IL-12a were downregulated in $p50^{-/-}$ mice in comparison to WT mice when exposed to a single dose of CNP. Furthermore, the opposite was observed for OPN levels in BALFs, and its mRNA levels were very similar in both genotypes, regardless of treatment (Table 5.2). Therefore, these results confirm that the lungs of $p50^{-/-}$ mice are more prone to produce specific NFkB1-dependent cytokines than WT mice in response to CNP exposure.

5.3.3.2 Other related genes

(i) p50/p50 target genes

p50/p50 homodimers are known to be (i) signal-specific transcriptional repressors of proinflammatory gene expression, selectively inhibiting transiently activated p65/p50 complexes, either by competing with p65 for dimerization [62,63] or by binding to identical NFkB binding sites [64]; and (ii) signal-specific transcriptional activators for antiinflammatory IL-10 [65]. Therefore, p50/p50 homodimer target genes such as IL-10 [189] and Bcl-2 [206] were profiled using the qPCR method (Table 5.2). Due to a shortage of p50/p50 homodimers in $p50^{-/-}$ mice, Bcl-2 was downregulated in $p50^{-/-}$ mice in comparison to WT mice in response to CNP exposure. In contrast, however, the mRNA profile of IL-10 showed an increased in $p50^{-/-}$ mice such that its regulation could be independently controlled by p50/p50 homodimers in CNP-induced acute lung inflammation systems.

(ii) NFkB and AP-1

To identify the impact of p50 deficiency on related gene expression of transcription factors in CNP-induced acute lung inflammation, genes for NFkB (such as IKBa, -ß, -z) and AP-1 (such as Fra1, -2, c-Jun, c-Fos and JunB) were profiled using the qPCR method. For the NFkB gene profiles (Table 5.2), our data showed that (i) CNP exposure did not change IKBz and IKBß gene expression in either genotype of mice, and (ii) CNP exposure decreased IKBa gene expression in $p50^{-/-}$ mice compared to WT mice. In addition, gene profiles for AP-1 showed that (Table 5.2): (i) c-Jun and c-Fos were unchanged; (ii) JunB was increased; and (iii) Fra1 and Fra2 were decreased, in $p50^{-/-}$ mice compared to WT mice.

(iii) Inflammatory proteases

Matrix metalloproteinases (MMPs) have been thought to be involved in the cleavage of cell surface receptors, the release of apoptotic ligands (such as the FAS ligand), and chemokine/cytokine in/activation on the one hand [207] as well as playing a major role on cell behaviors such as cell proliferation, migration (adhesion/dispersion), differentiation, angiogenesis, apoptosis, and host defense on the other hand [208-210]. In our CNP-induced acute lung inflammation system, Mmp7 was increased in both genotypes of mice, and increased more in $p50^{-/-}$ mice (Table 5.2). In contrast, Mmp9 was decreased in both genotypes of mice and decreased more in $p50^{-/-}$ mice (Table 5.2).

(iv) Th17 cell marker

T helper 17 cells (Th17) are a subset of T helper cells producing interleukin 17 (IL-17) that were discovered in 2007 [211]; they are thought to play a role in inflammation and tissue injury in various autoimmune and inflammatory diseases [212]. These inflammatory T cells produce the IL-17 family of cytokines, which mediate inflammation by recruiting innate immune cells and inducing proinflammatory cytokines [213,214]. Expression of Th17 marker genes, including those encoding the orphan nuclear hormone receptor Rorγt, IL-23r and IL-17f [215] in the lungs, were measured by qPCR. Data analysis showed decreased expression of these marker genes in $p50^{-/-}$ mice in comparison to WT mice in response to CNP exposure (Table 5.2). These results indicate that the p50 deficiency could cause a decreased frequency of Th17 cells at the site of inflammation.

(v) Cell adhesion

Cell adhesion molecules (Cams) are proteins located on the cell surface involved with binding with other cells or with the extracellular matrix (ECM) in a process called cell adhesion [216]. Cams are constitutively expressed, but LPS and gram-negative bacteria in the lungs result in increased expression [217,218] and Icam1 is required for maximal neutrophil emigration [219]. CNP exposure was found to increase Icam1 expression in WT and $p50^{-/-}$ mice, but there was no genotype effect. In contrast, however, CNP exposure decreased Vcam1 expression, but also had no genotype effect (Table 5.2). Therefore, the insufficient expression of cell adhesion molecules such as Icam1 and Vcam1 was not responsible for the effect of p50 deficiency on neutrophil recruitment elicited by CNP exposure in the lungs.

(vi) Oxidant stress

Superoxide dismutases (SOD) are a ubiquitous family of enzymes that function to catalyse the dismutation of superoxide anions efficiently [220]. However, in this study, CNP exposure was not found to change expression of related genes such as Sod2 and Sod3 in either genotype of mice (Table 5.2).

(vii) M2 macrophage marker

M1 macrophages produce large amounts of nitric oxide by expressing inducible nitric oxide synthase (iNOS) and tumor necrosis factor (TNF), and are essential for clearing bacterial, viral and fungal infections [221]. Other macrophages, called alternatively-activated macrophages or M2 macrophages, have an important role in the responses to parasite infection, tissue remodeling, angiogenesis and tumour progression [222]. M2 macrophages are characterized by their high expression of arginase-1 (Arg1), chitinase-like Ym1 (Chi3l3), resistin-like alpha (Retnla, also called Fizz-1), mannose receptor (Mrc1 encoding MR, also known as CD206), and chemokines such as CCL17 and CCL22 [223,224]. Therefore, M2 macrophage marker genes such as Arg1, Ccl22, Fizz-1 and IL-4 were measured in the lung by qPCR. Our results (Table 5.2) showed that in reponse to CNP exposure: (i) Arg1 and Fizz-1 were increased in both types of CNP-treated mice as compared to H_2O-treated mice, but only Arg1 (not Fizz-1) was significantly upregulated in $p50^{-/-}$ mice; (ii) IL-4 was not changed in either genotype of mice, regardless of treatment; and (iii) Ccl22 was only increased in WT mice, as compared with H_2O-treated mice, while p50 deficiency decreased its expression.

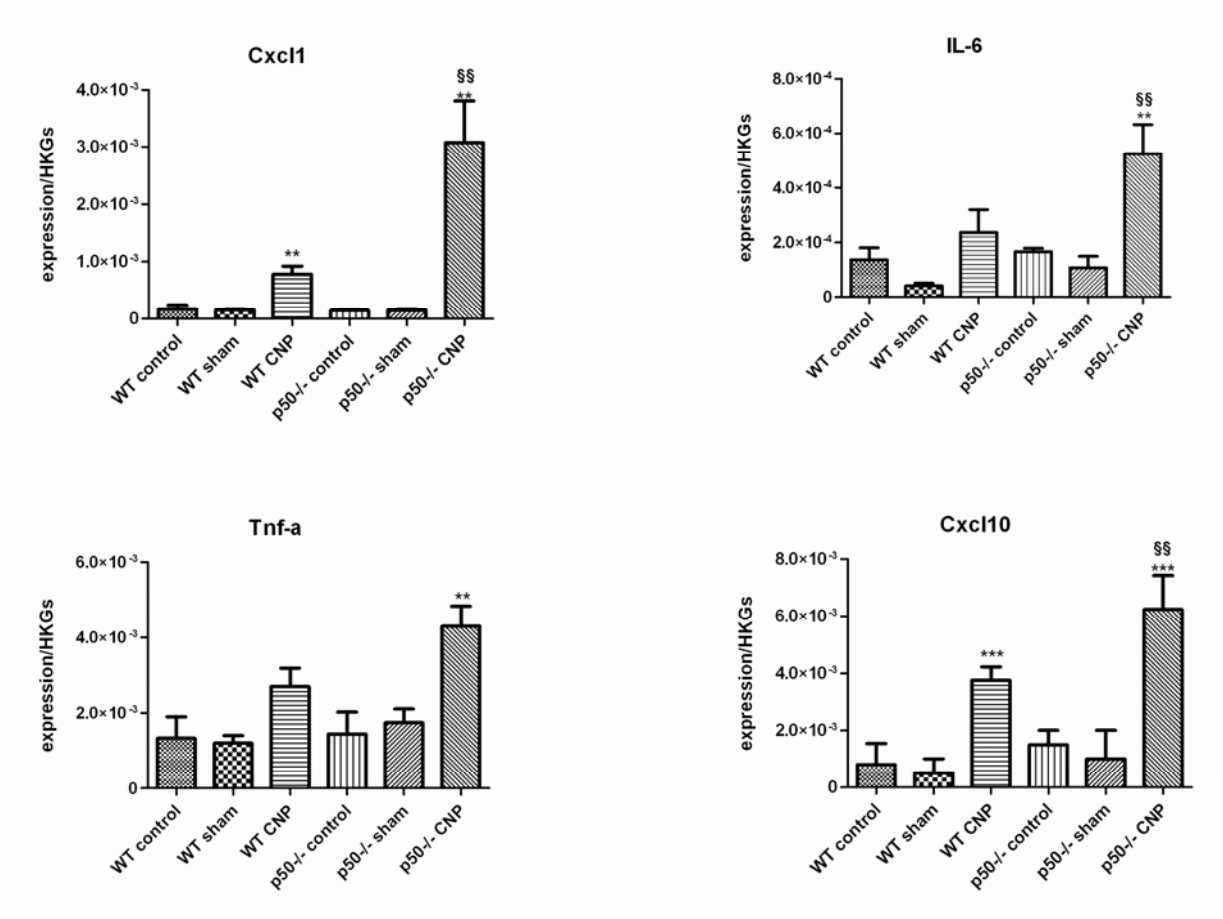

Figure 5.11: Genetic ablation of p50 led to increased proinflammatory mediators expression levels in lung homogenate in response to CNP exposure. Gene of interest (GOI) relative expression levels were detected by qPCR using the $2^{-\Delta Ct}$ method normalized to Actb, Gusb and Rpl13a. (*P < 0.05, ** P < 0.01, *** P < 0.001) indicate statistically significant changes in WT and $p50^{-/-}$ with respect to either untreated or H_2O-treated mice, while (§P < 0.05, §§ P <0.01, §§§ P <0.001) indicates statistically significant changes in CNP-treated WT mice. Data are shown as means ± SEM (n=7 to 12 per group).

Table 5.2: Summary of the gene expression in the lung tissue of WT and $p50^{-/-}$ mice in response to CNP exposure

		WT CNP	$p50^{-/-}$ CNP	$p50^{-/-}$ CNP
Function		(vs WT sham)	(vs $p50^{-/-}$ sham)	(vs WT CNP)
Inflammatory cytokine	Cxcl5	+++	+++	++
	Cxcl10	+++	+++	++

	Cxcl1	++	++	++
	Cxcl2	+	++	++
	IL-6	(+)	++	++
	Tnf-a	(+)	++	(+)
	Opn	~	~	~
	IL-1ß	(-)	(+)	(+)
	Gal-3	(+)	(+)	(-)
	IL-12ß	(+)	(-)	(-)
	Hmgb1	(+)	-	(-)
	Ppar-γ	(-)	-	(-)
	Lcn2	+	+	-
	IL-12a	(-)	(-)	-
p50/p50 target genes	IL-10	(-)	(+)	(+)
	Bcl-2	(-)	(-)	(-)
Inflammatory proteases	Mmp7	(+)	(+)	(+)
	Mmp9	(-)	---	-
Th17 cell marker	Rorγt	~	(-)	-
	IL-23r	(-)	--	(-)
	IL-17f	(+)	~	(-)
NFkB pathway	Ikbz	(-)	~	~
	Ikbß	(-)	(+)	~
	Ikba	~	(+)	(-)
Cell adhesion	Icam1	(+)	(+)	~
	Vcam1	(-)	(-)	~
AP-1 pathway	c-Jun	(-)	~	~
	c-Fos	(-)	(-)	~
	JunB	(-)	(-)	(+)
	Fra1	~	(-)	(-)
	Fra2	~	(-)	(-)
Oxidant stress	Sod2	~	~	~
	Sod3	(-)	~	~
M2 macrophge marker	Arg1	(+)	+	+
	Ccl22	(+)	~	(-)
	Fizz-1	+	+	~
	IL-4	~	~	~

Differences in gene expression in lungs between WT and $p50^{-/-}$ mice are shown after 24 hours of intratracheal instillation for a single dose of 20µg CNP per mouse. + $p<0.05$, ++ $p<0.01$ and +++ $p<0.001$

indicate statistically significant increases relative to sham mice; - $p<0.05$, -- $p<0.01$ and --- $p<0.001$ indicates statistically significant decreases relative to sham mice; (+) indicates increases which are not of statistical significance; (-) indicates decreases which are not of statistical significance; ~ indicates no change.

5.3.4 Analyse transcription factors in lungs of WT and $p50^{-/-}$ mice

Surprisingly, the acute inflammatory response, which in WT mice was characterized by an influx of 100 000-150 000 neutrophilic granulocytes into the alveolar compartment, was not changed in p50-deficient mice. To get an insight into the inflammatory gene expression, which is known to be regulated to a major extend by NFkB1 factors, the transcriptional signatures of the lung tissue from WT and $p50^{-/-}$ mice were analysed.

5.3.4.1 Analyse NFkB1 activation in lungs of WT and $p50^{-/-}$ mice

The transcription of proinflammatory cytokines, chemokines, and MMPs are regulated by the transcription factor NFkB, especially that of p65/p50 heterodimers [225,226]. Therefore the nuclear accumulations of NFkB subunits p65 and p50 in the lung tissue of $p50^{-/-}$ and WT mice upon CNP exposure were analysed using a TransAM® NFkB Family kit. Targeted disruption of p50 was verified in Fig. 5.12 which showed that p50 protein was undetectable in $p50^{-/-}$ mice. Interestingly, our data showed that an increased p65 and p50 nuclear accumulation occurred in WT mice, but not in $p50^{-/-}$ mice, upon CNP exposure; furthermore, this nuclear accumulation was significantly decreased to the basal level in $p50^{-/-}$ mice (Fig.5.12). Therefore the results suggest that $p50^{-/-}$ mice have an increased proinflammatory response to acute CNP exposure, despite the nuclear translocation of p65 and p50 occurring only in WT mice, and not in $p50^{-/-}$ mice.

An increase in NFkB DNA binding is reported to occur in response to combustion-derived nanoparticles, which results in an increased transactivation of proinflammatory genes [142,227-230]. To further investigate the proinflammatory response seen in the lungs of $p50^{-/-}$ mice, NFkB DNA binding activity was determined by the nuclear extraction of mouse lungs in response to CNP exposure by EMSA. In addition, untreated control mice also were analysed. As can be clearly seen in Fig. 5.12, CNP treatment strongly augmented NFkB activation in the lungs of WT mice, but not in $p50^{-/-}$ mice (Fig.5.13). Interestingly, no NFkB activation was detected in p50 untreated and CNP-treated mice. To verify NFkB DNA-binding activity and to determine NFkB subunit composition, a supershift analysis of lung samples from WT mice

was performed using antibodies against the p50 or p65 subunit of NFkB. In WT mice, the NFkB binding activity was composed of p50/p65 heterodimers, which are the major mediators of inflammatory responses, as well as p50/p50 homodimers. These results corroborate the above observations (Fig.5.12) showing no activation of NFkB in $p50^{-/-}$ mice in response to CNP exposure.

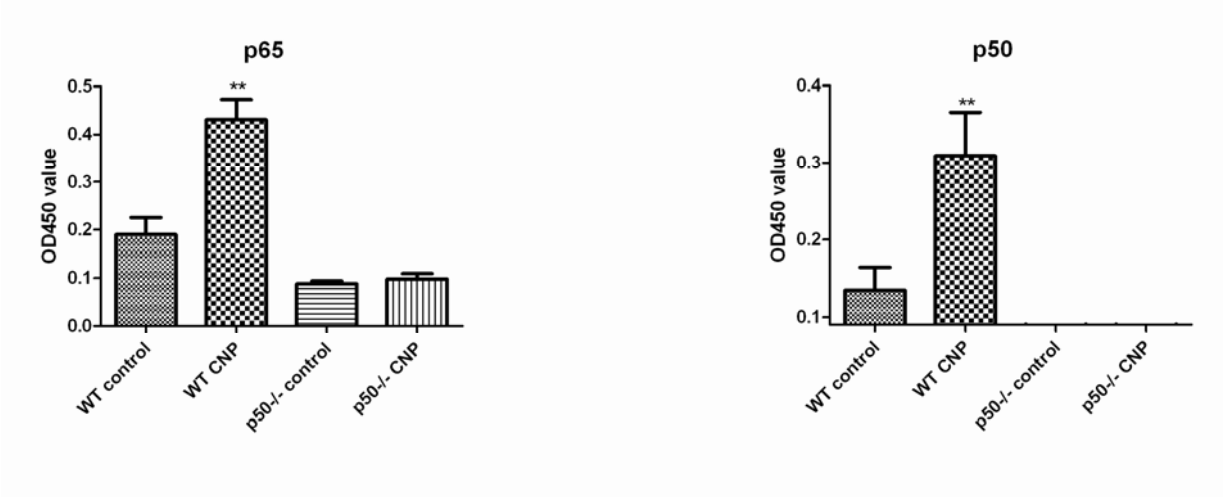

Figure 5.12: CNP-induced nuclear accumulation of both NFkB subunits p50 and RelA (p65) in WT, but not in $p50^{-/-}$ mice. Knockout of NFkB1 (p50) in the lungs of $p50^{-/-}$ mice was confirmed using a TransAM® NFκB Family kit. Data are shown as means ± SEM (*n* = 4–5 per group). ***P* < 0.01 indicates statistical significance compared with untreated mice. § p<0.05, §§§ p< 0.001 indicates statistical significance compared with WT mice.

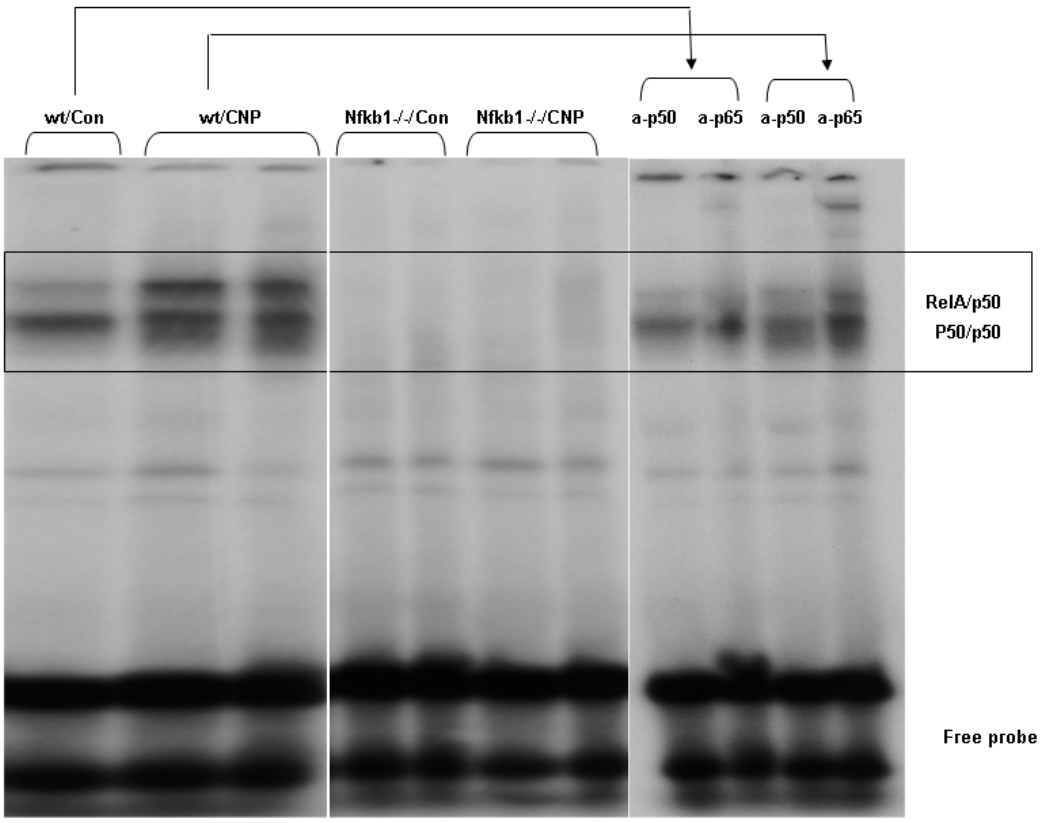

Figure 5.13: Electrophoretic mobility shift assay (EMSA) and supershift EMSA showing nuclear factor-kB activation in mouse lung nuclear extracts 24 hours after carbon nanoparticle exposure. The picture showed that CNP exposure induced a significant nuclear translocation of the NFkB1 subunits p50 and RelA (p65) in WT, but not in $p50^{-/-}$ mice after 24 hours of CNP instillation. One representative untreated WT lung and two samples per group for mice exposed to 20µg CNP per mouse for 24 hours were used. Supershift EMSA was performed for two representative samples from WT mice using antibodies against the two nuclear factor-kB subunits a-p65 and a-p50.

5.3.4.2 Analyse NFkB2 and AP-1 activation in lungs of WT and $p50^{-/-}$ mice

To gain insight into the mechanism of increased proinflammatory mediators in $p50^{-/-}$ mice, we investigated whether NFkB2 and AP-1 could compensatory regulate the CNP-mediated proinflammatory response in $p50^{-/-}$ mice in response to CNP exposure. Therefore, the nuclear accumulation of NFkB2 and AP-1-related protein in untreated and CNP-treated mice were analysed using a TransAM® NFkB Family

kit and a TransAM® AP-1 Family kit, respectively. Our results showed that CNP exposure did not significantly change the nuclear accumulation of p52 and Rel B in $p50^{-/-}$ mice, whereas it did significantly increase the levels of NFkB subunit p52 and Rel B in WT mice (Fig.5.14A). In addition, the data for AP-1 related proteins showed CNP exposure did not result in AP-1 activation in $p50^{-/-}$ and WT mice (Fig.5.14B). These results demonstrate that compensatory activation of neither NFkB2 (p52, RelB) nor AP-1 (c-Jun, Jun-D, c-Fos, FosB) pathways could be identified in $p50^{-/-}$ mice in response to CNP exposure.

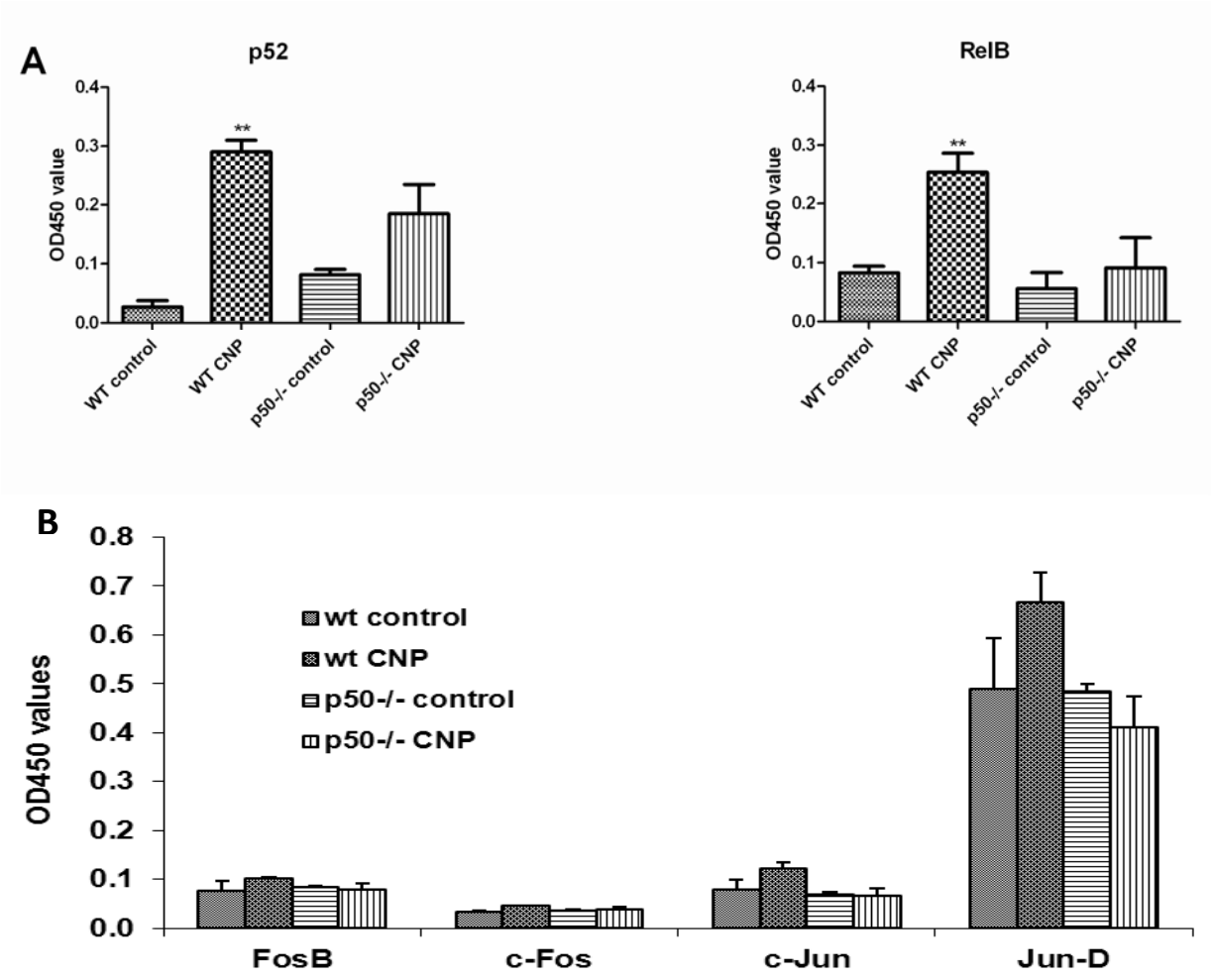

Figure 5.14: Compensatory activation of neither NFkB2 (p52, RelB) nor AP-1 (c-Jun, Jun-D, c-Fos, FosB) pathway was identified in $p50^{-/-}$ mice. Data are shown as means ± SEM (*n* = 4–5 per group). $^{**}P < 0.01$ indicates significance compared to untreated mice.

5.4 Roles of NFkB1 subunit p50 in alveolar macrophage polarization

Macrophages are the first line of defense against pathogens, and the mode of their activation will determine the success or failure of the host's response to pathogen aggression [105,106]. Meanwhile, plasticity is a hallmark of mononuclear phagocytes, and in response to environmental signals these cells undergo different forms of polarized activation, the extremes of which are called classic or M1 and alternative or M2 [102]. M1 macrophages (classically-activated macrophages) are induced by interferon-gamma or microbial products such as lipopolysaccharide (LPS) or tumor necrosis factor α (TNF-α), and are mediated by several signal transduction pathways involving signal transducer and activator of transcription (STAT), nuclear factor kappa-light-chain-enhancer of activated B cells (NFkB), and mitogen-activated protein kinases (MAPK) [118,231,232]. In contrast, M2 macrophages (alternatively-activated macrophages) are induced by Th2- or antiinflammatory cytokines and growth factors, including IL-4, IL-10 and transforming growth factor-β [118,232]. M1 macrophages typically take part in the initial immune response to invading microorganisms and promote the subsequent inflammatory immune responses by increasing antigen presentation capacity and inducing Th1 immunity through the production of cytokines, whereas M2 macrophages are induced during the resolution phase of inflammation and are involved in debris scavenging, tissue remodeling, and promotion of Th2 immunity [231,233,234].

Alveolar macrophages, along with mast cells, comprise the first line of immune defense in the lung, establishing an immune response upon encountering enviromental particles, such as combustion-derived nanoparticles [235,236]. To our knowledge, the molecular basis of alveolar macrophage polarization has not yet been fully elucidated. NFkB is a vital regulating factor in inflammation and resolution, and its activation is subject to multiple levels of regulation, including inhibitory, which finely tune macrophage functions [106,232]. Here we identified the roles of NFkB subunit p50 in the polarization of alveolar macrophages (AMs) *in vitro*.

5.4.1 Establishment of alveolar macrophage polarization model *in vitro*

To establish the macrophage polarization model *in vitro,* alveolar macrophages obtained from WT and $P50^{-/-}$ mice were treated with 4 hours of either IL-4 (20ng/ml) for M2 macrophages polarization or with LPS (1μg/ml) plus IFN gamma (20ng/ml) for M1 macrophage polarization. Total RNA was then extracted, and the expression of representative M1 and M2 genes was evaluated by qPCR (Fig.5.15 and Fig.5.16). In agreement with previous reports [237,238], expression of the prototypic M1 associated genes iNOS,

Cxcl1, Cxcl2, Cxcl5, IL-6 and IL-1ß were induced more in LPS+ IFN gamma-treated AMs, whereas its expression was drastically reduced in IL-4 treated AMs (Fig.5.16). In contrast, the mRNA level of M2-associated genes, such as Arg1, Fizz-1 and Ym1, were consistently higher in IL-4 treated AMs compared to the LPS+IFN gamma treated group (Fig.5.15). These results suggest that IL-4 treated primary alveolar macrophages cells acquire an alternative-activation programme that has a high expression of M2-associated genes; whereas LPS+IFN gamma-treated AMs acquire a classical-activation programme that has a high expression of M1-associated genes.

5.4.2 Roles of subunit p50 in alveolar macrophages polarization

5.4.2.1 Genetic ablation of p50 promotes M2 skewed inflammatory response of AMs

In the first step, the M2-associated gene expression profile expressed by IL-4 or with LPS +IFN gamma treated AMs (Fig.5.15) were characterized. The results showed that (i) M2-associated genes (Arg1, Fizz-1 and Ym1) were highly expressed in untreated and LPS+IFN gamma treated $p50^{-/-}$ AMs in comparison to WT AMs; (ii) targeted disruption of NFkB subunit p50 promotes M2-associated gene expression in IL-4-induced responses (except with Ym1). These results indicate that p50 is a negative regulator of M2-associated gene expression in AMs.

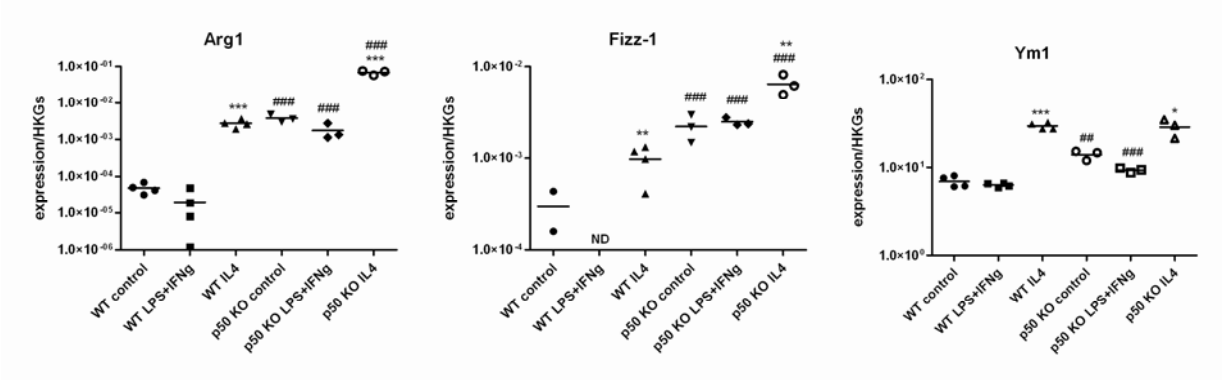

Figure 5.15: M2-associated markers were upregulated in $p50^{-/-}$ AMs. Alveolar macrophages from WT and $p50^{-/-}$ mice were either untreated (control), or with IL-4 (20ng/ml) or with LPS (1µg/ml) +IFN gamma (20ng/ml) challenge for 4 hours. Representative M2-associated genes were analysed by qPCR. Results were normalized to Actb and Hprt levels and calculated using the $2^{-\Delta Ct}$ method. Data are representative of two independent experiments, and the values shown are mean ± SEM from triplicate values. * p<0.05, ***P* < 0.01, ****P* < 0.001 compared to respective control group as well as # p<0.05, ##*P* < 0.01, ###*P* < 0.001 as compared to respective WT AMs. n=3-4. ND indicates no detectable.

5.4.2.2 Genetic ablation of p50 downregulated M1 skewed inflammatory response in AMs

To explore the role of p50 in the expression of an M1 phenotype of alveolar macrophages treated with either non-treatment, or IL-4 or LPS+IFN gamma, representative M1 cytokine genes were analysed by qPCR (Fig.5.16). IL-4 treatment failed to develop M1-like macrophages, assessed by the inducible expression of iNOS, Cxcl5, IL1ß, IL-6, Cxcl1 and Cxcl2; in contrast, LPS+IFN gamma treatment significantly upregulated the expression of these M1-associated genes in AMs. In addition, the absence of p50 significantly downregulated the LPS+IFN gamma induction of M1 associated genes in AMs. Thus, p50 is a positive regulator of M1-associated gene expression in AMs.

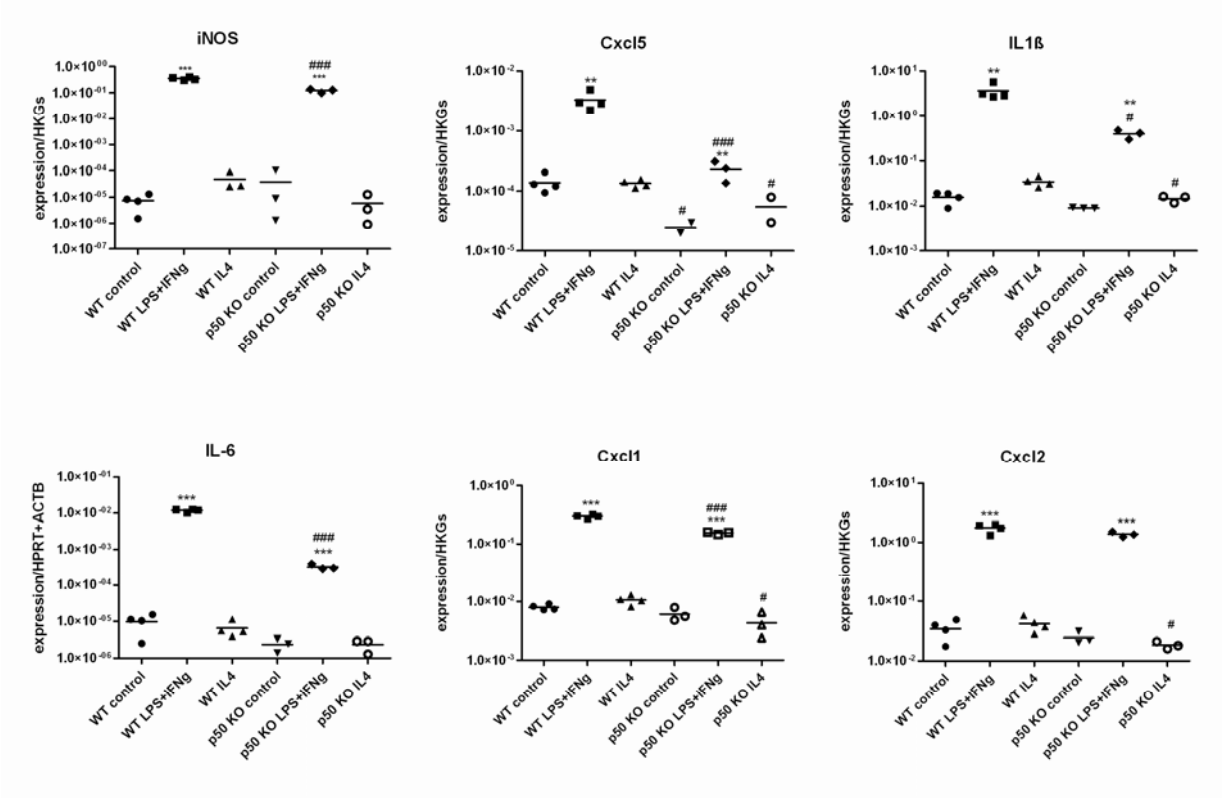

Figure 5.16: M1-associated markers were downregulated in p50$^{-/-}$ AMs. Alveolar macrophages from WT and p50$^{-/-}$ mice were treated with either non-treatment (control), with IL-4 (20ng/ml), or with LPS (1µg/ml) +IFN gamma (20ng/ml) challenge. Total RNA was then extracted and the expression of representative M1 genes was evaluated by qPCR. Results were normalized to Actb and Hprt levels and calculated using the $2^{-\Delta Ct}$ method. Data are representative of two independent experiments; the values shown are mean ± SEM from triplicate values. * p<0.05, ***P* < 0.01, ****P* < 0.001 compared to respective control group as well as # p<0.05, ##*P* < 0.01, ###*P* < 0.001 as compared to WT AMs. n=3-4.

5.4.2.3 NFkB related genes were downregulated, but Ppar-γ was upregulated in p50$^{-/-}$ M1 skewed inflammatory AMs

To seek the causes of downregulation of M1-associated genes and upregualtion of M2-associated genes in p50$^{-/-}$ AMs, the expression levels of IKB proteins as direct targets of the transcription factor NFkB and PPAR-γ as an important factor for M2 polarization were assessed by qPCR (Fig.5.17). The results showed that: (i) IL-4 did not affect IKBa and IKBß gene expression in WT mice, while LPS+IFN gamma significantly upregulated their expression in comparsion to untreated control AMs; (ii) the absence of p50 caused reduced IKBa, IKBß and IKBz gene expression in response to IL-4 and LPS+IFN gamma treatment; (iii) in contrast, however, in p50$^{-/-}$ AMs, Ppar-γ expression was significantly elevated in non-treated and LPS+IFN gamma-treated cells, as compared to WT AMs. These results indicate that increased expression of NFkB related genes promotes M1-skewed inflammation in AMs, while decreased expression of NFkB related genes could promote M2-skewed inflammation.

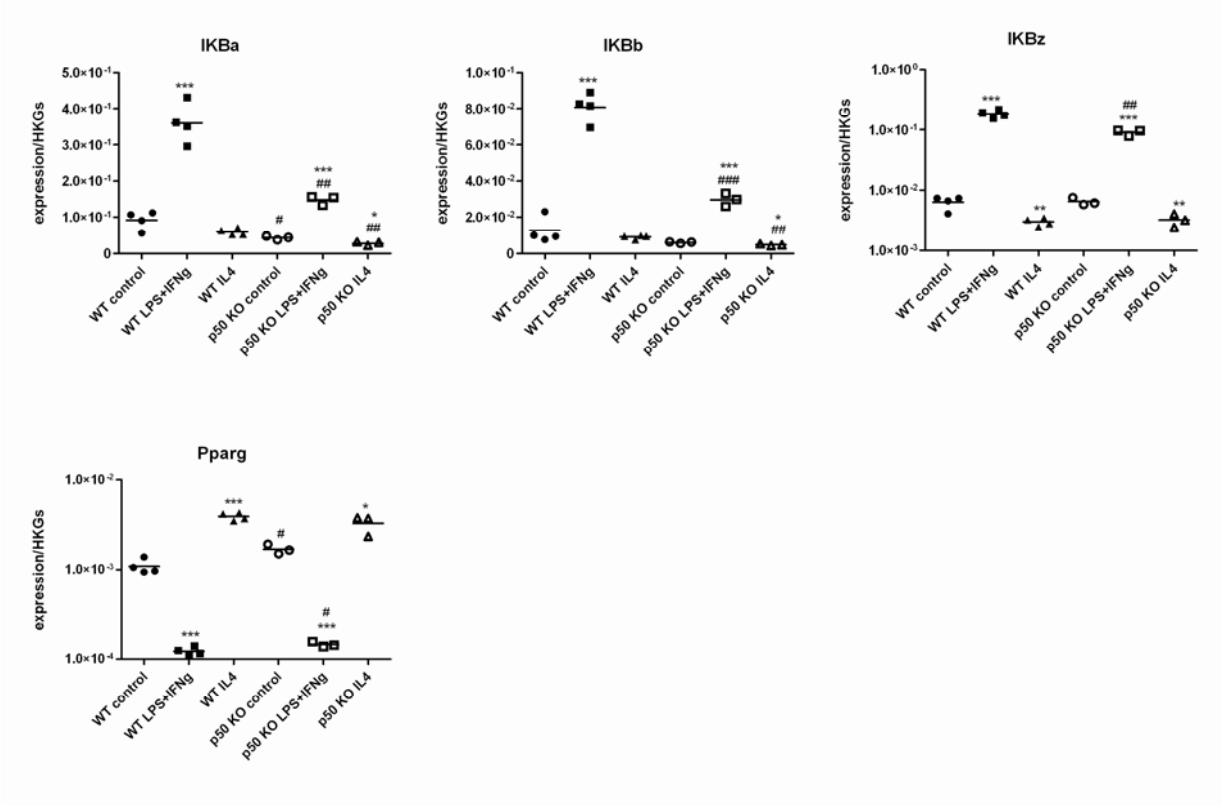

Figure 5.17: NFkB-related genes were downregulated, but Ppar-γ was upregulated in p50$^{-/-}$ AMs. Results were normalized to Actb and Hprt levels and calculated using the $2^{-\Delta Ct}$ method. Data are

representative of two independent experiments; the values shown are the mean ± SEM from triplicate values. * p<0.05, ***P* < 0.01, ****P* < 0.001 compared to the control group as well as # p<0.05, ##*P* < 0.01, ###*P* < 0.001 compared to WT AMs. n=3-4.

5.5 Impact of alveolar macrophages in particle-induced acute lung inflammation

To further investigate the role of alveolar macrophages in particle-induced aseptic acute lung inflammation in mice, the lavage macrophage obtained from mice treated for either 6 hours or 12 hours with CNP (the time-points with the highest levels of proinflammatory response, Fig.5.4), or for 12 hours with H_2O (sham), or left untreated (control) were characterized by qPCR. To isolate the alveolar macrophage, fresh BAL cells were incubated in a 48 well cell culture plate for 3 hours to allow adhesion and non-adherent cells were subsequently removed by two washes with 1X PBS. Adhered cells (alveolar macrophages) were isolated for total RNA preparation and macrophage-associated genes were analysed by qPCR.

Figs. 5.6 and 5.7A show that for proinflammatory marker genes of macrophages, such as iNOS, Tnf-a, IL-1ß and Cxcl2, transcripition levels in lung tissue reached a peak at 12 hours of CNP exposure. In contrast, the expression levels of these genes in alveolar macrophage obtained from mice with same treatment for 6 hours and 12 hours did not increase in comparison to the control and sham groups (Fig.5.18A).

Interestingly, in agreement with previous data (Fig.5.7B), M2 macrophage-associated genes such as Arg-1 and Fizz-1 were upregulated in mice lung tissue treated with 6 hours and 12 hours of CNP exposure in comparison to untreated mice. These genes in the alveolar macrophages obtained from mice under the same experimental circumstances were upregulated compared to untreated mice, but there was no difference in their levels compared to H_2O-treated mice (Fig.5.18B).

Furthermore, Fig.5.8 indicates that CNP-exposure-induced NFkB-related genes such as IKBß, IKBz and IKBa reach a peak in mice lung tissue at 12 hours post instillation. In contrast, however, there were no signs of CNP-exposure-induced NFkB or Ppar-γ activation in alveolar macrophages (Fig.5.18C).

In conclusion, the alveolar macrophage is not the cell responsible for producing proinflammatory mediators in the lung during particle-induced aseptic acute lung infllammation in mice.

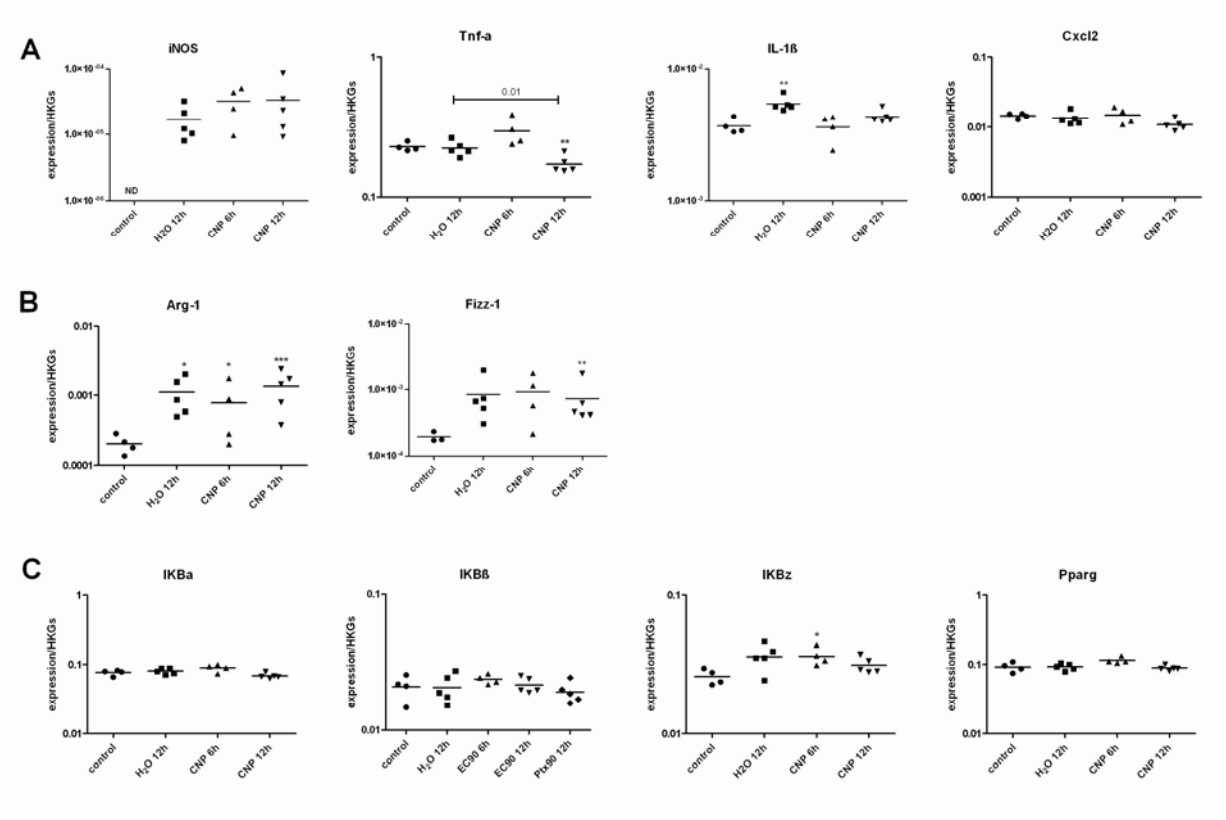

Figure 5.18: Alveolar macrophage is not the proinflammatory mediator producing cells during particle-induced aseptic acute lung inflammation in mice. Results were normalized to Actb and Hprt levels and calculated using the $2^{-\Delta Ct}$ method. Data are representative of two independent experiments; the values shown are mean ± SEM from triplicate values. Asterisks represent significance compared to the control group with * $p<0.05$, ** $P < 0.01$, *** $P < 0.001$. n=4-5.

6. Discussion

6.1 Intratracheal instillation of carbon nanoparticles (CNP) at a single dose of 20µg per mouse causes acute lung inflammation in mice

The increasing use of engineered nanoparticles (NP) in industrial and household applications as well as the emission of combustion derived nanoparticles will unavoidable lead to an rising release of such materials into the environment [84-87]. In contrast to a great number of studies investigating health effects of combustion derived particles, until now very little is known about the toxicity of man-made engineered nanoparticles for human health as well as the environment in general. There are only few effective techniques available that can directly measure the toxicity of these nanoparticles for our ecosystem [87,239]. In this context, the time course and molecular basis of the acute inflammatory reactions was investigated in the lungs of mice in response to a single dose of 20µg carbon nanoparticles (CNP) exposure at a single dose of 20µg per mouse. Particular emphasis was put on the role of the NFkB pathway in this model of aseptic lung inflammation, as this complex is known to be the key transcription factor for inflammatory gene expression in general.

Acute pulmonary inflammation has previously been described in mice as the major response to carbonaceous nanomaterial exposure by routes of inhalation and instillation [240,241]. The dose response for the inflammatory effect of the particles has been shown to be mainly determined by particle surface area, rather than other characteristics such as organic content, or primary particle size [136]. In line with this 20µg CNP induced an acute neutrophilic lung inflammation with highest inflammatory cells numbers generated in the airspace of the lungs at 24 hours post-instillation (Fig.5.3). This response was associated with increased NFkB activity (Fig.5.12, Fig.5.13, Fig.5.14 and Fig.5.8), as well as NFkB dependent proinflammatory cytokine gene expression (Fig.5.6 and Fig.5.7) and protein release (Fig.5.4 and Fig.5.5). At this 24 hour time point no AP-1 activation could be identified in the lungs (Fig.5.8), unless AP-1 is also known to be an important transcription factor associated with proinflammatory gene expression. From 3 to 7 days after instillation the inflammatory responses declined back to the basal levels and neutrophil cell numbers, the major cellular readout for inflammation, where virtually completely resolved by day 7.

During the acute inflammation response of the lungs to CNP exposure as discussed above, 12 hours of post-instillation, the initial raised total number of by bronchoalveolar lavage from the lungs retained cells drop down to the basal levels. This decrease was due to a significant reduction of the absolute number of alveolar macrophages (Fig.5.3), whereas the neutrophil number at the 12 hour

time point was significant increased compared to mice of the untreated control group and those prior to 12 hour exposure (Fig.5.3). Alveolar macrophages stand as the guardian of the alveolar–blood interface and represent the front line of cellular defense against respiratory pathogens. Alveolar macrophages are the primary phagocytes of the innate immune system of the lung, clearing the air spaces from infectious, toxic, or allergenic particles that have evaded the mechanical defenses of the respiratory tract such as the nasal passages, the glottis, and the mucociliary escalator system [120,242-245]. The decrease in the absolute number of alveolar macrophage s in the lung could indicate cytotoxicity of CNP to the scavenger cells, as indicated by increased LDH levels (an indicator of cell membrane injury and cell necrosis) (Fig.5.2). Also many proinflammatory mediator levels reach a peak (Fig.5.4 and Fig.5.5) at 12 hours of post-instillation. High levels of proinflammatory cytokines in the alveolar space of the lungs would subsequently attract more inflammatory cells such as macrophages and neutrophiles from lung tissue and blood to this site and indeed until 24 hours after instillation BAL cell numbers reach their highest levels. With the significant increase of alveolar macrophages in lungs tater than 12 hours of post-instillation, the inflammatory response alleviates, which fits to the concept that macrophages contribute to the resolution of the CNP induced aseptic acute lung inflammation, with significant reduces neutrophil counts at 3 days of post-instillation. We might therefore classify the time points prior to 24 hours as the acute response phase and that tater than 24h (around day 3 day) the resolution phase. Thus our study is well in line with many previous observations using the same challenge design (same stimulus and dose), showing most of inflammatory neutrophil cleared from the BAL fluid at time points around 3 days after challenge [134,197,246,247].

The transcription factors, NFkB and AP-1, a known to play a pivotal role in regulating genes involved in various physiological processes, including inflammatoy response, host defense, cell apoptosis and developmental processes [248-254]. CNP exposure increased during the acute activation phase NFkB–pathway genes in lungs, which was associated with upregulated expression of IKBß and IKBz (Fig.5.8). At this time point however, there was no sign for a CNP induced AP-1 pathway activation (Fig.5.8).

In conclusion, this part of the work classifies the response to a single dose of CNP exposure, (i) as an aseptic acute lung inflammation, which associated infiltration of inflammatory cells, including neutrophils and macrophages in the alveolar compartment of the mouse; (ii) with an influx of inflammatory cells such as neutrophils and macrophages into the airspace peaking 24 hours after CNP exposure; (iii) protein and transcription levels of proinflammatory cytokines significantly

increased 12 hours after CNP exposure; and (iv) CNP exposure only upregulating members of the NFkB, but not of the AP-1 pathway at the acute lung inflammation phase. To the best of our knowledge, this is the first study that describes the time course of carbon nanoparticle induced aseptic acute lung inflammation in the lungs of mice at the molecular level.

6.2 CNP triggered inflammatory cell influx into the lungs is not altered in $p50^{-/-}$ mice

CNP-induced proinflammatory response, especially the release of proinflammatory cytokines and chemokines, is mediated by recruiting inflammatory cells such as macrophages, neutrophils and lymphocytes into the lung spaces [255-258]. Sufficient related experimental evidence actually indicates that NFkB should be involved in the particle-mediated proinflammatory response in our CNP induced aseptic acute lung inflammation model [228,259-261]. However, very little is known about the role of the NFkB subunit p50, the main heterodimerization partner of p65, as transcriptional regulator during aseptic, particle-induced acute lung inflammation, as studied here with carbon nanoparticles. p50 knockout ($p50^{-/-}$) mice were used to shed some light on the role of p50 in aseptic lung inflammation in response to acute CNP exposure. Therefore, we exposed $p50^{-/-}$ and WT mice to CNP at a single dose of 20µg per mouse for 24 hours and investigated the inflammatory cell count in BAL fluid. No differences in the absolute number of macrophages, neutrophils and lymphocytes in BALF could be detected between $p50^{-/-}$ and WT mice when exposed to H_2O and clean air. In response to CNP exposure however, mice of both genotypes showed comparable decreases in alveolar macrophage numbers as well as significant increased neutrophil recruitment in (Fig.5.10). These findings are well in concert with previous *in vivo* observations showing that upon exposure to carbon nanotubes [262,263], and nanoparticles [247,264,265], which describe an association neutrophile recruitment and decreased alveolar macrophages.

Previous studies described that p50 deficiency increases BAL cytokine levels and recruitment of inflammatory cells to the alveolar air space in response to *E. coli* instillation [201,205] and cigarette smoke inhalation (CS) [68], suggesting that p50 limits proinflammatory gene expression and dangerous exacerbations of lung injury. LPS preparations from *E. coli* containing both LPS, which activates Toll-like receptor (TLR) 4, and bacterial products (such as heat-killed *E.coli*) that signal through TLR2 induced neutrophil recruitment that was decreased by p50 deficiency, TLR2 and TLR4 together p50 depentent pathways [200,266]. In our study, targeted disruption of p50 did not alter the numbers of inflammatory cells such as macrophages, neutrophils and lymphocytes emigrated into the airspace of the lungs upon CNP exposure (Fig.5.9 and Fig.5.10). Combustion derived nanoparticles, such as carbon nanaoparticle we used in this study, may differ from semipurified LPS

preparations in forming complexes with solube host proteins, such as complement, natural antibody, and surfactant proteins, which may alter host signaling and molecular pathways used the inflammatory cells emigration. Furthermore, there was no p50 genotype effect of transciptional levels of adhesion molecules Vcam-1 and Icam-1, which control the adhesion and transmigration of leukocytes [41,60], in mouse lungs in reponse to CNP exposure (Table 5.2). Therefore, our data suggests that bacterial toxins and products such as combustion derived nanoparticles, in contrast to LPS, trigger inflammatory cell recruitment not requiring p50.

6.3 Deletion of NFkB subunit p50 augments lung cytokine expression upon particle induced acute lung inflammation

Although targeted disruption of p50 did not alter inflammatory cells numbers in the lungs of mice upon CNP exposure, increased BAL levels of CNP induced proinflammatory mediators such as CXCL1, TNF-a, IL-6, CXCL10 and OPN were associated with p50-deficiency. Similar was observed for transcriptional levels of several proinflammatory genes such as Cxcl1, Cxcl2, Cxcl5 and IL-6 (Fig.5.11 and Table 5.1). Deficiency of p50 however did not amplify the protein leak into the lungs, indicating no increased genotype dependent lung injury upon CNP exposure (Fig 5.10). Similarly, p50 deficiency increases the expression of kB-regulated genes induced by *E.coli* pneumonia [200,205], IL-1 [267] and CS [68], which was associated with an augmented proinflammatory reponse.

NFkB is usually described as a dimer composed of the p50 and p65 subunits and is normally sequestered in the cytoplasm in complex with the specific inhibitors, classically IκBα or IκBβ [206]. The NFkB/Rel family members RelA, RelB and c-Rel all have a C-terminal transactivation domain. In contrast to these NFkB/Rel family members, p50 is considered to be transcriptionally mostly inactive because of the absence of a transactivation domain (TAD) in p50. Therefore p50 usually needs to form a heterodimers with TAD possessing factors to be transcriptionally active [268-270]. The exact molecular mechanisms determining p50 functions like a doule-edged sword which is either a repressor or an activator of gene expression remain to be determined, but may pathways involve intracellular signaling pathways which alter the respective nuclear proteins associating with p50 in dependence on the environmental circumstances [200]. For example, the p50/p50 homodimer is reported to inhibit NFkB dependent transcription of many proinflammatory genes by competing with other transcriptionally active NFkB dimers, such as p65/p50 for binding to the NFkB motif. Increased nuclear p50/50 levels result in increase of antiinflammatory and antiapoptotic genes [271-273], but p65/p50 heterodimer can recruit coactivators and mediate NFkB dependent gene expression [62,274-276]. Furthermore, under normal conditions, a small amount of p50 is present in the

nucleus, and binding of p50 to the proinflammatory gene promotor is reported to decrease gene expression [277,278]. NFkB subunit p50 may recruit different complexes to different promotors regions for different purposes during innate and adapted immune responses in the lungs, such as p50 is required for recruitment of the transcriptional repressor histone deacetylase (HDAC)-1 to kB sites in the Mmp-13 promoter [279].

The precise mechanism why targeted disruption of p50 caused increased cytokine levels upon CNP treatment but not altered inflammatory cell recruitment remains to be elucidated. We have analysed the expression over 20 genes related with the inflammatory responses at the mRNA level (Table 5.2), and most of them have been either increased or unchanged by p50 deficiency during CNP induced aseptic acute pulmonary inflammation. Actually none of these genes showed reduced levels in p50 mice. Previous studies observed that no significant decrease in gene expression during innate immune responses in $p50^{-/-}$ mice, which p50 clearly limits the expression of many kB-regulated genes during innate immune responses in the lungs [68,280,281]. Therefore, we favor the interpretation that p50 did not alter the inflammatory cells recruitment in the lungs by decreasing gene expression which brakes the inflammatory cells recruitment in the lungs upon CNP exposure.

6.4 No compensatory activation of either NFkB or AP-1 pathways in $p50^{-/-}$ mice in response to CNP exposure

Intratracheal infection of mice with *E. coli* has been associated with nuclear accumulation of p65/p50 heterodimers in the lungs within 3 hours and is followed by induction of p50/p50 homodimers post infection after 6 hours, which indicates a role for p50/p50 homodimers in the resolution of lung inflammation [200,205]. Interestingly, in our study, 24 hours after CNP exposure, we detected a significant nuclear accumulation of both p65 and p50 in WT mice, but no in $p50^{-/-}$ mice (Fig.5.12 and Fig.5.13). Therefore our data suggests that the CNP related activation and nuclear translocation of p65 requires p50 interaction and accordingly is only observed in CNP treated lungs of WT mice but not $p50^{-/-}$ mice.

The lack of nuclear p65 however opens the question of the respective transcription factor, substituting p65/p50 in the absence of p50. In this case it should be noted, that $p50^{-/-}$ mice showed augmentation of BAL cytokine levels and cytokine gene expression, arguing for enhanced inflammatory activation. To further elucidate this cause, we analysed the nuclear translocation of the NFkB related transcription factor and AP-1 factors in the lungs of $p50^{-/-}$ and WT mice in response to CNP exposure. Recent reports actually documented that inflammatory mediator expression such as

TNF-a, MMP1 require the simultaneous activation of AP-1 and NFkB working cooperatively together [77,83]. However in our case and in response to CNP exposure, no compensatory activation of NFkB1, NFkB2 or AP-1 pathways could be identified in $p50^{-/-}$ mice as compared to WT mice (Fig.5.14). Thus an unidentified transcription factor, obviously different from p65 and also the tested NFkB2 and AP1 factors seems to drive the transcription of proinflammatory genes such as Cxcl1, IL-6 and Tnf-a (Fig.5.11) in the absence of p65. And since the expression of p50 as well as its precursor p105 (IkBγ) is known to possess antiinflammatory activities, either via nuclear translocation of the p50/p50 homodimers or mediated by p105-ankyrin repeats which prevent nuclear translocation of Rel-like transcription factors, such as p65, the lack of p50/p105 might lead to an excessive proinflammatory gene expression, as has been observed in $p50^{-/-}$ lungs.

In conclusion, targeted disruption of p50 augments lung proinflammatory cytokine expression in the model of CNP induced aseptic acute lung inflammation in mice. The recruitment of inflammatory cells to the alveolar region is however not depending on the function of p50 and also not altered by the increased cytokine levels in p50 deficient, CNP exposed mice. The pathway however, which drives inflammatory gene expression in the absence of p50, which according to our data also impaired nuclear translocation of p65, remains unknown but NFkB2 and AP-1 are unlikely to compensate the response to CNP exposure in p50 deficient conditions. Therapeutically, increasing p105 or p50 like activities may therefore be an avenue for preventing or treating acute lung inflammation [205].

6.5 Alveolar macrophages from $p50^{-/-}$ mice show M2 skewed polarization profile

Macrophages play an essential role in homeostasis and defense against bacterial [105,106,282,283], viral [284], parasitic infection [285,286], and environmental particles [287-290]. Macrophage cells are characterized by high functional heterogeneity [102-104], and the mode of macrophage activation plays a central role in disease progression and/or its resolution [105-107]. Macrophages stimulated with LPS and/or IFN gamma has been shown to polarize into a proinflammatory phenotype named M1, or classically activated. These M1 polarized cells are characterized by a high expression level of iNOS (NOS2), receptors for antigen presentation, and induction of proinflammatory mediators such as TNF-α, IL-1β, and monocyte chemoattractant protein-1 (MCP-1) [105,123]; however, in contrast, alternatively activated, M2 polarized macrophages, which can be induced either by IL-4 or IL-13 stimulation for M2a, or immunoglobulin complexes in combination with TLR agonists for M2b or IL-10, TGF-β, or glucocorticoids for M2c. Cells of the latter subtype are mainly involved in the resolution of inflammation [291]. Thus M1 and M2 macrophages can serve distinct functions in the regulation of

the inflammatory response [123] and untimely or excessive M1 activity can mediate tissue injury and be detrimental to the host [292].

Therefore we tested the hypothesis whether p50-depletion changed the activation / polarization responsiveness of alveolar macrophages and thus contributes to the enhanced cytokine response to CNP exposure in $p50^{-/-}$ lungs. To our knowledge, the control of macrophage polarization has mainly been attributed to the function of a small group of transcription factors such as NFkB [102], AP-1 [293,294], HIFs [294], STATs [295], and PPARs [296]. Also our observations indicate that the transcription factor NFkB1 as contributor to this differentiation, more specifically we show that the NFkB subunit p50 as a critical factor in regulating M1/M2 polarization of alveolar macrophages (Fig.5.15 and 5.16). Several recent observations have implicated NFkB in myeloid cell biology [297-299]. With respect to the NFkB subunit p50, Alessandra Saccani et al. showed that tumor-associated macrophages (TAM) in established tumors generally have an M2 phenotype with defective production of IL-12 but high release of IL-10. He further suggested the defective responsiveness of TAMs to M1 activation signals, to be the reason for the inability of TAM to mount an effective M1 antitumor response capable of inhibiting tumor growth [300,301] and that this defect is associated with a massive nuclear localization of the p50 homodimers. These observations were extended by Chiara Porta et al., who pointed to p50 as a key transcription factor component in the orchestration of the M2 driven inflammatory reactions *in vitro* and *in vivo.* She showed that p50 inhibits NFkB driven, M1-polarization and IFN-β production in peritoneal macrophages [102].

In light of these observations, we hypothesized that alveolar macrophages from $p50^{-/-}$ mice should show a polarization phenotype and according to the previously described role of p50 for M2 polarization, possess a rather M1 skewed response profile. To get insight in the role of the NFkB1 subunit p50 in alveolar machophage polarization, we first established the macrophage polarization model *in vitro* using primary AMs obtained from WT and $p50^{-/-}$ mice, stimulated for 4 hours with either LPS+IFN gamma, for M1 polarization or IL-4 for M2 polarization. In agreement with many previous observations [237,238,302-304], for WT macrophages of different origin, in our study also primary alveolar macrophages (AMs) from both $p50^{-/-}$ and WT mice proved to be capable to change to M1 or M2 polarized phenotypes in dependence of the specific microenvironments (LPS+IFN gamma or IL4). In consequence the expression of the prototypic M1 associated genes iNOS, Cxcl1, Cxcl2, Cxcl5, IL-6 and IL-1ß were highly induced in LPS+IFN gamma treated AMs (Fig.5.16), but several markers such as iNOS, IL-1ß and IL-6 showed reduced response in $p50^{-/-}$ AM compared to WT cells.

On the other side however, even that the M2 markers Arg1, Fizz-1 and Ym1 were in consistently higher in IL-4 treated cells (Fig.5.15), the baseline values of $p50^{-/-}$ AM exceeded those of WT cells by magnitudes, but where still further inducible by IL-4 in a range similar to the response of the WT cells. AM from p50 deficient cells thus showed already in non-stimulated conditions an M2 skewed phenotype in comparison to WT cells. These results suggested that in the absence of p50, AMs acquired an alternative-activation program, resulting in elevated expression of M2 associated genes. In contrast, LPS+IFN gamma treated AMs acquire the classcical activation program, with high expression of M1 associated genes, but p50-deficiency seems to impair this classical activation to a certain extend. Additionally the NFkB-pathway genes IKBa, IKBß and IKBz were upregulated in LPS+IFN gamma treated AMs whileas downregulated in IL-4 treated AMs, and $p50^{-/-}$ AMs showed reduced responses. In light of the lack of p65/p50 nuclearization in CNP exposed $p50^{-/-}$ lungs, also a M1 defective response to LPS+IFN gamma could be explained. Therefore our findings are corroborated with these observations that NFkB, especially in p65/p50 heterodimer, is involved in proinflammatory repsonses in macrophages when stimulated with LPS, IFN gamma and TNF-a [305-307].

However, our data contrast with that from Antonio Sica [308-311], who suggested that the ablation of the NFkB subunit p50, selective restored M1 mediators (e.g., iNOS and Tnf-α) and thus inhibited M2 cytokine release, in response to LPS rechallenge in endotoxin-tolerant macrophages. In our case, in AMs, the targeted disruption of the NFkB subunit p50 promoted the M2 skewed antiinflammatory gene expression (e.g., Arg1, Fizz-1 and Ym1) and even down-regulated M1-like proinflammatory genes such as iNOS, Cxcl-1, -2, -5, IL-1ß and IL-6. In addition to the increased antiinflammatory gene expression response to IL-4 for $p50^{-/-}$ AMs, AMs from $p50^{-/-}$ mice also showed higher basal levels of these genes as compared to WT mice, whereas no changes in basal levels were observed for M1 associated genes.

Taken together our macrophage results highlight the well described role of the NFkB1 subunit p50 in the LPS stimulated response, since p50-deficient macrophages where characterized by impaired induction of target gene expression such as iNOS, IL-1ß and IL-6 which obviously require interaction with p65. On the other hand p50/p50 homodimers seem not to be required to mount a M2 related gene expression in response to IL4, which might be different for the alternative activation during LPS mediated tolerance. In fact, the lack of p50 seems to skew the basal activation of AM to a M2 like phenotype, eventually because of the lack of p50/p65 availability for transcriptional activation of M1 related genes.

6.6 Little impact of alveolar macrophage on particle induced acute lung inflammation in mice

AM are considered to be within the most important cellular constituents of the lower respiratory tract. By analogy to macrophage biology in general, they are thought to play a key role in innate immune recognition of microbial pathogens or other danger signals, generation of inflammatory responses, control of intracellular pathogens and homeostatic regulation of immune responses [312]. Innate immune responses by AMs are crucial for immunosurveillance and host protection against all kinds of inhaled pathogens, but excessive inflammatory responses by these cells also underpins the pathogenesis of numerous diseases including pulmonary fibrosis, tuberculosis and *Streptococcus pneumoniae* infection [312-314].

In the model of experimental pneumococcal pneumonia, depletion of alveolar macrophages leads primarily to failure to clear apoptotic neutrophils, with the consequence of persistent production of proinflammatory cytokines, influx of activated neutrophils, and alveolar capillary injury [120,315]. Also in our model of aseptic inflammation, particle exposure triggered release of alveolar macrophage derived cytokines such as CXCL2 and TNF-a into the alveolar lumen (Fig.5.4), as well as rapidly induced macrophage related gene expression such as iNOS, Tnf-a, IL-1ß, Arg-1 and Fizz-1 in the lung tissue (Fig.5.7). On the other hand and as discussed in the paragraph 6.5., AM from p50-deficient lungs seemed not to contribute to the elevated cytokine levels detected in CNP treated p50 knock out mice, which questions the contribution of alveolar macrophages to the cytokine response. To gain insight whether alveolar macrophages are the respective cells responsible for the proinflammatory mediator secretion upon CNP exposure, alveolar macrophages obtained from mice treated with CNP for 6 and 12 hours were analysed by qPCR for their inflammatory response and compared to AMs from untreated and H_2O instilled mice.

Interestingly, none of the proinflammatory macrophage marker genes investigated, such as iNOS, Tnf-a, IL-1ß and Cxcl2, indicated that the alveolar macrophage obtained from CNP treated mice differs from control and sham groups (Fig.5.18A). Also M2 macrophage-associated genes, such as Arg-1 and Fizz-1 were equally expressed in H_2O-treated, sham mice, and CNP exposed mice. Also NFkB pathway genes did not indicate any inflammatory activation of alveolar macrophages (Fig.5.18C) in response to CNP, unless all these genes have been observed to be induced in lung homogenates at the same time points (Fig.5.7). We therefore need to challenge the tenets, that AM will be the cells responsible for the release of the inflammatory cytokine storm observed during the first 24h after CNP exposure. Either other macrophages, such as by BAL not accessible tissue

macrophages, or even epithelial cells might be more relevant cytokine producers and also interact with the deposited particles in an inflammatory manner not involving AM activation. This would at least explain the inconsistencies and contradictions discussed for the M2 skewed macrophages in $p50^{-/-}$ lungs before.

In conclusion, the NFkB1 subunit p50 is dispensable and the alveolar macrophage seems not to be the responsible cell for producing proinflammatory mediators in the lumen during carbon particle induced aseptic acute lung infllammation in mice.

7. Reference

1. West JB (2008) Respiratory physiology : the essentials. Philadelphia: Wolters Kluwer Health/Lippincott Williams & Wilkins. ix, 186 p. p.
2. Cotes JE, Chinn DJ, Miller MR (2006) Lung function : physiology, measurement and application in medicine. Malden, Mass. ; Oxford: Blackwell Pub. xi, 636 p. p.
3. Weibel ER (1963) Morphometry of the human lung. Berlin,: Springer. xi, 151 p. p.
4. Hayek Hv (1960) The human lung. New York,: Hafner Pub. Co. 372 p. p.
5. Hamid Q, Shannon J, Martin J (2005) Physiologic basis of respiratory disease. Hamilton: BC Decker, Inc. xxii, 793 p. p.
6. Griesenbach U, Alton EW, Consortium UKCFGT (2009) Gene transfer to the lung: lessons learned from more than 2 decades of CF gene therapy. Adv Drug Deliv Rev 61: 128-139.
7. Shields TW (2009) General thoracic surgery. Philadelphia: Wolters Kluwer Health/Lippincott Williams & Wilkins.
8. Patton JS (1996) Mechanisms of macromolecule absorption by the lungs. Adv Drug Deliv Rev 19: 3-36.
9. West JB (2012) Respiratory physiology : the essentials. Philadelphia: Wolters Kluwer Health/Lippincott Williams & Wilkins. viii, 200 p. p.
10. Thurlbeck WM (1967) The internal surface area of nonemphysematous lungs. Am Rev Respir Dis 95: 765-773.
11. Weibel ER (1973) Morphological basis of alveolar-capillary gas exchange. Physiol Rev 53: 419-495.
12. Bellingan G (1999) Inflammatory cell activation in sepsis. Br Med Bull 55: 12-29.
13. Patton JS, Byron PR (2007) Inhaling medicines: delivering drugs to the body through the lungs. Nature Reviews Drug Discovery 6: 67-74.
14. Rogers DF (1994) Airway goblet cells: responsive and adaptable front-line defenders. Eur Respir J 7: 1690-1706.
15. Rock JR, Onaitis MW, Rawlins EL, Lu Y, Clark CP, et al. (2009) Basal cells as stem cells of the mouse trachea and human airway epithelium. Proceedings of the National Academy of Sciences of the United States of America 106: 12771-12775.
16. Kling MA (2011) A review of respiratory system anatomy, physiology, and disease in the mouse, rat, hamster, and gerbil. Vet Clin North Am Exot Anim Pract 14: 287-337, vi.
17. Forstner K, Faust U (1990) [Physiology of the respiratory system]. Biomed Tech (Berl) 35 Suppl 1: 6-15.
18. Yoshizawa S, Tateda K, Matsumoto T, Gondaira F, Miyazaki S, et al. (2005) Legionella pneumophila evades gamma interferon-mediated growth suppression through interleukin-10 induction in bone marrow-derived macrophages. Infect Immun 73: 2709-2717.
19. Rannels DE, Swisher JW, Lee YC (1996) Alveolar epithelial cell-macrophage interactions in response to coal dust. Chest 109: 34S-35S.
20. Burns CA, Zarkower A (1982) The effects of silica and fly ash dust inhalation on alveolar macrophage effector cell function. J Reticuloendothel Soc 32: 449-459.
21. Lambrecht BN (2006) Alveolar macrophage in the driver's seat. Immunity 24: 366-368.
22. Szulakowski P, Crowther AJ, Jimenez LA, Donaldson K, Mayer R, et al. (2006) The effect of smoking on the transcriptional regulation of lung inflammation in patients with chronic obstructive pulmonary disease. Am J Respir Crit Care Med 174: 41-50.
23. Hoogendoorn M, Feenstra TL, Hoogenveen RT, Rutten-van Molken MP (2010) Long-term effectiveness and cost-effectiveness of smoking cessation interventions in patients with COPD. Thorax 65: 711-718.

24. Galli SJ, Tsai M, Piliponsky AM (2008) The development of allergic inflammation. Nature 454: 445-454.
25. Nakanishi K, Tsutsui H, Yoshimoto T (2010) Importance of IL-18-induced super Th1 cells for the development of allergic inflammation. Allergol Int 59: 137-141.
26. Cho YS, Oh SY, Zhu Z (2008) Tyrosine phosphatase SHP-1 in oxidative stress and development of allergic airway inflammation. Am J Respir Cell Mol Biol 39: 412-419.
27. Chen HI (2009) From neurogenic pulmonary edema to fat embolism syndrome: a brief review of experimental and clinical investigations of acute lung injury and acute respiratory distress syndrome. Chin J Physiol 52: 339-344.
28. Wheeler AP, Bernard GR (2007) Acute lung injury and the acute respiratory distress syndrome: a clinical review. Lancet 369: 1553-1564.
29. Tan WC, Vollmer WM, Lamprecht B, Mannino DM, Jithoo A, et al. (2012) Worldwide patterns of bronchodilator responsiveness: results from the Burden of Obstructive Lung Disease study. Thorax.
30. Menezes AM, Perez-Padilla R, Hallal PC, Jardim JR, Muino A, et al. (2008) Worldwide burden of COPD in high- and low-income countries. Part II. Burden of chronic obstructive lung disease in Latin America: the PLATINO study. Int J Tuberc Lung Dis 12: 709-712.
31. Wijagkanalan W, Kawakami S, Higuchi Y, Yamashita F, Hashida M (2011) Intratracheally instilled mannosylated cationic liposome/NFkappaB decoy complexes for effective prevention of LPS-induced lung inflammation. J Control Release 149: 42-50.
32. Rahman I, MacNee W (1998) Role of transcription factors in inflammatory lung diseases. Thorax 53: 601-612.
33. Walker C, Bauer W, Braun RK, Menz G, Braun P, et al. (1994) Activated T cells and cytokines in bronchoalveolar lavages from patients with various lung diseases associated with eosinophilia. Am J Respir Crit Care Med 150: 1038-1048.
34. Rom WN (2011) Role of oxidants in interstitial lung diseases: pneumoconioses, constrictive bronchiolitis, and chronic tropical pulmonary eosinophilia. Mediators Inflamm 2011: 407657.
35. Ciencewicki J, Trivedi S, Kleeberger SR (2008) Oxidants and the pathogenesis of lung diseases. J Allergy Clin Immunol 122: 456-468; quiz 469-470.
36. Rahman I, Yang SR, Biswas SK (2006) Current concepts of redox signaling in the lungs. Antioxid Redox Signal 8: 681-689.
37. Papavassiliou AG (1995) Molecular medicine. Transcription factors. N Engl J Med 332: 45-47.
38. Keller U, Nilsson JA, Maclean KH, Old JB, Cleveland JL (2005) Nfkb 1 is dispensable for Myc-induced lymphomagenesis. Oncogene 24: 6231-6240.
39. Bowie A, O'Neill LA (2000) Oxidative stress and nuclear factor-kappaB activation: a reassessment of the evidence in the light of recent discoveries. Biochem Pharmacol 59: 13-23.
40. Baeuerle PA, Henkel T (1994) Function and activation of NF-kappa B in the immune system. Annu Rev Immunol 12: 141-179.
41. Tak PP, Firestein GS (2001) NF-kappaB: a key role in inflammatory diseases. J Clin Invest 107: 7-11.
42. Zandi E, Chen Y, Karin M (1998) Direct phosphorylation of I kappa B by IKK alpha and IKK beta: Discrimination between free and NF-kappa B-bound substrate. Science 281: 1360-1363.
43. Chen F, Castranova V, Shi X, Demers LM (1999) New insights into the role of nuclear factor-kappaB, a ubiquitous transcription factor in the initiation of diseases. Clinical Chemistry 45: 7-17.
44. Hennighausen L, Furth PA (1990) NF-kB and HIV. Nature 343: 218-219.
45. Grimm S, Baeuerle PA (1993) The inducible transcription factor NF-kappa B: structure-function relationship of its protein subunits. Biochem J 290 (Pt 2): 297-308.

46. Ghosh S (1999) Regulation of inducible gene expression by the transcription factor NF-kappaB. Immunol Res 19: 183-189.
47. Dobrzanski P, Ryseck RP, Bravo R (1993) Both N- and C-terminal domains of RelB are required for full transactivation: role of the N-terminal leucine zipper-like motif. Mol Cell Biol 13: 1572-1582.
48. Fusco AJ, Savinova OV, Talwar R, Kearns JD, Hoffmann A, et al. (2008) Stabilization of RelB requires multidomain interactions with p100/p52. J Biol Chem 283: 12324-12332.
49. Ghosh S, Gifford AM, Riviere LR, Tempst P, Nolan GP, et al. (1990) Cloning of the p50 DNA binding subunit of NF-kappa B: homology to rel and dorsal. Cell 62: 1019-1029.
50. Inoue J, Kerr LD, Kakizuka A, Verma IM (1992) I kappa B gamma, a 70 kd protein identical to the C-terminal half of p110 NF-kappa B: a new member of the I kappa B family. Cell 68: 1109-1120.
51. Sha WC, Liou HC, Tuomanen EI, Baltimore D (1995) Targeted disruption of the p50 subunit of NF-kappa B leads to multifocal defects in immune responses. Cell 80: 321-330.
52. Oeckinghaus A, Hayden MS, Ghosh S (2011) Crosstalk in NF-kappaB signaling pathways. Nat Immunol 12: 695-708.
53. Gilmore TD (2006) Introduction to NF-kappa B: players, pathways, perspectives. Oncogene 25: 6680-6684.
54. Ghosh S, May MJ, Kopp EB (1998) NF-kappa B and Rel proteins: evolutionarily conserved mediators of immune responses. Annu Rev Immunol 16: 225-260.
55. Bonizzi G, Karin M (2004) The two NF-kappa B activation pathways and their role in innate and adaptive immunity. Trends Immunol 25: 280-288.
56. Gilboa-Geffen A, Wolf Y, Hanin G, Melamed-Book N, Pick M, et al. (2011) Activation of the Alternative NFkB Pathway Improves Disease Symptoms in a Model of Sjogren's Syndrome. PLoS One 6.
57. Jaeschke H, Smith CW, Clemens MG, Ganey PE, Roth RA (1996) Mechanisms of inflammatory liver injury: adhesion molecules and cytotoxicity of neutrophils. Toxicol Appl Pharmacol 139: 213-226.
58. Lukacs NW, Ward PA (1996) Inflammatory mediators, cytokines, and adhesion molecules in pulmonary inflammation and injury. Adv Immunol 62: 257-304.
59. Albelda SM, Smith CW, Ward PA (1994) Adhesion molecules and inflammatory injury. FASEB J 8: 504-512.
60. Chen CC, Rosenbloom CL, Anderson DC, Manning AM (1995) Selective inhibition of E-selectin, vascular cell adhesion molecule-1, and intercellular adhesion molecule-1 expression by inhibitors of I kappa B-alpha phosphorylation. J Immunol 155: 3538-3545.
61. Chen CC, Manning AM (1995) Transcriptional regulation of endothelial cell adhesion molecules: a dominant role for NF-kappa B. Agents Actions Suppl 47: 135-141.
62. Gadjeva M, Tomczak MF, Zhang M, Wang YY, Dull K, et al. (2004) A role for NF-kappa B subunits p50 and p65 in the inhibition of lipopolysaccharide-induced shock. J Immunol 173: 5786-5793.
63. Urban MB, Baeuerle PA (1991) The role of the p50 and p65 subunits of NF-kappa B in the recognition of cognate sequences. New Biol 3: 279-288.
64. Tong X, Yin L, Washington R, Rosenberg DW, Giardina C (2004) The p50-p50 NF-kappa B complex as a stimulus-specific repressor of gene activation. Molecular and Cellular Biochemistry 265: 171-183.
65. Cao SJ, Zhang X, Edwards JP, Mosser DM (2006) NF-kappa B1 (p50) homodimers differentially regulate pro- and anti-inflammatory cytokines in macrophages. Journal of Biological Chemistry 281: 26041-26050.
66. O'Connor S, Shumway SD, Amanna IJ, Hayes CE, Miyamoto S (2004) Regulation of constitutive p50/c-rel activity via proteasome inhibitor-resistant I kappa B alpha degradation in B cells. Molecular and Cellular Biology 24: 4895-4908.

67. Wessells J, Baer M, Young HA, Claudio E, Brown K, et al. (2004) BCL-3 and NF-kappa B p50 attenuate lipopolysaccharide-induced inflammatory responses in macrophages. Journal of Biological Chemistry 279: 49995-50003.
68. Rajendrasozhan S, Chung S, Sundar IK, Yao H, Rahman I (2010) Targeted disruption of NF-{kappa}B1 (p50) augments cigarette smoke-induced lung inflammation and emphysema in mice: a critical role of p50 in chromatin remodeling. Am J Physiol Lung Cell Mol Physiol 298: L197-209.
69. T. Rangasamy GP, R. Tuder, S. Bhatt, W. Mitzner, S. Georas (2010) Disruption Of P50 Subunit Of NF-κB Enhances Susceptibility To Pulmonary Emphysema In Mice. B38 CHRONIC OBSTRUCTIVE PULMONARY DISEASE PATHOGENESIS II.
70. Eferl R, Wagner EF (2003) AP-1: A double-edged sword in tumorigenesis. Nature Reviews Cancer 3: 859-868.
71. Reddy NM, Vegiraju S, Irving A, Paun BC, Luzina IG, et al. (2012) Targeted Deletion of Jun/AP-1 in Alveolar Epithelial Cells Causes Progressive Emphysema and Worsens Cigarette Smoke-Induced Lung Inflammation. American Journal of Pathology 180: 562-574.
72. Eferl R, Wagner EF (2003) AP-1: a double-edged sword in tumorigenesis. Nat Rev Cancer 3: 859-868.
73. Angel P, Szabowski A, Schorpp-Kistner M (2001) Function and regulation of AP-1 subunits in skin physiology and pathology. Oncogene 20: 2413-2423.
74. Karin M, Liu Z, Zandi E (1997) AP-1 function and regulation. Curr Opin Cell Biol 9: 240-246.
75. Guo RF, Lentsch AB, Sarma JV, Sun L, Riedemann NC, et al. (2002) Activator protein-1 activation in acute lung injury. Am J Pathol 161: 275-282.
76. Wagner EF, Nebreda AR (2009) Signal integration by JNK and p38 MAPK pathways in cancer development. Nat Rev Cancer 9: 537-549.
77. Roebuck KA, Carpenter LR, Lakshminarayanan V, Page SM, Moy JN, et al. (1999) Stimulus-specific regulation of chemokine expression involves differential activation of the redox-responsive transcription factors AP-1 and NF-kappaB. J Leukoc Biol 65: 291-298.
78. Zagariya A, Mungre S, Lovis R, Birrer M, Ness S, et al. (1998) Tumor necrosis factor alpha gene regulation: enhancement of C/EBPbeta-induced activation by c-Jun. Mol Cell Biol 18: 2815-2824.
79. Ray N, Kuwahara M, Takada Y, Maruyama K, Kawaguchi T, et al. (2006) c-Fos suppresses systemic inflammatory response to endotoxin. Int Immunol 18: 671-677.
80. Takada Y, Ray N, Ikeda E, Kawaguchi T, Kuwahara M, et al. (2010) Fos proteins suppress dextran sulfate sodium-induced colitis through inhibition of NF-kappaB. J Immunol 184: 1014-1021.
81. Zenz R, Eferl R, Kenner L, Florin L, Hummerich L, et al. (2005) Psoriasis-like skin disease and arthritis caused by inducible epidermal deletion of Jun proteins. Nature 437: 369-375.
82. Vaz M, Reddy NM, Rajasekaran S, Reddy SP (2012) Genetic disruption of Fra-1 decreases susceptibility to endotoxin-induced acute lung injury and mortality in mice. Am J Respir Cell Mol Biol 46: 55-62.
83. Divya CS, Pillai MR (2006) Antitumor action of curcumin in human papillomavirus associated cells involves downregulation of viral oncogenes, prevention of NFkB and AP-1 translocation, and modulation of apoptosis. Mol Carcinog 45: 320-332.
84. Nowack B, Bucheli TD (2007) Occurrence, behavior and effects of nanoparticles in the environment. Environmental Pollution 150: 5-22.
85. Banfield JF, Zhang HZ (2001) Nanoparticles in the environment. Nanoparticles and the Environment 44: 1-58.
86. Sanchez A, Recillas S, Font X, Casals E, Gonzalez E, et al. (2011) Ecotoxicity of, and remediation with, engineered inorganic nanoparticles in the environment. Trac-Trends in Analytical Chemistry 30: 507-516.

87. Howard AG (2010) On the challenge of quantifying man-made nanoparticles in the aquatic environment. Journal of Environmental Monitoring 12: 135-142.
88. Zhang FY, Li LP, Krafft T, Lv JM, Wang WY, et al. (2011) Study on the Association between Ambient Air Pollution and Daily Cardiovascular and Respiratory Mortality in an Urban District of Beijing. Int J Environ Res Public Health 8: 2109-2123.
89. Katanoda K, Sobue T, Satoh H, Tajima K, Suzuki T, et al. (2011) An Association Between Long-Term Exposure to Ambient Air Pollution and Mortality From Lung Cancer and Respiratory Diseases in Japan. Journal of Epidemiology 21: 132-143.
90. Willis A, Jerrett M, Burnett RT, Krewski D (2003) The association between sulfate air pollution and mortality at the county scale: An exploration of the impact of scale on a long-term exposure study. Journal of Toxicology and Environmental Health-Part A 66: 1605-1624.
91. Raghavendran K, Notter RH, Davidson BA, Helinski JD, Kunkel SL, et al. (2009) Lung contusion: inflammatory mechanisms and interaction with other injuries. Shock 32: 122-130.
92. Moldoveanu B, Otmishi P, Jani P, Walker J, Sarmiento X, et al. (2009) Inflammatory mechanisms in the lung. J Inflamm Res 2: 1-11.
93. Floss C, Stadermann FJ, Bradley J, Dai ZR, Bajt S, et al. (2004) Carbon and nitrogen isotopic anomalies in an anhydrous interplanetary dust particle. Science 303: 1355-1358.
94. Donaldson K, Tran L, Jimenez LA, Duffin R, Newby DE, et al. (2005) Combustion-derived nanoparticles: a review of their toxicology following inhalation exposure. Part Fibre Toxicol 2: 10.
95. Hashimoto S, Gon Y, Takeshita I, Matsumoto K, Jibiki I, et al. (2000) Diesel exhaust particles activate p38 MAP kinase to produce interleukin 8 and RANTES by human bronchial epithelial cells and N-acetylcysteine attenuates p38 MAP kinase activation. Am J Respir Crit Care Med 161: 280-285.
96. Takizawa H, Ohtoshi T, Kawasaki S, Kohyama T, Desaki M, et al. (1999) Diesel exhaust particles induce NF-kappa B activation in human bronchial epithelial cells in vitro: importance in cytokine transcription. J Immunol 162: 4705-4711.
97. Muller L, Riediker M, Wick P, Mohr M, Gehr P, et al. (2010) Oxidative stress and inflammation response after nanoparticle exposure: differences between human lung cell monocultures and an advanced three-dimensional model of the human epithelial airways. Journal of the Royal Society Interface 7: S27-S40.
98. Ikeda M, Shitashige M, Yamasaki H, Sagai M, Tomita T (1995) Oxidative modification of low density lipoprotein by diesel exhaust particles. Biol Pharm Bull 18: 866-871.
99. Li N, Venkatesan MI, Miguel A, Kaplan R, Gujuluva C, et al. (2000) Induction of heme oxygenase-1 expression in macrophages by diesel exhaust particle chemicals and quinones via the antioxidant-responsive element. J Immunol 165: 3393-3401.
100. Nel AE, Diaz-Sanchez D, Li N (2001) The role of particulate pollutants in pulmonary inflammation and asthma: evidence for the involvement of organic chemicals and oxidative stress. Curr Opin Pulm Med 7: 20-26.
101. Stoeger T, Takenaka S, Frankenberger B, Ritter B, Karg E, et al. (2009) Deducing in vivo toxicity of combustion-derived nanoparticles from a cell-free oxidative potency assay and metabolic activation of organic compounds. Environ Health Perspect 117: 54-60.
102. Porta C, Rimoldi M, Raes G, Brys L, Ghezzi P, et al. (2009) Tolerance and M2 (alternative) macrophage polarization are related processes orchestrated by p50 nuclear factor kappaB. Proc Natl Acad Sci U S A 106: 14978-14983.
103. Goerdt S, Orfanos CE (1999) Other functions, other genes: alternative activation of antigen-presenting cells. Immunity 10: 137-142.
104. Gordon S, Taylor PR (2005) Monocyte and macrophage heterogeneity. Nat Rev Immunol 5: 953-964.

105. Mege JL, Mehraj V, Capo C (2011) Macrophage polarization and bacterial infections. Curr Opin Infect Dis 24: 230-234.
106. Benoit M, Desnues B, Mege JL (2008) Macrophage polarization in bacterial infections. J Immunol 181: 3733-3739.
107. Satoh T, Takeuchi O, Vandenbon A, Yasuda K, Tanaka Y, et al. (2010) The Jmjd3-Irf4 axis regulates M2 macrophage polarization and host responses against helminth infection. Nat Immunol 11: 936-944.
108. Gordon S, Martinez FO (2010) Alternative activation of macrophages: mechanism and functions. Immunity 32: 593-604.
109. Gordon S (2003) Alternative activation of macrophages. Nat Rev Immunol 3: 23-35.
110. Rodriguez-Prados JC, Traves PG, Cuenca J, Rico D, Aragones J, et al. (2010) Substrate fate in activated macrophages: a comparison between innate, classic, and alternative activation. J Immunol 185: 605-614.
111. Jenkins SJ, Ruckerl D, Cook PC, Jones LH, Finkelman FD, et al. (2011) Local macrophage proliferation, rather than recruitment from the blood, is a signature of TH2 inflammation. Science 332: 1284-1288.
112. Isbel NM, Nikolic-Paterson DJ, Hill PA, Dowling J, Atkins RC (2001) Local macrophage proliferation correlates with increased renal M-CSF expression in human glomerulonephritis. Nephrol Dial Transplant 16: 1638-1647.
113. Yang N, Wu LL, Nikolic-Paterson DJ, Ng YY, Yang WC, et al. (1998) Local macrophage and myofibroblast proliferation in progressive renal injury in the rat remnant kidney. Nephrol Dial Transplant 13: 1967-1974.
114. Tomioka H, Tatano Y, Maw WW, Sano C, Kanehiro Y, et al. (2012) Characteristics of Suppressor Macrophages Induced by Mycobacterial and Protozoal Infections in relation to Alternatively Activated M2 Macrophages. Clin Dev Immunol 2012: 635451.
115. Edwards JP, Zhang X, Frauwirth KA, Mosser DM (2006) Biochemical and functional characterization of three activated macrophage populations. J Leukoc Biol 80: 1298-1307.
116. Cho WS, Choi M, Han BS, Cho M, Oh J, et al. (2007) Inflammatory mediators induced by intratracheal instillation of ultrafine amorphous silica particles. Toxicol Lett 175: 24-33.
117. Lee S, Zhang J (2012) Heterogeneity of macrophages in injured trigeminal nerves: Cytokine/chemokine expressing vs. phagocytic macrophages. Brain Behav Immun.
118. Mosser DM, Edwards JP (2008) Exploring the full spectrum of macrophage activation. Nat Rev Immunol 8: 958-969.
119. Ward PA (1996) Role of complement, chemokines, and regulatory cytokines in acute lung injury. Ann N Y Acad Sci 796: 104-112.
120. Rubins JB (2003) Alveolar macrophages: wielding the double-edged sword of inflammation. Am J Respir Crit Care Med 167: 103-104.
121. Sica A, Mantovani A (2012) Macrophage plasticity and polarization: in vivo veritas. J Clin Invest 122: 787-795.
122. Bouhlel MA, Derudas B, Rigamonti E, Dievart R, Brozek J, et al. (2007) PPAR gamma activation primes human monocytes into alternative M2 macrophages with anti-inflammatory properties. Cell Metab 6: 137-143.
123. Liao X, Sharma N, Kapadia F, Zhou G, Lu Y, et al. (2011) Kruppel-like factor 4 regulates macrophage polarization. J Clin Invest 121: 2736-2749.
124. Pello OM, De Pizzol M, Mirolo M, Soucek L, Zammataro L, et al. (2012) Role of c-MYC in alternative activation of human macrophages and tumor-associated macrophage biology. Blood 119: 411-421.

125. Sica A, Bronte V (2007) Altered macrophage differentiation and immune dysfunction in tumor development. J Clin Invest 117: 1155-1166.
126. Covin RB, Brock TG, Bailie MB, Peters-Golden M (1998) Altered expression and localization of 5-lipoxygenase accompany macrophage differentiation in the lung. Am J Physiol 275: L303-310.
127. Auffray C, Sieweke MH, Geissmann F (2009) Blood monocytes: development, heterogeneity, and relationship with dendritic cells. Annu Rev Immunol 27: 669-692.
128. Soehnlein O, Lindbom L (2010) Phagocyte partnership during the onset and resolution of inflammation. Nat Rev Immunol 10: 427-439.
129. Kang K, Reilly SM, Karabacak V, Gangl MR, Fitzgerald K, et al. (2008) Adipocyte-derived Th2 cytokines and myeloid PPARdelta regulate macrophage polarization and insulin sensitivity. Cell Metab 7: 485-495.
130. Heilbronn LK, Campbell LV (2008) Adipose tissue macrophages, low grade inflammation and insulin resistance in human obesity. Curr Pharm Des 14: 1225-1230.
131. Laskin DL (2009) Macrophages and Inflammatory Mediators in Chemical Toxicity: A Battle of Forces. Chem Res Toxicol 22: 1376-1385.
132. Roth C, Ferron GA, Karg E, Lentner B, Schumann G, et al. (2004) Generation of ultrafine particles by spark discharging. Aerosol Science and Technology 38: 228-235.
133. Gotz AA, Vidal-Puig A, Rodel HG, de Angelis MH, Stoeger T (2011) Carbon-nanoparticle-triggered acute lung inflammation and its resolution are not altered in PPAR gamma-defective (P465L) mice. Particle and Fibre Toxicology 8.
134. Ganguly K, Upadhyay S, Irmler M, Takenaka S, Pukelsheim K, et al. (2009) Pathway focused protein profiling indicates differential function for IL-1B, -18 and VEGF during initiation and resolution of lung inflammation evoked by carbon nanoparticle exposure in mice. Part Fibre Toxicol 6: 31.
135. Nicklas W, Baneux P, Boot R, Decelle T, Deeny AA, et al. (2002) Recommendations for the health monitoring of rodent and rabbit colonies in breeding and experimental units. Lab Anim 36: 20-42.
136. Stoeger T, Reinhard C, Takenaka S, Schroeppel A, Karg E, et al. (2006) Instillation of six different ultrafine carbon particles indicates a surface area threshold dose for acute lung inflammation in mice. Environ Health Perspect 114: 328-333.
137. Brown RH, Walters DM, Greenberg RS, Mitzner W (1999) A method of endotracheal intubation and pulmonary functional assessment for repeated studies in mice. Journal of Applied Physiology 87: 2362-2365.
138. Shaw DJ (1992) Introduction to colloid and surface chemistry. Oxford ; Boston: Butterworth-Heinemann. vi, 306 p. p.
139. Kodavanti UP, Schladweiler MC, Ledbetter AD, Hauser R, Christiani DC, et al. (2002) Temporal association between pulmonary and systemic effects of particulate matter in healthy and cardiovascular compromised rats. Journal of Toxicology and Environmental Health-Part A 65: 1545-1569.
140. Andre E, Stoeger T, Takenaka S, Bahnweg M, Ritter B, et al. (2006) Inhalation of ultrafine carbon particles triggers biphasic pro-inflammatory response in the mouse lung. Eur Respir J 28: 275-285.
141. Krappmann D, Emmerich F, Kordes U, Scharschmidt E, Dorken B, et al. (1999) Molecular mechanisms of constitutive NF-kappaB/Rel activation in Hodgkin/Reed-Sternberg cells. Oncogene 18: 943-953.
142. Alessandrini F, Beck-Speier I, Krappmann D, Weichenmeier I, Takenaka S, et al. (2009) Role of oxidative stress in ultrafine particle-induced exacerbation of allergic lung inflammation. Am J Respir Crit Care Med 179: 984-991.

143. Chanteux H, Guisset AC, Pilette C, Sibille Y (2007) LPS induces IL-10 production by human alveolar macrophages via MAPKinases- and Sp1-dependent mechanisms. Respir Res 8: 71.
144. Thellin O, Zorzi W, Lakaye B, De Borman B, Coumans B, et al. (1999) Housekeeping genes as internal standards: use and limits. Journal of Biotechnology 75: 291-295.
145. Dheda K, Huggett JF, Bustin SA, Johnson MA, Rook G, et al. (2004) Validation of housekeeping genes for normalizing RNA expression in real-time PCR. Biotechniques 37: 112-114, 116, 118-119.
146. Banda M, Bommineni A, Thomas RA, Luckinbill LS, Tucker JD (2008) Evaluation and validation of housekeeping genes in response to ionizing radiation and chemical exposure for normalizing RNA expression in real-time PCR. Mutat Res 649: 126-134.
147. Vandesompele J, De Preter K, Pattyn F, Poppe B, Van Roy N, et al. (2002) Accurate normalization of real-time quantitative RT-PCR data by geometric averaging of multiple internal control genes. Genome Biol 3: RESEARCH0034.
148. Andersen CL, Jensen JL, Orntoft TF (2004) Normalization of real-time quantitative reverse transcription-PCR data: a model-based variance estimation approach to identify genes suited for normalization, applied to bladder and colon cancer data sets. Cancer Res 64: 5245-5250.
149. Pfaffl MW, Tichopad A, Prgomet C, Neuvians TP (2004) Determination of stable housekeeping genes, differentially regulated target genes and sample integrity: BestKeeper - Excel-based tool using pair-wise correlations. Biotechnology Letters 26: 509-515.
150. Nolan T, Hands RE, Bustin SA (2006) Quantification of mRNA using real-time RT-PCR. Nature Protocols 1: 1559-1582.
151. Bustin SA (2002) Quantification of mRNA using real-time reverse transcription PCR (RT-PCR): trends and problems. Journal of Molecular Endocrinology 29.
152. Aguilera M, Querci M, Pastor S, Bellocchi G, Milcamps A, et al. (2009) Assessing Copy Number of MON 810 Integrations in Commercial Seed Maize Varieties by 5 ' Event-Specific Real-Time PCR Validated Method Coupled to 2(-Delta Delta CT) Analysis. Food Analytical Methods 2: 73-79.
153. D'hulst AI, Vermaelen KY, Brusselle GG, Joos GF, Pauwels RA (2005) Time course of cigarette smoke-induced pulmonary inflammation in mice. European Respiratory Journal 26: 204-213.
154. Canonica GW (2002) Introduction to nasal and pulmonary allergy cascade. Allergy 57: 8-12.
155. Kwon KY, Lee HW, Park JY, Jung HR, Hwang IS, et al. (2010) Effects of small airway and lung parenchyma in short and long. Histopathology 57: 226-226.
156. D'Angelo E, Koulouris NG, Della Valle P, Gentile G, Pecchiari M (2008) The fall in exhaled nitric oxide with ventilation at low lung volumes in rabbits: An index of small airway injury. Respir Physiol Neurobiol 160: 215-223.
157. Beyerle A, Braun A, Banerjee A, Ercal N, Eickelberg O, et al. (2011) Inflammatory responses to pulmonary application of PEI-based siRNA nanocarriers in mice. Biomaterials 32: 8694-8701.
158. Wagner JG, Roth RA (2000) Neutrophil migration mechanisms, with an emphasis on the pulmonary vasculature. Pharmacol Rev 52: 349-374.
159. Lee YH, Kim SH, Kim Y, Lim Y, Ha K, et al. (2012) Inhibitory effect of the antidepressant imipramine on NF-kappaB-dependent CXCL1 expression in TNFalpha-exposed astrocytes. Int Immunopharmacol 12: 547-555.
160. Cai S, Batra S, Lira SA, Kolls JK, Jeyaseelan S (2010) CXCL1 regulates pulmonary host defense to Klebsiella Infection via CXCL2, CXCL5, NF-kappaB, and MAPKs. J Immunol 185: 6214-6225.
161. Yang RH, Strong JA, Zhang JM (2009) NF-kappaB mediated enhancement of potassium currents by the chemokine CXCL1/growth related oncogene in small diameter rat sensory neurons. Mol Pain 5: 26.
162. Locksley RM, Killeen N, Lenardo MJ (2001) The TNF and TNF receptor superfamilies: integrating mammalian biology. Cell 104: 487-501.

163. Smirnova MG, Kiselev SL, Gnuchev NV, Birchall JP, Pearson JP (2002) Role of the pro-inflammatory cytokines tumor necrosis factor-alpha, interleukin-1 beta, interleukin-6 and interleukin-8 in the pathogenesis of the otitis media with effusion. Eur Cytokine Netw 13: 161-172.
164. Wang KX, Denhardt DT (2008) Osteopontin: role in immune regulation and stress responses. Cytokine Growth Factor Rev 19: 333-345.
165. Yachie A, Niida Y, Wada T, Igarashi N, Kaneda H, et al. (1999) Oxidative stress causes enhanced endothelial cell injury in human heme oxygenase-1 deficiency. J Clin Invest 103: 129-135.
166. Buelow R, Tullius SG, Volk HD (2001) Protection of grafts by hemoxygenase-1 and its toxic product carbon monoxide. American Journal of Transplantation 1: 313-315.
167. Cerretti DP, Kozlosky CJ, Mosley B, Nelson N, Van Ness K, et al. (1992) Molecular cloning of the interleukin-1 beta converting enzyme. Science 256: 97-100.
168. Mariathasan S, Newton K, Monack DM, Vucic D, French DM, et al. (2004) Differential activation of the inflammasome by caspase-1 adaptors ASC and Ipaf. Nature 430: 213-218.
169. Bazan JF, Bacon KB, Hardiman G, Wang W, Soo K, et al. (1997) A new class of membrane-bound chemokine with a CX3C motif. Nature 385: 640-644.
170. Holness CL, Simmons DL (1993) Molecular cloning of CD68, a human macrophage marker related to lysosomal glycoproteins. Blood 81: 1607-1613.
171. Stoeger T, Takenaka S, Frankenberger B, Ritter B, Karg E, et al. (2009) Deducing in Vivo Toxicity of Combustion-Derived Nanoparticles from a Cell-Free Oxidative Potency Assay and Metabolic Activation of Organic Compounds. Environmental Health Perspectives 117: 54-60.
172. Churg A, Xie CS, Wang XS, Vincent R, Wang RD (2005) Air pollution particles activate NF-kappa B on contact with airway epithelial cell surfaces. Toxicology and Applied Pharmacology 208: 37-45.
173. Thorne PS, Hadina S, Kulhankova K, Wohlford-Lenane C, McCray PB, et al. (2006) Monitoring of endotoxin-induced pulmonary inflammation in vivo in NF-kB luciferase transgenic mice. Journal of Allergy and Clinical Immunology 117: S147-S147.
174. Lancaster LH, Christman JW, Blackwell TR, Koay MA, Blackwell TS (2001) Suppression of lung inflammation in rats by prevention of NF-kappa B activation in the liver. Inflammation 25: 25-31.
175. Hayden MS, Ghosh S (2004) Signaling to NF-kappaB. Genes Dev 18: 2195-2224.
176. Hunter RB, Kandarian SC (2004) Disruption of either the Nfkb1 or the Bcl3 gene inhibits skeletal muscle atrophy. Journal of Clinical Investigation 114: 1504-1511.
177. Keller U, Nilsson JA, Maclean KH, Old JB, Cleveland JL (2005) Nfkb1 is dispensable for Myc-induced lymphomagenesis. Oncogene 24: 6231-6240.
178. Zhao XX, Ross EJ, Wang YY, Horwitz BH (2012) Nfkb1 Inhibits LPS-Induced IFN-beta and IL-12 p40 Production in Macrophages by Distinct Mechanisms. PLoS One 7.
179. Sager TM, Castranova V (2009) Surface area of particle administered versus mass in determining the pulmonary toxicity of ultrafine and fine carbon black: comparison to ultrafine titanium dioxide. Part Fibre Toxicol 6: 15.
180. Stefaniak AB, Hoover MD, Dickerson RM, Day GA, Breysse PN, et al. (2007) Differences in estimates of size distribution of beryllium powder materials using phase contrast microscopy, scanning electron microscopy, and liquid suspension counter techniques. Part Fibre Toxicol 4: 3.
181. Warheit DB, Webb TR, Sayes CM, Colvin VL, Reed KL (2006) Pulmonary instillation studies with nanoscale TiO2 rods and dots in rats: toxicity is not dependent upon particle size and surface area. Toxicol Sci 91: 227-236.
182. Kimura S, Egashira K, Ling C, Tsujimoto H, Hara K, et al. (2007) A novel anti-inflammatory therapeutic approach for pulmonary arterial hypertension: Blockade of NF-kB by Nano-DDS of NF-kB decoy to the lung ameliorates monocrotaline-induced PAH. Circulation 116: 193-193.

183. Deng JO, Fujimoto J, Ye XF, Men TY, Van Pelt CS, et al. (2010) Knockout of the Tumor Suppressor Gene Gprc5a in Mice Leads to NF-KB Activation in Airway Epithelium and Promotes Lung Inflammation and Tumorigenesis. Cancer Prev Res (Phila) 3: 424-437.
184. Matsuda N, Hattori Y, Yamamoto S, Teramae H, Koike K (2009) Inhaled Tak1 Sirna Improves Lung Inflammation and Apoptosis by Reduced Transcriptional Activity of Nf-Kb and Ap-1 in Septic Mice. Critical Care Medicine 37: A21-A21.
185. Pasparakis M (2011) Ikk/Nf-Kb Signalling in Chronic Inflammation. Inflammation Research 60: 15-15.
186. Wilson HM, Rees AJ, Kluth DC (2003) Anti-inflammatory effect of NF-kB inhibited macrophages on glomerular inflammation. Journal of the American Society of Nephrology 14: 173a-173a.
187. Schulze-Luehrmann J, Ghosh S (2006) Antigen-receptor signaling to nuclear factor kappa B. Immunity 25: 701-715.
188. Sen R (2006) Control of B lymphocyte apoptosis by the transcription factor NF-kappaB. Immunity 25: 871-883.
189. Saccani A, Schioppa T, Porta C, Biswas SK, Nebuloni M, et al. (2006) p50 nuclear factor-kappaB overexpression in tumor-associated macrophages inhibits M1 inflammatory responses and antitumor resistance. Cancer Res 66: 11432-11440.
190. Driscoll KE, Carter JM, Hassenbein DG, Howard B (1997) Cytokines and particle-induced inflammatory cell recruitment. Environ Health Perspect 105 Suppl 5: 1159-1164.
191. Driscoll KE (2000) TNFalpha and MIP-2: role in particle-induced inflammation and regulation by oxidative stress. Toxicol Lett 112-113: 177-183.
192. Provoost S, Maes T, Pauwels NS, Vanden Berghe T, Vandenabeele P, et al. (2011) NLRP3/caspase-1-independent IL-1beta production mediates diesel exhaust particle-induced pulmonary inflammation. J Immunol 187: 3331-3337.
193. Waller A, Nayee P, Czaplewski LG (2000) Identification and characterization of a rat macrophage inflammatory protein-1alpha receptor. J Hematother Stem Cell Res 9: 703-709.
194. Beutler B, Greenwald D, Hulmes JD, Chang M, Pan YC, et al. (1985) Identity of tumour necrosis factor and the macrophage-secreted factor cachectin. Nature 316: 552-554.
195. Barna BP, Thomassen MJ, Zhou P, Pettay J, Singh-Burgess S, et al. (1996) Activation of alveolar macrophage TNF and MCP-1 expression in vivo by a synthetic peptide of C-reactive protein. J Leukoc Biol 59: 397-402.
196. Wang MJ, Jeng KC, Shih PC (2000) Differential expression and regulation of macrophage inflammatory protein (MIP)-1alpha and MIP-2 genes by alveolar and peritoneal macrophages in LPS-hyporesponsive C3H/HeJ mice. Cell Immunol 204: 88-95.
197. Gotz AA, Vidal-Puig A, Rodel HG, de Angelis MH, Stoeger T (2011) Carbon-nanoparticle-triggered acute lung inflammation and its resolution are not altered in PPARgamma-defective (P465L) mice. Part Fibre Toxicol 8: 28.
198. Saiga H, Nishimura J, Kuwata H, Okuyama M, Matsumoto S, et al. (2008) Lipocalin 2-dependent inhibition of mycobacterial growth in alveolar epithelium. J Immunol 181: 8521-8527.
199. Jeyaseelan S, Manzer R, Young SK, Yamamoto M, Akira S, et al. (2005) Induction of CXCL5 during inflammation in the rodent lung involves activation of alveolar epithelium. Am J Respir Cell Mol Biol 32: 531-539.
200. Mizgerd JP, Lupa MM, Spieker MS (2004) NF-kappaB p50 facilitates neutrophil accumulation during LPS-induced pulmonary inflammation. BMC Immunol 5: 10.
201. Ziegler-Heitbrock L (2001) The p50-homodimer mechanism in tolerance to LPS. J Endotoxin Res 7: 219-222.
202. Ziegler-Heitbrock HW, Petersmann I, Frankenberger M (1997) p50 (NF-kappa B1) is upregulated in LPS tolerant P388D1 murine macrophages. Immunobiology 198: 73-80.

203. Ju J, Naura AS, Errami Y, Zerfaoui M, Kim H, et al. (2010) Phosphorylation of p50 NF-kappaB at a single serine residue by DNA-dependent protein kinase is critical for VCAM-1 expression upon TNF treatment. J Biol Chem 285: 41152-41160.
204. Fakhrzadeh L, Laskin JD, Laskin DL (2004) Ozone-induced production of nitric oxide and TNF-alpha and tissue injury are dependent on NF-kappaB p50. Am J Physiol Lung Cell Mol Physiol 287: L279-285.
205. Mizgerd JP, Lupa MM, Kogan MS, Warren HB, Kobzik L, et al. (2003) Nuclear factor-kappaB p50 limits inflammation and prevents lung injury during Escherichia coli pneumonia. Am J Respir Crit Care Med 168: 810-817.
206. Kurland JF, Kodym R, Story MD, Spurgers KB, McDonnell TJ, et al. (2001) NF-kappaB1 (p50) homodimers contribute to transcription of the bcl-2 oncogene. J Biol Chem 276: 45380-45386.
207. Van Lint P, Libert C (2007) Chemokine and cytokine processing by matrix metalloproteinases and its effect on leukocyte migration and inflammation. J Leukoc Biol 82: 1375-1381.
208. Androulakis E, Tousoulis D, Papageorgiou N, Latsios G, Siasos G, et al. (2012) The Role of Matrix Metalloproteinases in Essential Hypertension. Curr Top Med Chem 12: 1149-1158.
209. Kampoli AM, Tousoulis D, Papageorgiou N, Antoniades C, Androulakis E, et al. (2012) Matrix Metalloproteinases in Acute Coronary Syndromes: Current Perspectives. Curr Top Med Chem 12: 1192-1205.
210. Tsioufis C, Bafakis I, Kasiakogias A, Stefanadis C (2012) The Role of Matrix Metalloproteinases in Diabetes Mellitus. Curr Top Med Chem 12: 1159-1165.
211. Stockinger B, Veldhoen M (2007) Differentiation and function of Th17 T cells. Curr Opin Immunol 19: 281-286.
212. Steinman L (2007) A brief history of T(H)17, the first major revision in the T(H)1/T(H)2 hypothesis of T cell-mediated tissue damage. Nat Med 13: 139-145.
213. Kolls JK, Linden A (2004) Interleukin-17 family members and inflammation. Immunity 21: 467-476.
214. Dong C (2006) Diversification of T-helper-cell lineages: finding the family root of IL-17-producing cells. Nat Rev Immunol 6: 329-333.
215. Chang M, Lee AJ, Fitzpatrick L, Zhang M, Sun SC (2009) NF-kappa B1 p105 regulates T cell homeostasis and prevents chronic inflammation. J Immunol 182: 3131-3138.
216. Nott P, Temple M (2009) New cell adhesion research. New York: Nova Biomedical Books. xii, 296 p. p.
217. Burns AR, Takei F, Doerschuk CM (1994) Quantitation of ICAM-1 expression in mouse lung during pneumonia. J Immunol 153: 3189-3198.
218. Beck-Schimmer B, Schimmer RC, Warner RL, Schmal H, Nordblom G, et al. (1997) Expression of lung vascular and airway ICAM-1 after exposure to bacterial lipopolysaccharide. Am J Respir Cell Mol Biol 17: 344-352.
219. Kumasaka T, Quinlan WM, Doyle NA, Condon TP, Sligh J, et al. (1996) Role of the intercellular adhesion molecule-1(ICAM-1) in endotoxin-induced pneumonia evaluated using ICAM-1 antisense oligonucleotides, anti-ICAM-1 monoclonal antibodies, and ICAM-1 mutant mice. J Clin Invest 97: 2362-2369.
220. Zelko IN, Mariani TJ, Folz RJ (2002) Superoxide dismutase multigene family: a comparison of the CuZn-SOD (SOD1), Mn-SOD (SOD2), and EC-SOD (SOD3) gene structures, evolution, and expression. Free Radic Biol Med 33: 337-349.
221. Satoh T, Takeuchi O, Vandenbon A, Yasuda K, Tanaka Y, et al. (2010) The Jmjd3-Irf4 axis regulates M2 macrophage polarization and host responses against helminth infection. Nature Immunology 11: 936-U989.

222. Kigerl KA, Gensel JC, Ankeny DP, Alexander JK, Donnelly DJ, et al. (2009) Identification of Two Distinct Macrophage Subsets with Divergent Effects Causing either Neurotoxicity or Regeneration in the Injured Mouse Spinal Cord. Journal of Neuroscience 29: 13435-13444.
223. Nair MG, Gallagher LJ, Taylor MD, Loke P, Coulson PS, et al. (2005) Chitinase and Fizz family members are a generalized feature of nematode infection with selective Upregulation of Ym1 and F10.1 by antigen-presenting cells. Infection and Immunity 73: 385-394.
224. Stein M, Keshav S, Harris N, Gordon S (1992) Interleukin 4 potently enhances murine macrophage mannose receptor activity: a marker of alternative immunologic macrophage activation. J Exp Med 176: 287-292.
225. Pahl HL (1999) Activators and target genes of Rel/NF-kappaB transcription factors. Oncogene 18: 6853-6866.
226. Vlahos R, Bozinovski S, Jones JE, Powell J, Gras J, et al. (2006) Differential protease, innate immunity, and NF-kappaB induction profiles during lung inflammation induced by subchronic cigarette smoke exposure in mice. Am J Physiol Lung Cell Mol Physiol 290: L931-945.
227. Clohisy JC, Hirayama T, Frazier E, Han SK, Abu-Amer Y (2004) NF-kB signaling blockade abolishes implant particle-induced osteoclastogenesis. Journal of Orthopaedic Research 22: 13-20.
228. Yamanaka Y, Karuppaiah K, Abu-Amer Y (2011) Polyubiquitination events mediate polymethylmethacrylate (PMMA) particle activation of NF-kappaB pathway. J Biol Chem 286: 23735-23741.
229. Nishanth RP, Jyotsna RG, Schlager JJ, Hussain SM, Reddanna P (2011) Inflammatory responses of RAW 264.7 macrophages upon exposure to nanoparticles: role of ROS-NFkappaB signaling pathway. Nanotoxicology 5: 502-516.
230. van Berlo D, Knaapen AM, van Schooten FJ, Schins RP, Albrecht C (2010) NF-kappaB dependent and independent mechanisms of quartz-induced proinflammatory activation of lung epithelial cells. Part Fibre Toxicol 7: 13.
231. Wang YC, He F, Feng F, Liu XW, Dong GY, et al. (2010) Notch signaling determines the M1 versus M2 polarization of macrophages in antitumor immune responses. Cancer Res 70: 4840-4849.
232. Martinez FO, Helming L, Gordon S (2009) Alternative activation of macrophages: an immunologic functional perspective. Annu Rev Immunol 27: 451-483.
233. Yamamoto S, Yancey PG, Zuo Y, Ma LJ, Kaseda R, et al. (2011) Macrophage polarization by angiotensin II-type 1 receptor aggravates renal injury-acceleration of atherosclerosis. Arterioscler Thromb Vasc Biol 31: 2856-2864.
234. Wu C, Li A, Leng Y, Li Y, Kang J (2012) Histone deacetylase inhibition by sodium valproate regulates polarization of macrophage subsets. DNA Cell Biol 31: 592-599.
235. Kreyling WG (1992) Intracellular particle dissolution in alveolar macrophages. Environ Health Perspect 97: 121-126.
236. Chono S, Tanino T, Seki T, Morimoto K (2007) Uptake characteristics of liposomes by rat alveolar macrophages: influence of particle size and surface mannose modification. J Pharm Pharmacol 59: 75-80.
237. Mantovani A, Sozzani S, Locati M, Allavena P, Sica A (2002) Macrophage polarization: tumor-associated macrophages as a paradigm for polarized M2 mononuclear phagocytes. Trends Immunol 23: 549-555.
238. Benoit M, Ghigo E, Capo C, Raoult D, Mege JL (2008) The uptake of apoptotic cells drives Coxiella burnetii replication and macrophage polarization: a model for Q fever endocarditis. PLoS Pathog 4: e1000066.
239. Matranga V, Corsi I (2012) Toxic effects of engineered nanoparticles in the marine environment: Model organisms and molecular approaches. Marine Environmental Research 76: 32-40.

240. Roursgaard M, Poulsen SS, Poulsen LK, Hammer M, Jensen KA, et al. (2010) Time-response relationship of nano and micro particle induced lung inflammation. Quartz as reference compound. Hum Exp Toxicol 29: 915-933.
241. Larsen ST, Roursgaard M, Jensen KA, Nielsen GD (2010) Nano titanium dioxide particles promote allergic sensitization and lung inflammation in mice. Basic Clin Pharmacol Toxicol 106: 114-117.
242. Wang J, Nikrad MP, Travanty EA, Zhou B, Phang T, et al. (2012) Innate immune response of human alveolar macrophages during influenza A infection. PLoS One 7: e29879.
243. Robinson AB, Johnson KD, Bennion BG, Reynolds PR (2012) RAGE signaling by alveolar macrophages influences tobacco smoke-induced inflammation. Am J Physiol Lung Cell Mol Physiol 302: L1192-1199.
244. Sunahara KK, Martins JO (2012) Alveolar macrophages in diabetes: friends or foes? J Leukoc Biol 91: 871-876.
245. Sibille Y, Reynolds HY (1990) Macrophages and polymorphonuclear neutrophils in lung defense and injury. Am Rev Respir Dis 141: 471-501.
246. Gotz AA, Rozman J, Rodel HG, Fuchs H, Gailus-Durner V, et al. (2011) Comparison of particle-exposure triggered pulmonary and systemic inflammation in mice fed with three different diets. Part Fibre Toxicol 8: 30.
247. Ganguly K, Upadhyay S, Irmler M, Takenaka S, Pukelsheim K, et al. (2011) Impaired resolution of inflammatory response in the lungs of JF1/Msf mice following carbon nanoparticle instillation. Respir Res 12: 94.
248. Ling J, Kumar R (2012) Crosstalk between NFkB and glucocorticoid signaling: A potential target of breast cancer therapy. Cancer Lett 322: 119-126.
249. Demchenko YN, Kuehl WM (2010) A critical role for the NFkB pathway in multiple myeloma. Oncotarget 1: 59-68.
250. Sarada S, Himadri P, Mishra C, Geetali P, Ram MS, et al. (2008) Role of oxidative stress and NFkB in hypoxia-induced pulmonary edema. Exp Biol Med (Maywood) 233: 1088-1098.
251. Perrin-Schmitt F (1992) rel, NFKB, and the Brachyury T gene. Biochim Biophys Acta 1171: 129-131.
252. Schonthaler HB, Guinea-Viniegra J, Wagner EF (2011) Targeting inflammation by modulating the Jun/AP-1 pathway. Ann Rheum Dis 70 Suppl 1: i109-112.
253. Reddy NM, Vegiraju S, Irving A, Paun BC, Luzina IG, et al. (2012) Targeted deletion of Jun/AP-1 in alveolar epithelial cells causes progressive emphysema and worsens cigarette smoke-induced lung inflammation. Am J Pathol 180: 562-574.
254. Rahman I, Gilmour PS, Jimenez LA, MacNee W (2002) Oxidative stress and TNF-alpha induce histone acetylation and NF-kappaB/AP-1 activation in alveolar epithelial cells: potential mechanism in gene transcription in lung inflammation. Mol Cell Biochem 234-235: 239-248.
255. Rao KM, Ma JY, Meighan T, Barger MW, Pack D, et al. (2005) Time course of gene expression of inflammatory mediators in rat lung after diesel exhaust particle exposure. Environ Health Perspect 113: 612-617.
256. Schleh C, Rothen-Rutishauser BM, Blank F, Lauenstein HD, Nassimi M, et al. (2012) Surfactant Protein D modulates allergen particle uptake and inflammatory response in a human epithelial airway model. Respir Res 13: 8.
257. Jia YQ, Zhao XH, Guo XB (2006) [Effects of the inhalable particle (PM10) on secretion of inflammatory factors in human lung fibroblasts and mouse alveolar macrophage cell]. Wei Sheng Yan Jiu 35: 557-560.
258. Maier KL, Alessandrini F, Beck-Speier I, Hofer TP, Diabate S, et al. (2008) Health effects of ambient particulate matter--biological mechanisms and inflammatory responses to in vitro and in vivo particle exposures. Inhal Toxicol 20: 319-337.

259. Donaldson K, Tran CL (2002) Inflammation caused by particles and fibers. Inhal Toxicol 14: 5-27.
260. Hubbard AK, Timblin CR, Shukla A, Rincon M, Mossman BT (2002) Activation of NF-kappaB-dependent gene expression by silica in lungs of luciferase reporter mice. Am J Physiol Lung Cell Mol Physiol 282: L968-975.
261. Takahashi K, Onodera S, Tohyama H, Kwon HJ, Honma K, et al. (2011) In vivo imaging of particle-induced inflammation and osteolysis in the calvariae of NFkappaB/luciferase transgenic mice. J Biomed Biotechnol 2011.
262. Luo X, Matranga C, Tan S, Alba N, Cui XT (2011) Carbon nanotube nanoreservior for controlled release of anti-inflammatory dexamethasone. Biomaterials 32: 6316-6323.
263. Minnikanti S, Pereira MG, Jaraiedi S, Jackson K, Costa-Neto CM, et al. (2010) In vivo electrochemical characterization and inflammatory response of multiwalled carbon nanotube-based electrodes in rat hippocampus. J Neural Eng 7: 16002.
264. Victor EG, Silveira PC, Possato JC, da Rosa GL, Munari UB, et al. (2012) Pulsed ultrasound associated with gold nanoparticle gel reduces oxidative stress parameters and expression of pro-inflammatory molecules in an animal model of muscle injury. J Nanobiotechnology 10: 11.
265. Howard KA, Paludan SR, Behlke MA, Besenbacher F, Deleuran B, et al. (2009) Chitosan/siRNA nanoparticle-mediated TNF-alpha knockdown in peritoneal macrophages for anti-inflammatory treatment in a murine arthritis model. Mol Ther 17: 162-168.
266. Lee HK, Lee J, Tobias PS (2002) Two lipoproteins extracted from Escherichia coli K-12 LCD25 lipopolysaccharide are the major components responsible for Toll-like receptor 2-mediated signaling. J Immunol 168: 4012-4017.
267. Campbell SJ, Anthony DC, Oakley F, Carlsen H, Elsharkawy AM, et al. (2008) Hepatic nuclear factor kappa B regulates neutrophil recruitment to the injured brain. J Neuropathol Exp Neurol 67: 223-230.
268. Kollander R, Solovey A, Milbauer LC, Abdulla F, Kelm RJ, Jr., et al. (2010) Nuclear factor-kappa B (NFkappaB) component p50 in blood mononuclear cells regulates endothelial tissue factor expression in sickle transgenic mice: implications for the coagulopathy of sickle cell disease. Transl Res 155: 170-177.
269. Oikawa K, Odero GL, Platt E, Neuendorff M, Hatherell A, et al. (2012) NF-kappaB p50 subunit knockout impairs late LTP and alters long term memory in the mouse hippocampus. BMC Neurosci 13: 45.
270. Karadimas SK, Klironomos G, Papachristou DJ, Papanikolaou S, Papadaki E, et al. (2012) Immunohistochemical Profile of NF-kappaB/p50, NF-kappaB/p65, MMP-9, MMP-2 and u-PA in Experimental Cervical Spondylotic Myelopathy. Spine (Phila Pa 1976).
271. Courtine E, Cagnard N, Mazzolini J, Antona M, Pene F, et al. (2012) Combined loss of cRel/p50 subunits of NF-kappaB leads to impaired innate host response in sepsis. Innate Immun.
272. Kabuta T, Hakuno F, Cho Y, Yamanaka D, Chida K, et al. (2010) Insulin receptor substrate-3, interacting with Bcl-3, enhances p50 NF-kappaB activity. Biochem Biophys Res Commun 394: 697-702.
273. Escalante CR, Shen L, Thanos D, Aggarwal AK (2002) Structure of NF-kappaB p50/p65 heterodimer bound to the PRDII DNA element from the interferon-beta promoter. Structure 10: 383-391.
274. Saldana M, Mullol J, Aguilar E, Bonastre M, Marin C (2007) Nuclear factor kappa-B p50 and p65 subunits expression in dementia with Lewy bodies. Neuropathol Appl Neurobiol 33: 308-316.
275. Gadjeva M, Wang Y, Horwitz BH (2007) NF-kappaB p50 and p65 subunits control intestinal homeostasis. Eur J Immunol 37: 2509-2517.

276. Dooher JE, Paz-Priel I, Houng S, Baldwin AS, Jr., Friedman AD (2011) C/EBPalpha, C/EBPalpha oncoproteins, or C/EBPbeta preferentially bind NF-kappaB p50 compared with p65, focusing therapeutic targeting on the C/EBP:p50 interaction. Mol Cancer Res 9: 1395-1405.
277. Martinez-Micaelo N, Gonzalez-Abuin N, Terra X, Richart C, Ardevol A, et al. (2012) Omega-3 docosahexaenoic acid and procyanidins inhibit cyclo-oxygenase activity and attenuate NF-kappaB activation through a p105/p50 regulatory mechanism in macrophage inflammation. Biochem J 441: 653-663.
278. Wessells J, Baer M, Young HA, Claudio E, Brown K, et al. (2004) BCL-3 and NF-kappaB p50 attenuate lipopolysaccharide-induced inflammatory responses in macrophages. J Biol Chem 279: 49995-50003.
279. Elsharkawy AM, Oakley F, Lin F, Packham G, Mann DA, et al. (2010) The NF-kappaB p50:p50:HDAC-1 repressor complex orchestrates transcriptional inhibition of multiple pro-inflammatory genes. J Hepatol 53: 519-527.
280. Conner JR, Smirnova, II, Moseman AP, Poltorak A (2010) IRAK1BP1 inhibits inflammation by promoting nuclear translocation of NF-kappaB p50. Proc Natl Acad Sci U S A 107: 11477-11482.
281. Park HJ, Lee SH, Son DJ, Oh KW, Kim KH, et al. (2004) Antiarthritic effect of bee venom: inhibition of inflammation mediator generation by suppression of NF-kappaB through interaction with the p50 subunit. Arthritis Rheum 50: 3504-3515.
282. Serbina NV, Jia T, Hohl TM, Pamer EG (2008) Monocyte-mediated defense against microbial pathogens. Annu Rev Immunol 26: 421-452.
283. Mege JL, Capo C (2010) [Is macrophage polarization the Gordian knot of bacterial infections?]. Med Sci (Paris) 26: 83-88.
284. Aldridge JR, Jr., Moseley CE, Boltz DA, Negovetich NJ, Reynolds C, et al. (2009) TNF/iNOS-producing dendritic cells are the necessary evil of lethal influenza virus infection. Proc Natl Acad Sci U S A 106: 5306-5311.
285. De Trez C, Magez S, Akira S, Ryffel B, Carlier Y, et al. (2009) iNOS-producing inflammatory dendritic cells constitute the major infected cell type during the chronic Leishmania major infection phase of C57BL/6 resistant mice. PLoS Pathog 5: e1000494.
286. Lykens JE, Terrell CE, Zoller EE, Divanovic S, Trompette A, et al. (2010) Mice with a selective impairment of IFN-gamma signaling in macrophage lineage cells demonstrate the critical role of IFN-gamma-activated macrophages for the control of protozoan parasitic infections in vivo. J Immunol 184: 877-885.
287. Ferin J (1982) Pulmonary alveolar pores and alveolar macrophage-mediated particle clearance. Anat Rec 203: 265-272.
288. Lehnert BE, Valdez YE, Tietjen GL (1989) Alveolar macrophage-particle relationships during lung clearance. Am J Respir Cell Mol Biol 1: 145-154.
289. Kleinman MT, Sioutas C, Chang MC, Boere AJ, Cassee FR (2003) Ambient fine and coarse particle suppression of alveolar macrophage functions. Toxicol Lett 137: 151-158.
290. Tao F, Kobzik L (2002) Lung macrophage-epithelial cell interactions amplify particle-mediated cytokine release. Am J Respir Cell Mol Biol 26: 499-505.
291. Mantovani A, Sica A, Sozzani S, Allavena P, Vecchi A, et al. (2004) The chemokine system in diverse forms of macrophage activation and polarization. Trends Immunol 25: 677-686.
292. Bosschaerts T, Morias Y, Stijlemans B, Herin M, Porta C, et al. (2011) IL-10 limits production of pathogenic TNF by M1 myeloid cells through induction of nuclear NF-kappaB p50 member in Trypanosoma congolense infection-resistant C57BL/6 mice. Eur J Immunol 41: 3270-3280.

293. Kizaki T, Suzuki K, Hitomi Y, Iwabuchi K, Onoe K, et al. (2001) Negative regulation of LPS-stimulated expression of inducible nitric oxide synthase by AP-1 in macrophage cell line J774A.1. Biochem Biophys Res Commun 289: 1031-1038.
294. Zhou J, Dehne N, Brune B (2009) Nitric oxide causes macrophage migration via the HIF-1-stimulated small GTPases Cdc42 and Rac1. Free Radic Biol Med 47: 741-749.
295. Hu X, Herrero C, Li WP, Antoniv TT, Falck-Pedersen E, et al. (2002) Sensitization of IFN-gamma Jak-STAT signaling during macrophage activation. Nat Immunol 3: 859-866.
296. Dubourdeau M, Pipy B, Rousseau D (2010) [Roles of PPAR and p21WAF1/CIP1 in monocyte/macrophage differentiation: are circulating monocytes able to proliferate?]. Med Sci (Paris) 26: 481-486.
297. Ellrichmann G, Thone J, Lee DH, Rupec RA, Gold R, et al. (2012) Constitutive activity of NF-kappa B in myeloid cells drives pathogenicity of monocytes and macrophages during autoimmune neuroinflammation. J Neuroinflammation 9: 15.
298. Nakagawa M, Shimabe M, Watanabe-Okochi N, Arai S, Yoshimi A, et al. (2011) AML1/RUNX1 functions as a cytoplasmic attenuator of NF-kappaB signaling in the repression of myeloid tumors. Blood 118: 6626-6637.
299. Maeda S, Hikiba Y, Sakamoto K, Nakagawa H, Hirata Y, et al. (2011) Colon cancer-derived factors activate NF-kappaB in myeloid cells via TLR2 to link inflammation and tumorigenesis. Mol Med Report 4: 1083-1088.
300. Saccani A, Schioppa T, Porta C, Biswas SK, Nebuloni M, et al. (2006) P50 nuclear factor-kappa B overexpression in tumor-associated macrophages inhibits M1 inflammatory responses and antitumor resistance. Cancer Research 66: 11432-11440.
301. Porta C, Rimoldi M, Mantovani A, Sica A (2008) p50 NF-kappa B overexpression in tumor associated macrophages inhibits M1 inflammatory responses and antitumor resistance. Cytokine 43: 274-275.
302. Joshi AD, Oak SR, Hartigan AJ, Finn WG, Kunkel SL, et al. (2010) Interleukin-33 contributes to both M1 and M2 chemokine marker expression in human macrophages. BMC Immunol 11: 52.
303. Zhang HL, Hassan MY, Zheng XY, Azimullah S, Quezada HC, et al. (2012) Attenuated EAN in TNF-alpha Deficient Mice Is Associated with an Altered Balance of M1/M2 Macrophages. PLoS One 7: e38157.
304. Heusinkveld M, de Vos van Steenwijk PJ, Goedemans R, Ramwadhdoebe TH, Gorter A, et al. (2011) M2 macrophages induced by prostaglandin E2 and IL-6 from cervical carcinoma are switched to activated M1 macrophages by CD4+ Th1 cells. J Immunol 187: 1157-1165.
305. Yoo MS, Lee KT (2011) Anti-Inflammatory Effects of Fucosterol Via the Suppression of Nf-Kb Pathway and P38 Pathway in Lps-Induced Raw264.7 Macrophage Cells. Inflammation Research 60: 282-282.
306. Prabhu KS, Davis F, Bhat D, Reddy CC (2004) Selenium suppresses LPS-induced NF-kB activation of cyclooxygenase-2 by inhibiting IkBa phosphorylation in a mouse macrophage cell. Faseb Journal 18: C99-C99.
307. Kluth DC, Wilson HM, Rees AJ (2003) Inhibition of NF-kB attenuates macrophage IFN-gamma responses. Journal of the American Society of Nephrology 14: 168a-169a.
308. Sica A, Mantovani A (2012) Macrophage plasticity and polarization: in vivo veritas. Journal of Clinical Investigation 122: 787-795.
309. Porta C, Rimoldi M, Raes G, Brys L, Ghezzi P, et al. (2009) Tolerance and M2 (alternative) macrophage polarization are related processes orchestrated by p50 nuclear factor kappa B. Proceedings of the National Academy of Sciences of the United States of America 106: 14978-14983.

310. Hagemann T, Biswas SK, Lawrence T, Sica A, Lewis CE (2009) Regulation of macrophage function in tumors: the multifaceted role of NF-kappa B. Blood 113: 3139-3146.
311. Martinez FO, Sica A, Mantovani A, Locati M (2008) Macrophage activation and polarization. Frontiers in Bioscience-Landmark 13: 453-461.
312. Tomlinson GS, Booth H, Petit SJ, Potton E, Towers GJ, et al. (2012) Adherent human alveolar macrophages exhibit a transient pro-inflammatory profile that confounds responses to innate immune stimulation. PLoS One 7: e40348.
313. Wynn TA (2011) Integrating mechanisms of pulmonary fibrosis. J Exp Med 208: 1339-1350.
314. Xu F, Droemann D, Rupp J, Shen H, Wu X, et al. (2008) Modulation of the inflammatory response to Streptococcus pneumoniae in a model of acute lung tissue infection. Am J Respir Cell Mol Biol 39: 522-529.
315. Knapp S, Leemans JC, Florquin S, Branger J, Maris NA, et al. (2003) Alveolar macrophages have a protective antiinflammatory role during murine pneumococcal pneumonia. Am J Respir Crit Care Med 167: 171-179.

8. Abbreviations

°C	Degrees Celsius
µl	Microliter
Ab	antibody
Actb	Actin, beta
ALI	acute lung injury
AMs	Aveloar macrophages
AP-1	Activator protein 1
BAL	Bronchoalveolar lavage
BALF	BAL flluid
BET	Brunauer, Emmett, and Teller
BSA	Bovine serum albumin
cDNA	Complementary DNA
CNP	Carbon nanoparticle
COPD	chronic obstructive pulmonary disease
C_t	Threshold cycle
CS	cigarette smoke
DMEM	Dulbecco's Modified Eagle Medium
DNA	Deoxyribonucleic acid
DTT	Dithiothreitol
E.coli	Escherichia coli
EDTA	Ethyldiaminetetraacetate
ELISA	Enzyme-linked immunosorbent assay
EMSA	Electrophoretic mobility shift assay
g	gram
Gapdh	Glyceraldehyde-3-phosphate dehydrogenase
GM-CSF	Granulocyte-macrophage colony-stimulating factor
GOI	Gene of interest
HKGs	Housekeeping genes
Hprt	hypoxanthine phosphoribosyltransferase
HRP	horseradish peroxidase
JNK	Jun-N-terminal kinases
KO, -/-	Knock out
L	Liter
LDH	lactate dehydrogenase
LPS	Lipopolysaccharides
M1 macrophages	classic activated macrophages
M2 macrophages	alternative activated macrophages
MAPK	Mitogen-activated protein kinases
M-CSF	Macrophage colony-stimulating factor
ml	Milliliter

mm	Millimetre
NFkB	nuclear factor kappa-light-chain-enhancer of activated B cells
OC	organic content
OD	optical density
PBS	Phosphate buffer saline
PBST	phosphate buffered saline with Tween 20
PCR	Polymerase chain reaction
PMNs	polymorphonuclear leukocytes
qPCR	quantitative real-time polymerase chain reaction
RIPA	radioimmunoprecipitation assay buffer
RNA	Ribose nucleic acid
Rpl13a	ribosomal protein L13A
RT-PCR	Reverse transcription PCR
SDS-PAGE	sodium dodecyl sulfate polyacrylamide gel electrophoresis
SEM	standard error of the mean
SPF	Specific pathogen-free
STAT	signal transducer and activator of transcription
TAE	tris acetate with EDTA
TAM	tumor-associated macrophages
TBE	tris borate with EDTA
TBP	TATA box binding protein
TEM	transmission electron microscopy
TLR	Toll-like receptor
WT	Wild type

Appendix 1

R. Yin, X. Liu, C. Liu, Z. Ding, X. Zhang, F. Tian, W. Liu, J. Yu, L. Li, M.H. de Angelis, T. Stoeger, Systematic selection of housekeeping genes for gene expression normalization in chicken embryo fibroblasts infected with Newcastle disease virus, Biochem Biophys Res Commun 413(2011) 537-540.

Renfu Yin's contributions:

Renfu Yin was conceived and designed of the whole study, performed statistical data analysis and wrote the paper.

Biochemical and Biophysical Research Communications 413 (2011) 537–540

Contents lists available at SciVerse ScienceDirect

Biochemical and Biophysical Research Communications

journal homepage: www.elsevier.com/locate/ybbrc

Systematic selection of housekeeping genes for gene expression normalization in chicken embryo fibroblasts infected with Newcastle disease virus

Renfu Yin [a,b,c,1], Xinxin Liu [e,1], Chang Liu [f,1], Zhuang Ding [a,*], Xiaodong Zhang [a], Furong Tian [c], Weihong Liu [e], Jinghai Yu [e], Lin Li [g], Martin Hrabé de Angelis [b,d], Tobias Stoeger [c]

[a] Department of Veterinary Preventive Medicine, College of Animal Science and Veterinary Medicine, Jilin University, Xi'an Road 5333, Changchun, Jilin 130062, China
[b] Lehrstuhl für Experimentelle Genetik, Technische Universität München, Freising-Weihenstephan 85354, Germany
[c] Comprehensive Pneumology Center, Institute of Lung Biology and Disease, Helmholtz Zentrum München, Ingolstädter Landstraße 1, D-85764 Munich, Germany
[d] Institute of Experimental Genetics, Helmholtz Zentrum München, Ingolstädter Landstraße 1, D-85764 Munich, Germany
[e] College of Quartermaster Technology, Jilin University, Xi'an Road 5333, Changchun, Jilin 130062, China
[f] Department of Food Science, College of Agriculture, Yanbian University, Gongyuan 977, Yanji, Jilin 133002, China
[g] Institute of Animal Husbandry and Veterinary Science of Jilin, Xi'an Road 4510, Changchun, Jilin 130062, China

ARTICLE INFO

Article history:
Received 10 August 2011
Available online 6 September 2011

Keywords:
Newcastle disease virus
Housekeeping gene
qRT-PCR
Chicken embryo fibroblasts

ABSTRACT

Gene expression analysis is frequently used to analyze the response to viral infection, and 18S RNA, SHDA and GAPDH represent popular house keeping genes (HKGs) often used to normalize gene expression. Here we describe the first systematic selection and evaluation of suitable HKGs for gene expression analysis in chicken embryo fibroblasts (CEF) infected with NDV adapted to the guidelines from Gorzelniak and Ferguson. Our results indicate that ACTB, HPRT1 and HMBS were valuable and stable HKGs, while 18S RNA, GAPDH and SHDA are considerably regulated during the course of infection and thus precluded for normalization. Normalizing the infection dependent gene IFN-a and the infection independent gene B2M to inappropriate HKGs consequently misleads to significant errors in estimating their regulations. Our study emphasizes that even the most popular HKGs like 18S RNA and GAPDH can lead to divergent and inaccurate data interpretation of significant magnitude if not carefully analyzed for stability before.

1. Introduction

With the current rise in NDV-caused economic losses [1] on the one hand and its use as a promising oncolytic agent [2] on the other hand, real-time quantitative reverse transcription-polymerase chain reaction (qRT-PCR) has become a widely used method to assess transcriptional profiles of NDV-related target genes. However, this widely used method relies on a correction for intersample variability by normalizing to one or more HKGs whose expression should not change due to treatment or study conditions [3,4]. Therefore, it is import to distinguish technical variability from true biological changes in gene expression. To our knowledge, there are so far no studies aiming to optimize the HKG selection for gene expression studies upon NDV infection.

For this purpose, we chose to use the guidelines previously described by Gorzelniak and Ferguson [4,5], applying the criterion of $\Delta Ct \leqslant \pm 0.5$ as a delimiter of reference gene suitability. This criteria bases on the assumption that relative expression levels of HKG varying between 0.7 and 1.4, are considered as fluctuations in gene expression which is largely due to technical variance that should be reflected similarly between both housekeeping and target genes; while $\Delta Ct > \pm 0.5$ (relative expression beyond out between 0.7 and 1.4) are suggestive of biological variability resulting from treatment or experimental conditions, precluding the use of such HKG for target gene normalization.

2. Material and methods

In the present study, NDV strain NA-1 was purified directly from the allantoic fluid and primary CEF were prepared from 10-day-old specific pathogen-free (SPF) chicken eggs as has been described previously [6]. 0.4×10^6 CEF cells per well were seeded into 24-well plates 1 day before viral treatment. When the cells reached 70–80% confluence, the cells were washed and overlaid with 100 μl serum-free E-MEM medium containing virus suspensions at a multiplicity of infection (MOI) of 10. CEF supernatant was completely removed at 12, 24, 48 and 72 h after viral infection and 800 μl of ZR RNA Buffer (ZYMO, Beijing, China) were directly

* Corresponding author. Fax: +86 431 87836171
E-mail address: renfu.yin@helmholtz-muenchen.de (Z. Ding).
[1] These authors contributed equal to this study.

0006-291X/$ - see front matter © 2011 Elsevier Inc. All rights reserved.
doi:10.1016/j.bbrc.2011.08.131

9. Appendix

Table 1
Primer sequences and amplicon characteristics of housekeeping genes and target genes in this study.

Symbol	Gene name	Sequence	Ampicon (bp)	Accession number
ACTB	Beta-actin	F: cagacatcagggtgtgatgg R: tcaggggctactctcagctc	183	L08165.1
GAPDH	Glyceraldehyde-3-phosphate dehydrogenase	F: tgggcagatgcaggtgctga R: tggtgcacgatgcattgctgaga	201	X01578.1
18S RNA	18S ribosomal RNA	F: ggcggctttggtgactctag R: atcgaaccctgattccccgt	148	AF173612.1
HMBS	Hydroxymethylbilane synthase	F: ggctgggagaatcgcatagg R: tcctgcagggcagataccat	131	XM 417846.2
HPRT1	Hypoxanthine phosphorribosyltransferase 1	F: tggtggggatgacctctcaa R: ggccgatatcccacacttcg	177	NM 204848.1
SDHA	Succinate dehydrogenase complex, subunit A	F: ttcccgttttgcctacggtg R: ctgcctcgccacaagcatat	126	XM 419054.2
IFN-a	Interferon alpha	F: agcaatgcttggacagcag R:aggcgctgtaatcgttgtct	123	GU119896.1
B2M	Beta-2-microglobulin	F:aaggagccgcaggtctac R: cttgctctttgccgtcatac	151	NM 001001750.1

added into each well for total RNA isolation. First strand cDNA synthesis, qRT-PCR performance with SYBR green and statistical data analysis have been described in our previous studies [6,7]. Sample reactions, including negative controls, were performed in triplicate in a 96 well plate. All experiments were performed in two independent repetitions. All validation data were converted to fold-changes using the $2^{-\Delta Ct}$ method for the raw data or $2^{-\Delta\Delta Ct}$ for normalized data. All experimental protocols were reviewed and approved by the Experimental Animal Council of Jilin University, China.

3. Results

3.1. Transcription of candidate housekeeping genes in CEF is affected upon NDV infection

The transcriptional profiles of six commonly used HKGs (for gene information see Table 1) in NDV infected CEFs over a time of up to 72 h were examined using absolute Ct values. All HKGs showed moderate to high expression with a mean Ct value below 25 for each gene (Fig. 1A). As shown in Fig. 1A, the expression levels of 18S RNA

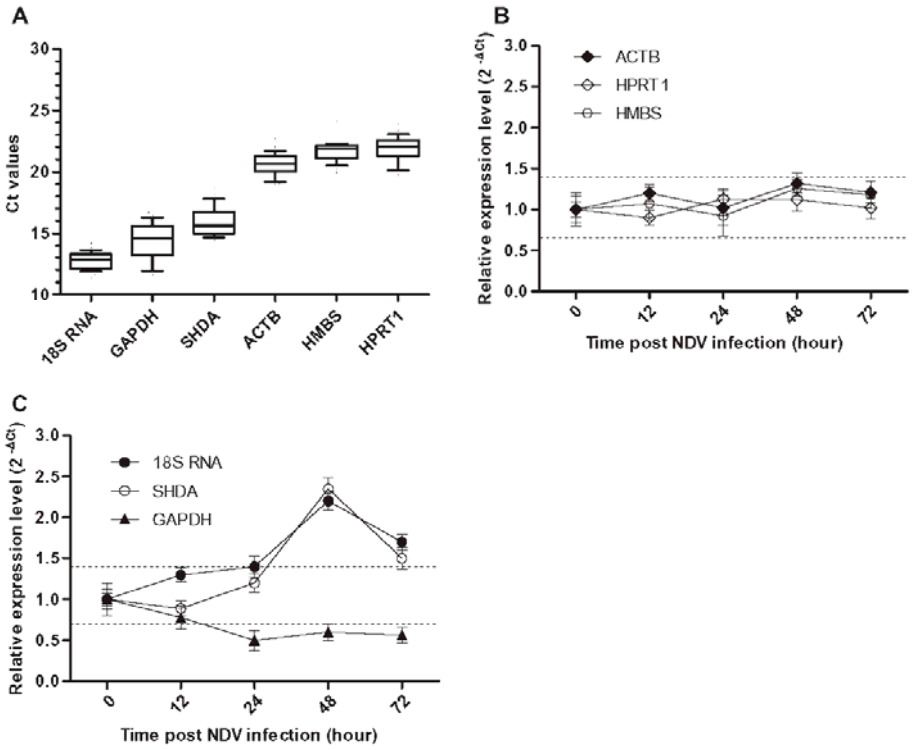

Fig. 1. Transcriptional profiles of 6 housekeeping genes in chicken embryo fibroblasts over time up to 72 h infected with Newcastle disease virus strain NA-1 at an MOI of 10. The raw cycle threshold (Ct) values of each housekeeping gene in all samples ($n = 27$) are plotted in a box-and-whisker diagram (A). Boxes represent the interquartile interval (25–75%) with median value (50%); whiskers represent the 90th and 10th percentiles, respectively. Fold changes in housekeeping genes that fell within (B) and outside (C) the $\Delta Ct \leqslant \pm 0.5$ limits of suitability ($n = 5$–6).

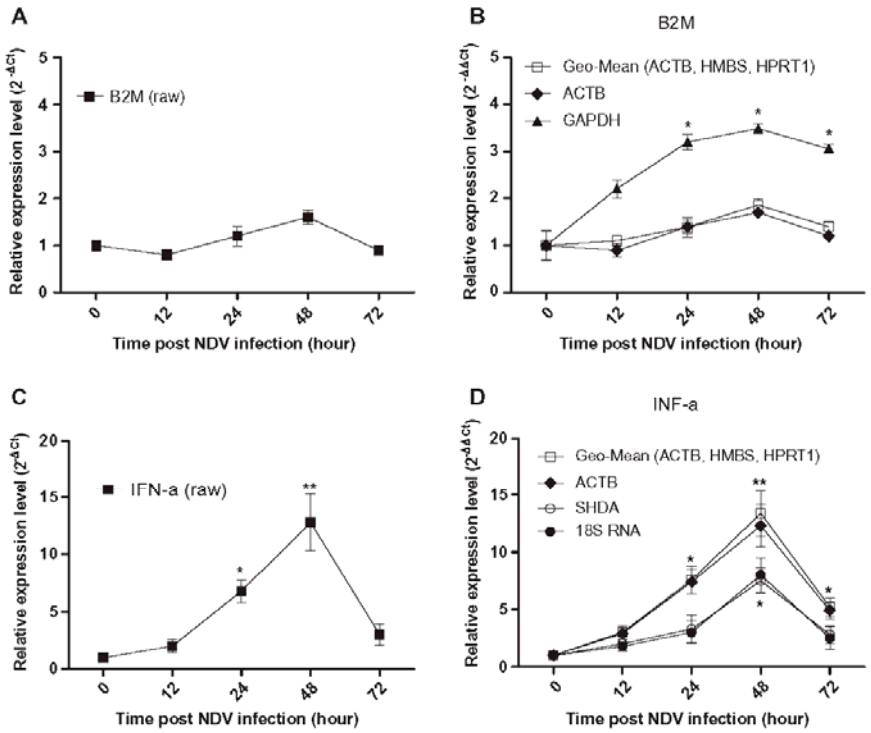

Fig. 2. Gain or loss of statistical significance of target genes with inappropriate housekeeping gene selection in CEF infected with NDV. Fold changes for both, B2M gene expression without (A) or with normalization (B) to the geometric mean of three housekeeping genes (ACTB, SHDA and HMBS), ACTB, or GAPDH and IFN-a gene expression without (C) or with normalization (D) to the geometric mean of three housekeeping genes (ACTB, SHDA and HMBS), ACTB, SHDA, or 18s RNA. Asterisks indicates significant differences between treated and untreated samples ($n = 5–6$; $^{*}p < 0.05$; $^{**}p < 0.01$).

was highest, with mean Ct values at 13 cycles, followed by the HKGs GAPDH and SHDA, with mean Ct values between 15 and 16 whereas ACT, HMBS and HPRT displayed the lowest levels with median Ct values between 21 and 22. Among the 6 HKGs, the maximum and the minimum variation of the expression range during the course of infection were 5.1 cycles for GAPDH and 1.7 cycles for HMBS, respectively. In a next step, these HKGs as a delimiter of HKG suitability were evaluated using the criterion of $\Delta Ct \leqslant \pm 0.5$. As illustrated in Fig. 1B, the relative expression of 50% of the HKGs tested (ACTB, HPRT1 and HMBS) fluctuated within the $\Delta Ct \leqslant \pm 0.5$ limits in a manner that would be consistent as tolerable intersample variability and thus, considered suitable for the use as normalization gene in our study (Fig. 1B). However, 18S RNA and SHDA increased steadily and exceeded the $\Delta Ct \leqslant \pm 0.5$ ranges at more one time point (Fig. 1C); in contrast, GAPDH was the only one HKG that steadily and consistently dropped and crossed the $\Delta Ct \leqslant \pm 0.5$ limit 24 h post-NDV infection (Fig. 1C). The relative fold changes for GAPDH, 18S RNA or SHDA were likely to be due to biological variability, possibly related to the cellular response to NDV infection, thus precluding these commonly used HKGs for normalization under these experimental conditions.

3.2. Gain of statistical significance with the error using housekeeping gene

To assess the impact of the error using GAPDH as a HKG, we examined relative expression of B2M without and with normalization to either ACTB, the geometric mean of three stable HKGs (ACTB, HMBS and HPRT1) or GAPDH in CEF treated with NDV over the time up to 72 h. B2M was chosen for this experiment as a target gene that is assumingly not responsive to NDV infection [8]. Fig. 2B illustrates that the fold changes in B2M gene expression, either normalized to ACTB or the geometric mean of the three stable HKGs matches well with the changes observed for the raw B2M levels without normalization (Fig. 2A), where all data points during the treatment remain unchanged compared to the untreated control. In contrast, when B2M was normalized to GAPDH, the decline in GAPDH abundance relates to a fatal overestimation of the B2M expression, suggesting levels significantly different from the untreated control in particular for those time points where the $\Delta Ct \leqslant \pm 0.5$ delimiter range was exceed (Fig. 2B). Thus, normalizing B2M to GAPDH resulted in an inaccurate gain of significance that did not occur with ACTB or the geometric mean of stable HKGs.

3.3. Loss of statistical significance with inappropriate housekeeping gene selection

Next we examined the impact of the $\Delta Ct \leqslant \pm 0.5$ limits exceeding HKGs on IFN-a, a target gene whose expression is known to be significantly increase upon NDV infection [9,10]. We evaluated its relative expression without and with normalization to either ACTB, the geometric mean of three stable HKGs (ACTB, HMBS and HPRT1), SHDA or 18S RNA under the same experimental condition. Normalization of IFN-a to ACTB or the geometric mean of the three stable HKGs resulted in fold changes of gene expression (Fig. 2D) that were nearly identical to fold changes of the raw expression without normalization (Fig. 2C) where 24 h post-infection yielded 7.6-fold induction in target gene expression that increased to

13-fold induction by 48 h following a decrease to a 5-fold induction for 72 h. These results were very similar to the well-documented expression profile of IFN-a during NDV infection as analyzed by qPCR [10,11]. In contrast, however, the increases in gene expression at 24 h and 72 h post-infection were not significant when IFN-a was normalized to SHDA or 18S RNA, where the 7.6-fold and 5-fold induction of the HKG ablated the 4.6-fold and 2.5-fold induction of the target gene (Fig. 2D). Although considering the normalization to ACTB, INF-a expression appeared to be significantly increased by 7-fold 48 h post-infection, this is remarkably enough a 5-fold decreased induction as compared to normalization of the geometric mean of the three stable HKGs. Thus, normalizing IFN-a to SHDA or 18S RNA upon NDV infection over a time up to 72 h resulted in an inaccurate loss of significance in change of gene expression that did not occur with ACTB or the geometric mean of three stable HKGs.

4. Discussion

Our here presented data reconfirms that a statistically significant difference in gene expressions between experimental groups may be present or absent in dependence on the HKG used for expression normalization, and this even if the variability in HKG expression seems marginal [4,12–15]. Comparing the outcome of normalizing to among ACTB, 18S RNA or GAPDH, we present data from two genes; B2M, whose raw profile did not vary over time following NDV treatment; and IFN-a, which significantly increased under the same experimental conditions. Neither the expression profile nor the significance in gene expression of either gene was markedly influenced by normalized to ACTB or the geometric mean of three stable HKGs. In contrast, normalizing B2M to GAPDH resulted in an inaccurate gain of significance as well as IFN-a to either 18S RNA or SHDA resulted in an inappropriate loss of significance, respectively, demonstrating even small variation in HKG can have a significance influence on statistical outcome.

In summary, we validated six commonly used HKGs for the purpose of interpreting the impact of HKG selection on normalization of two target genes in chicken embryo fibroblast following NDV treatment over a time up to 72 h. Here presented data plausibly demonstrates that the use of unvalidated controls can led to flawed outcomes where reported changes in target gene expression were actually due to changes in HKG expression. Until HKGs are evaluated with respect to the individual conditions, the erroneous impact of inappropriate HKG selection on data interpretation and biological outcome will undoubtedly continue to contribute to inaccurate conclusions and inconsistencies between reports.

Acknowledgments

Financial support was provided by National Natural Science Foundation of China (30771606) and China Scholarship Council (CSC). R.Y. is the recipient of a fellowship of CSC (200817097).

References

[1] Y.M. Saif, H.J. Barnes, Diseases of poultry, 12th ed., Blackwell Publishing Professional, Ames, Iowa, 2008.
[2] J.G. Sinkovics, J.C. Horvath, Newcastle disease virus (NDV): brief history of its oncolytic strains, J. Clin. Virol. 16 (2000) 1–15.
[3] J. Huggett, K. Dheda, S. Bustin, A. Zumla, Real-time RT-PCR normalisation; strategies and considerations, Genes Immun. 6 (2005) 279–284.
[4] B.S. Ferguson, H. Nam, R.G. Hopkins, R.F. Morrison, Impact of reference gene selection for target gene normalization on experimental outcome using real-time qRT-PCR in adipocytes, PLoS One 5 (2010) e15208.
[5] K. Gorzelniak, J. Janke, S. Engeli, A.M. Sharma, Validation of endogenous controls for gene expression studies in human adipocytes and preadipocytes, Horm. Metab. Res. 33 (2001) 625–627.
[6] R. Yin, Z. Ding, X. Liu, L. Mu, Y. Cong, T. Stoeger, Inhibition of Newcastle disease virus replication by RNA interference targeting the matrix protein gene in chicken embryo fibroblasts, J. Virol. Methods 167 (2010) 107–111.
[7] R. Yin, F. Tian, B. Frankenberger, M.H. de Angelis, T. Stoeger, Selection and evaluation of stable housekeeping genes for gene expression normalization in carbon nanoparticle-induced acute pulmonary inflammation in mice, Biochem. Biophys. Res. Commun. 399 (2010) 531–536.
[8] P. Chitra, B. Bakthavatsalam, T. Palvannan, Beta-2 microglobulin as an immunological marker to assess the progression of human immunodeficiency virus infected patients on highly active antiretroviral therapy, Clin. Chim. Acta 412 (2011) 1151–1154.
[9] M. Balenovic, V. Savic, A. Ekert Kabalin, L. Jurinovic, W.L. Ragland, Abundance of IFN-alpha and IFN-gamma gene transcripts and absence of IL-2 transcripts in the blood of chickens vaccinated with live or inactivated NDV, Acta Vet. Hung. 59 (2011) 141–148.
[10] H. Schwarz, O. Harlin, A. Ohnemus, B. Kaspers, P. Staeheli, Synthesis of IFN-beta by virus-infected chicken embryo cells demonstrated with specific antisera and a new bioassay, J. Interferon Cytokine Res. 24 (2004) 179–184.
[11] A. Hoss, E.C. Zwarthoff, R. Zawatzky, Differential expression of interferon alpha and beta induced with Newcastle disease virus in mouse macrophage cultures, J. Gen. Virol. 70 (Pt 3) (1989) 575–589.
[12] K. Dheda, J.F. Huggett, J.S. Chang, L.U. Kim, S.A. Bustin, M.A. Johnson, G.A. Rook, A. Zumla, The implications of using an inappropriate reference gene for real-time reverse transcription PCR data normalization, Anal. Biochem. 344 (2005) 141–143.
[13] N.V. Demidenko, M.D. Logacheva, A.A. Penin, Selection and validation of reference genes for quantitative real-time PCR in buckwheat (*Fagopyrum esculentum*) based on transcriptome sequence data, PLoS One 6 (2011) e19434.
[14] S. Wierschke, S. Gigout, P. Horn, T.N. Lehmann, C. Dehnicke, A.U. Brauer, R.A. Deisz, Evaluating reference genes to normalize gene expression in human epileptogenic brain tissues, Biochem. Biophys. Res. Commun. 403 (2010) 385–390.
[15] M.B. Maess, S. Sendelbach, S. Lorkowski, Selection of reliable reference genes during THP-1 monocyte differentiation into macrophages, BMC Mol. Biol. 11 (2010) 90.

Appendix 2

R. Yin, F. Tian, B. Frankenberger, M.H. de Angelis, T. Stoeger, Selection and evaluation of stable housekeeping genes for gene expression normalization in carbon nanoparticle-induced acute pulmonary inflammation in mice, Biochem Biophys Res Commun 399 (2010) 531-536.

Renfu Yin's contributions:

Renfu Yin was involved in the conceiving and designing of the study, was responsible for all experimental parts of the study, performed statistical data analysis and wrote the paper.

Biochemical and Biophysical Research Communications 399 (2010) 531–536

Contents lists available at ScienceDirect

Biochemical and Biophysical Research Communications

journal homepage: www.elsevier.com/locate/ybbrc

Selection and evaluation of stable housekeeping genes for gene expression normalization in carbon nanoparticle-induced acute pulmonary inflammation in mice

Renfu Yin [a,c,d], Furong Tian [a], Birgit Frankenberger [a], Martin Hrabé de Angelis [b,c], Tobias Stoeger [a,*]

[a] Comprehensive Pneumology Center, Institute of Lung Biology and Disease (iLBD), Helmholtz Zentrum München, Ingolstädter Landstraße 1, D-85764 Neuherberg/Munich, Germany
[b] Institute of Experimental Genetics, Helmholtz Zentrum München, Ingolstädter Landstraße 1, D-85764 Neuherberg/Munich, Germany
[c] Lehrstuhl für Experimentelle Genetik, Technische Universität München, Freising Weihenstephan 85354, Germany
[d] Department of Veterinary Preventive Medicine, College of Animal Science and Veterinary Medicine, Jilin University, Xi'an Road 5333, Changchun, Jilin 130062, China

ARTICLE INFO

Article history:
Received 16 July 2010
Available online 1 August 2010

Keywords:
Housekeeping genes
Acute lung inflammation
NF-κB
Quantitative RT-PCR

ABSTRACT

Quantitative reverse transcription-polymerase chain reaction (qRT-PCR) is a highly specific and sensitive technique for the quantification of gene expression on the mRNA levels. But use of unconfirmed housekeeping genes (HKGs) could lead to misinterpretation of the expression of genes of interest (GOI). In this study, the stability and suitability of 11 frequently used housekeeping genes, namely 18S rRNA, ACTB, B2M, CYPA, GADPH, GUSB, HMBS, HPRT1, RPL13A, SDHA and TBP in 36 lung tissues isolated from either wild-type (WT) mice or p50 knock out (p50 /) mice or p105 knock-out (p105 /) mice which were treated with either carbon nanoparticle (CNP) or H_2O or non-treated, have been validated by geNorm, NormFinder and BestKeeper programs. The expression levels of ACTB, GUSB and RPL13A were the most constant in lung tissues across three genotypes and three kinds of treatments. A set of three most stable genes is found sufficient to be used as housekeeping genes for lung tissues in studies of similar design.

1. Introduction

Inhalation of carbon nanoparticles (CNP), a main constituent of urban air pollution, is believed to trigger pulmonary or even systemic inflammation via the generation of oxidative stress [1,2]. The redox-sensitive transcription factor NF-κB, which controls a majority of inflammatory genes, is thought to play an important role in onset of pulmonary inflammation [3,4]. In mammalian cells, the NF-κB family is composed of five members, NF-κB1 (p50, precursor p105), NF-κB2 (p52, precursor p100), RelA, RelB and c-Rel, which function as various hetero- and homo-dimmers [5]. It has been reported that NF-κB1 (p50 and p105) plays import roles in NF-κB functions, however, whether the subunit p50 and p105 of NF-κB could control acute pulmonary inflammation and injury after 24 h upon CNP treatment is not clear.

One approach to understanding p50 and p105 roles in CNP-induced acute pulmonary inflammation is to study gene expression in animal models using qRT-PCR. The data obtained by qRT-PCR are typically normalized with an internal control, often referred to as a housekeeping gene. However, the use of unconfirmed HKGs may lead to misinterpretation of the expression of GOI. Up to now, several mathematical methods, such as geNorm [6], NormFinder [7] and BestKeeper [8], have been developed to analyze the variability of the expression of candidate HKG. The ideal HKG for qRT-PCR would be one whose mRNA is consistently expressed at the same level in all samples under investigation, regardless of tissue type, disease state, medication or experimental conditions, and could have expression levels comparable to that of the target [9–11].

However, a systematic study of the suitability of HKGs for qRT-PCR normalization in the field of CNP-induced acute pulmonary inflammation has thus far been lacking. Therefore, the aim of the present study is to identify candidate genes in the CNP-induced acute pulmonary inflammation models that could be used in qRT-PCR experiments as housekeeping genes to normalize the expression of GOI.

2. Methods

2.1. Animal treatment and lung tissue processing

Animal treatment and lung tissue processing as described in our previous studies [1,35]. Briefly, all mice were female, 10–12 weeks of age with body weights between 17.39 and 20.5 g during the study. Each of three genetically modified mice consisted of three

* Corresponding author at: Institute of Lung Biology and Disease (iLBD), Helmholtz Zentrum München, Ingolstädter Landstraße 1, D-85764 Neuherberg/Munich, Germany. Fax: +49 (0) 89 3187 2400.
E-mail address: tobias.stoeger@helmholtz-muenchen.de (T. Stoeger).

0006-291X/$ - see front matter © 2010 Elsevier Inc. All rights reserved.
doi:10.1016/j.bbrc.2010.07.104

9. Appendix

groups (each group consisted of between 6 and 8 animals), and one group was instillated with 20 μg CNP (previous called UfCP [1]; primary particle size: 10 nm, OC < 5%), the other two served as control and sham exposed groups. After 24 h, mice were anesthetized by intraperitoneal injection of a mixture of xylazine (4.1 mg/kg body weight) and ketamine (188.3 mg/kg body weight) and killed by exsanguination. Lung tissue after bronchoalveolar lavage (BAL) was stored at −80 °C. Four lung of each group were chose for gene expression analysis. We treated animals humanely and with regard for alleviation of suffering; experimental protocols were reviewed and approved by the Bavarian Animal Research Authority (Approval No. 55.2-1-54-2351-115-05).

2.2. Total RNA extraction and first strand cDNA synthesis

Total RNA was isolated using the RNeasy Mini Kit (Qiagen, Hilden, Germany) following the manufacturer's instructions with an additional peqGOLD TriFast (Peqlab, Erlangen, Germany) extraction to improve protein exclusion. RNA concentration and purity was determined by A_{260} and A_{280} measurements using a NanoDrop® ND-1000 spectrophotometer (Thermo Scientific, Wilmington, USA). The mean value of A_{260}/A_{280} ratio for all RNA samples was 2.05 ± 0.4, reflecting high purity and protein absence. RNA integrity was evaluated by the ratio of 28S/18S ribosomal RNA bands after electrophoresis in denaturing 1% agarose gel. To guarantee the quality necessary for expression analysis all samples used in this study presented a 28S/18S rRNA ratio ⩾ 1.7.

One microgram total RNA was reverse-transcribed using the Superscript™ II Reverse Transcriptase kit (Invitrogen, Karlsruhe, Germany) for first strand cDNA synthesis with 5 μM Random Nonamer (N9; MWG Biotech, AG, Ebersberg, Germany) primer according to the manufacture's recommendations. In brief, RNA and primers were mixed and incubated at 70 °C for 5 min followed by cooling on ice for 5 min and room temperature for 5–10 min before transcription. The first strand cDNA synthesis was started after adding transcription mixture at 42 °C lasting 1 h for reverse transcription reaction. Finally, the reaction was inactivated by heating to 70 °C for 15 min. All cDNA samples were diluted 1:5 with DNase- and RNase- free H_2O and stored at −20 °C.

2.3. Real-time quantitative PCR with SYBR green

qRT-PCR was conducted using the ABI PRISM® 7000 detection system (Applied Biosystems, Foster city, CA, USA), based on ABsolute™ QPCR SYBR® Green ROX Mix (Thermo Scientific, Wilmington, USA). The PCR reaction mixture contained 1 μl cDNA (10 ng/μl), 1 μl (5 μM) of each primer, 12.5 μl ROX mix and PCR-grade H_2O up to a total volume of 25 μl. After initial enzyme activation (one cycle at 95 °C for 15 min), 40 cycles amplification (95 °C for 15 s, 60 °C for 30 s and 72 °C 30 s) were performed in 96-well optical reaction plates (Applied Biosystems, Foster city, CA, USA). To verify that the used primer pair produced only a single product, a dissociation protocol was added after thermocycling, determining dissociation of the PCR products from 60 to 95 °C by increasing 0.5 °C per cycle. In all negative control samples no amplification signal was detected.

2.4. Statistical data analysis

The C_t is defined as the number of cycles needed for fluorescence to reach a specific threshold level of detection and is inversely correlated with the amount of RNA or DNA template present in the reaction [36]. The stability of HKGs expression was analyzed with geNorm (http://medgen.ugent.be/~jvdesomp/genorm/), NormFinder (http://www.mdl.dk/publicationsnormfinder.htm) and BestKeeper (http://www.gene-quantification.de/bestkeeper.html) software packages. Relative expression of GOI was analyzed by $\Delta\Delta C_t$ method was used where $\Delta\Delta C_t = (C_t$ target gene, test sample $- C_t$ endogenous control, test sample$) - (C_t$ target gene, calibrator sample $- C_t$ endogenous control, calibrator sample) [37]. Relative quantities were corrected for efficiency of amplification and fold change in gene expression between groups was calculated as $E^{\Delta\Delta C_t} \pm$ SEM. Where more than one endogenous control is used, fold change estimates were calculated using the geometric mean of HKGs quantities relative to the calibrator sample which could be the minimum, maximum or a named sample or an average.

3. Results

3.1. Selection of housekeeping genes and identification of primers

For the selection and evaluation of stable housekeeping genes for gene expression normalization in during CNP induced acute pulmonary inflammation in mice we selected 11 commonly used HKGs (18S rRNA, ACTB, B2M, CYPA, GAPDH, GUSB, HMBS, HPRT1, RPL13A, SDHA and TBP) of varying functional classes (for full gene information see Table 1). Particular attention was paid to selecting HKGs that belong to different functional classes, which significantly reduces the chance that genes might be co-regulated [12,13]. Primers were then designed and tested (Table 2). The specificity of the amplifications was confirmed by the presence of a single band of expected size for each primer pairs in agarose gels following electrophoresis and by the single peak dissociation curves of the amplicon. Efficiency of PCRs ranged between 94.97% for TBP and 112.19% for GUSB, and correlation coefficients varied from 0.9887 to 1 for HMBS and ACTB, respectively (Table 2).

3.2. Transcriptional profiles of housekeeping genes

For comparison of HKGs transcriptional profiles, the cycle threshold (C_t) values were plotted directly and indicated in Fig. 1. The median expression range of the 11 tested HKGs was calculated from raw C_t values and spanned 16.43 cycles for ACTB to 24.76 cycles for HMBS. As presented in Fig. 1, expression levels of GUSB, HMBS, HPRT1 and TBP were low, with median C_t values between 22 and 25 cycles. GADPH, RPL13A and SHDA displayed intermediate expression levels with median C_t values between 20 and 21.74 cycles. In contrast, high expression of 18S rRNA, ACTB, B2M and CYPA was detected, with C_t values between 16.5 and 19 cycles. Among the 11 HGKs, the maximum and minimum expression range was 2.63 cycles for HPRT1 and 1.13 cycles for CYPA, respectively.

3.3. Expression stabilities of candidate housekeeping genes

Our main objective was to identify HKGs with minimal variability among our set of samples. In order to determine the least variable HKGs, we evaluated expression stabilities of the 11 candidate HKGs using the three most commonly used Excel-based tools: geNorm, NormFinder and BestKeeper.

3.3.1. geNorm analysis

For ranking the various candidate HKGs, geNorm is a useful program using the principle that the expression ratio of two ideal HKGs is identical in all tested samples [6]. The 11 candidate HKGs for normalization were ranked according to their expression stability M values using the geNorm program. The M value is defined as the average pair-wise variation of a certain gene with all other tested HKGs. Consequently, genes with low M value have a low variation and a stable expression, while genes with high M value

9. Appendix

Table 1
Name, function and accession number of candidate housekeeping genes considered in this work.

Symbol	Gene name	Function	Accession No.
18S rRNA	18S ribosomal RNA	Cytosolic small ribosome subunit, translation	NR 003278
ACTB	Actin, β	Cytoskeletal structural protein	NM 007393
B2M	β-2 Microglobulin	β-Chain of major histocompatibility complex class I molecules	NM 009735
CYPA (Ppia)	Cyclophilin A (peptidyprolyl isomerase A)	Catalyzes the *cis–trans* isomerization of proline imidic peptide bonds in oligopeptides, accelerating folding	NM 008907
GAPDH	Glyceraldehyde-3 -phosphate dehydrogenase	Catalysis of conversion of D-glyceraldehyde -3-phosphate to 3-phospho-D-glyceroyl phosphate	NM 008084
GUSB	β-Glucuronidase	Exoglycosidase in lysosomes	NM 010368
HMBS (PBGD)	Hydroxymethylbilane synthase	Third enzyme of the heme biosynthetic pathway and catalyzes the head to tail condensation of four porphobilinogen molecules into the linear hydroxymethylbilane	NM 013551
HPRT1	Hypoxanthine guanine phosphoribosyl transferase	Purine synthesis in salvage pathway	NM 013556
RPL13A	Ribosomal protein L13A	Structural component of the large 60S ribosomal subunit	NM 009438
SDHA	Succinate dehydrogenase complex, subunit A, flavoprotein (Fp)	Succinate dehydrogenase/fumarate reductase, flavoprotein subunit involved in energy production and conversion	NM 023281
TBP	TATA box binding protein	General RNA polymerase II transcription factor	NM 013684

have a high variation and a less stable expression. The average expression *M* values of the 11 HKGs were plotted in Fig. 2. As shown in the upper line of Fig. 2, *M* value of RPL13A and ACTB were the lowest (0.218), and that of 18S rRNA was the highest (0.466), indicating that RPL13A and ACTB had the most stable expression and that 18S rRNA was expressed most variably.

3.3.2. NormFinder

NormFinder, another visual basic for applications (VBA) applet, is a model-based program calculating HKGs expression stability (more stable gene expression is indicated by lower average expression stability values) based on the intra-group variance, and includes the inter-group variance if applicable [7]. In this sense, using this program, we identified the same HKGs as having the greatest stability: GUSB, ACTB and RPL13A (stability values 0.005, 0.008 and 0.009, respectively, Fig. 2 downer line), although here GUSB was more stable than ACTB and RPL13A. The three least HKGs were 18S rRNA, HPRT1 and B2M (stability values 0.037, 0.022 and 0.017, respectively).

3.3.3. BestKeeper

The Excel-based program BestKeeper, determines the optimal HKGs employing the pair-wise correlation analysis of all pairs of candidate genes (up to 10 HKGs) and calculates the geometric mean of the best suited ones by raw C_t values of each gene. More importantly, comparing all genes of interest to this BestKeeper index, enables to decide whether they are differentially expressed under an applied treatment [8]. The 10 HKGs studied in our analysis compared by their BestKeeper index, also correlated gene one with each other, except for 18S rRNA (the least stable gene determined by geNorm and NormFinder). BestKeeper analysis showed that the four most stable genes were CYPA, GUSB, ACTB and RPL13A (BestKeeper index 0.949, 0.945, 0.928 and 0.900, respectively), while the three most variable genes were GADPH, HPRT1 and TBP (BestKeeper index 0.744, 0.756 and 0.831, respectively).

3.4. The optimal number of HKGs for normalization

To evaluate the optimal number of HKGs for accurate normalization, pair-wise variations V_n/V_{n+1} between two sequential normalization factors (NF) are calculated to determine the effect of adding the next HKG in normalization [6]. A large variation implies that the added gene has a significant effect and should preferably be included for calculation of a reliable NF. As shown in Fig. 3, the threshold of 0.15 is not exceeded at any point, indicating that two HKGs would be sufficient under this condition. However, normalization using three HKGs, instead of two, is generally considered as a more robust manner to generate a much more accurate and reliable estimate of the actual transcript level of GOI [14,6]. So the three most stable HKGs (ACTB, RPL13A and GUSB) we selected using geNorm, NormFinder and BestKeeper would be sufficient for accurate normalization of GOI.

3.5. Evaluation of selected candidate HKGs and normalization approach

In order to assess the value of the validation of housekeeping genes, the relative expression of CXCL1 which is known to be involved in acute pulmonary inflammation [18,19], was normalized using the following approach: (i) the three best HKGs combination (NF) selected by geNorm, NormFinder and BestKeeper ACTB, RPL13A and GUSB; (ii) the frequently cited endogenous gene 18S rRNA [15–17]; (iii) ACTB, RPL13A and GUSB were used individually.

CXCL1 protein concentration was measured by ELISA in lung BAL fluids collected 24 h after treatment with 20 μg CNP. Results indicated that concentration of CXCL1 was 40.97-fold induced in p50−/− mice (130.29 ± 29.70 pg/ml), 12.3-fold induced in p105−/− mice (39.13 ± 0.79 pg/ml) and 9.02-fold induced in WT mice (28.67 ± 7.43 pg/ml) upon CNP exposure, as compared with WT control mice (3.18 ± 1.07 pg/ml).

In accordance to the protein, Fig. 4 showed a significant increase in CXCL1 expression for the CNP exposure group normalized either to the HKGs selected in this study or the commonly cited housekeeping gene 18S rRNA, in comparison to the WT control group. When normalized to the top three stable HKGs (ACTB, GUSB and RPL13A), CXCL1 was up-regulated (in comparison to the WT control group) in WT mice by 6.03-fold, p50−/− mice by 15.71-fold and p105−/− mice by 10.25-fold, respectively, upon CNP exposure. However, normalization to the commonly used 18s rRNA, CXCL1 was up-regulated (also in comparison to the WT control group) in WT mice by 3.95-fold, p50−/− mice by 9.57-fold and p105−/− mice by 7.21-fold, respectively, in response to CNP exposure. Remarkably enough there is a decrease of approximately 1.53-fold in WT mice, 1.64-fold in p50−/− mice and 1.42-fold in p105−/− mice was seen in the same treatment group when normalizing

Table 2
Primer sequences and amplicon characteristics of housekeeping genes and genes of interest.

Name	Sequence (5′ → 3′)	Amplicon (bp)	TM (°C)[a]	E (%)[b]	R^2
18S rRNA	F: GAC TGT CTC GCC GGT GTC R: GGA GAG CCG GAA CGT CGA	98	88.86 ± 0.03	96.8	0.9983
ACTB	F: TCC ATC ATG AAG TGT GAC GT R: GAG CAA TGA TCT TGA TCT TCA T	154	83.02 ± 0.03	99.3	1.0000
B2M	F: CTG ACC GGC CTG TAT GCT A R: CAG TCT CAG TGG GGG TGA AT	244	82.95 ± 0.04	98.33	0.9998
CYPA	F: TTT GCA GAC GCC ACT GTC R: CAG TGC TCA GAG CTC GAA AG	165	87.09 ± 0.05	107.5	0.9988
GAPDH	F: TGC ACC ACC AAC TGC TTA GC R: GGC ATG GAC TGT GGT CAT GAG	101	83.6 ± 0.04	102.8	0.9981
GUSB	F: CAG GGT CAA CTT CAG GTT CC R: GCT CTT TGT GAC AGC CAC TG	165	84.16 ± 0.04	112.19	0.9948
HMBS	F: GGT CCC TGT TCA GCA AGA AG R: AAG CCA GAA GTA GGC AGT GG	242	86.8 ± 0.00	109.8	0.9887
HPRT1	F: GTT GGA TAC AGG CCA GAC TTT GT R: CAC AGG ACT AGA ACA CCT GC	224	81.56 ± 0.03	97.6	0.9985
RPL13A	F: CCC TCC ACC CTA TGA CAA GA R: CTG CCT GTT TCC GTA ACC TC	221	85.45 ± 0.06	105.93	0.997
SDHA	F: CAG TTC CAC CCC ACA GGT AT R: GAT CTT TCT CAG GGC CAC AG	208	84.8 ± 0.06	102.7	0.9978
TBP	F: GCC TTC CAC CTT ATG CTC AG R: GCT ACT GCC TGC TGT TGT TG	202	84.22 ± 0.03	94.97	0.991
KC	F: CCG AAG TCA TAG CCA CAC R: GTG CCA TCA GAG CAG TCT	139	83.14 ± 0.07	110	0.99

[a] The dissociation temperature of amplicon was calculated by ABI PRISM® 7000 Sequence Detection System.
[b] Amplification efficiency calculation was performed from the slopes of the dissociation curve according to the equation $E = 10^{(-1/\text{slope})}$.

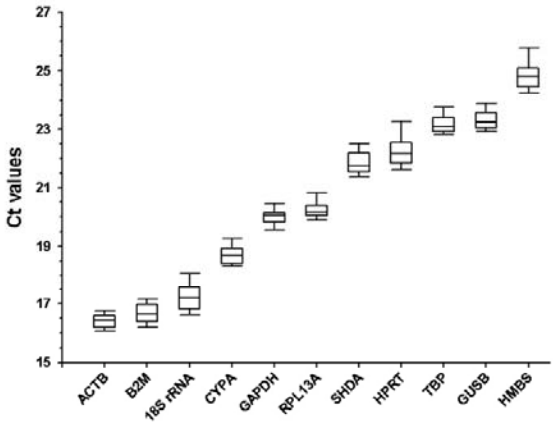

Fig. 1. Transcriptional profiles of 11 candidate housekeeping genes in lungs of mice during carbon nanoparticle induced acute pulmonary inflammation. Raw C_t values are represented for each gene by box-plot. The central box represents the interquartile interval (25–75%), the line inside the box is the median value (50%), and whiskers (error bars) above and below the box indicate the 90th and 10th percentiles. C_t, real-time PCR cycle threshold number).

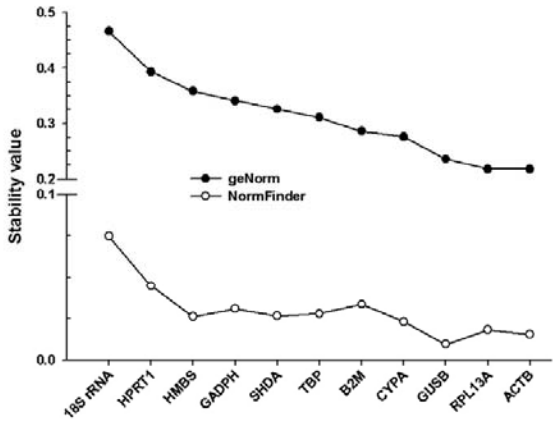

Fig. 2. Gene expression stability and ranking of the 11 candidate housekeeping genes were calculated using the software packages geNorm and NormFinder, respectively. The average expression stability M values (M) and the best combination of two genes for 11 HKGs were calculated by geNorm program (upper line with solid circle) in lung tissue. The cut-off for an unstable gene is $M \geqslant 1.5$. The lower M, the more stable the gene among the candidate HKGs; The lower line with open circle results from NormFinder, here the stability M value is inversely proportional to the stability of the candidate gene. With both approaches, the most stable genes (lowest stability value) are identified as ACTB, RPL13A and GUSB, whereas 18S rRNA and HPRT1 are two least stable HKGs.

against 18S rRNA, compared with normalized to top three stable HKGs combination. When normalization to ACTB and RPL13A, the relative expression of CXCL1 less than 1-fold compared with normalizing against the top three HKGs combination, while normalizing to GUSB up-regulated 1.14- to 1.27-fold compared with the top three stable HKGs combination.

Therefore, these results demonstrate how the explanation of GOI expression levels can be affected by the choice of the HKGs in real-time quantitative RT-PCR analysis.

4. Discussion

In this study we have selected and evaluated the stability of several housekeeping genes for their use as qRT-PCR normalizing factors in CNP-induced acute pulmonary inflammation. Based on our results, we conclude that use of a single normalization

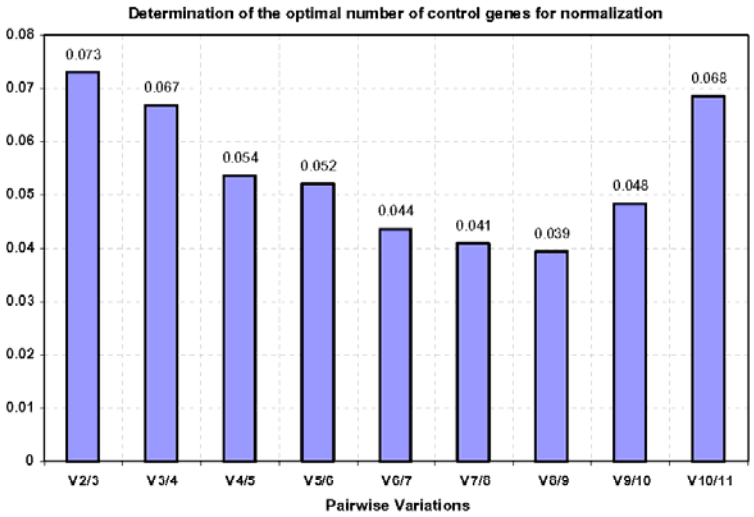

Fig. 3. The optimal number of HKGs for normalization was determined using geNorm. Pair-wise variation ($V_n/<V_{n+1}$) analysis between the normalization factor NF_n and NF_{n+1} was performed to determine the number of HKGs required for accurate normalization. Each bar represents the variation between the means of n most stable genes versus the group of $n + 1$ most stable genes (e.g., column 1 represents the variation between the mean of the two most stable genes, that is, ACTB, RPL13A and three most stable genes, that is ACTB, RPL13A and GUSB).

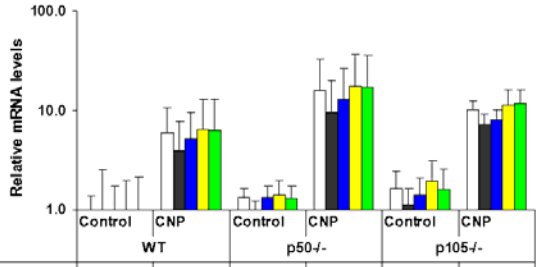

	WT		p50-/-		p105-/-	
	Control	CNP	Control	CNP	Control	CNP
NF	1.00	6.03	1.35	15.71	1.64	10.25
18S rRNA	1.00	3.95	0.97	9.57	1.10	7.21
GUSB	1.00	5.30	1.33	12.84	1.40	8.05
ACTB	1.00	6.53	1.41	17.69	1.95	11.38
RPL13A	1.00	6.34	1.31	17.08	1.62	11.76

Fig. 4. Relative expression of CXCL1 normalized different HKGs combinations. The relative expression of CXCL1 in lung homogenates 24 h after instillation with CNP were calculated using the $E^{\Delta\Delta C_T}$ method and normalized to NF (the most stable three HKGs, ACTB, GUSB and RPL13A, determined by geNorm, NormFinder and BestKeeper), or frequently used 18s rRNA or individual of the most three stable HKGs, respectively. Each bar represents the mean of two measurements from four animals, ±SEM.

housekeeping gene is potentially misleading, and suggest a panel of housekeeping genes for more accurate transcript quantification.qRT-PCR is a sensitive and accurate technique for measuring gene expression [20], and constitutes a powerful tool for increasing our understanding of the subunit p50 and p105 of NF-κB functions in CNP-induced acute pulmonary inflammation. However, in the CNP-induced acute pulmonary inflammation system, little is known about the ideal genes to use for normalization and many previous studies have only utilized a single housekeeping gene for normalizing gene expression data [21–23]. Normalization of real-time RT-PCR data using a single, non-validated housekeeping gene may lead to inaccurate biological conclusions, and previous studies have highlighted the need to validate housekeeping genes for each experimental condition [24–28,13].

The geNorm [6], NormFinder [7] and BestKeeper [8] algorithms are now widely used to determine the most stable housekeeping genes from a set of candidate genes with invariable expression [29–34]. Among 11 candidate housekeeping genes in this study, both geNorm and NormFinder identified ACTB, GUSB and RPL13A as the most stable combination of housekeeping gens for the CNP-induced acute pulmonary inflammation. And BestKeeper identified CYPA, GUSB, ACTB and RPL13A as the top four stable housekeeping according to the BestKeeper index (shown in Table 3). Considering both results, ACTB, GUSB and RPL13A could

Table 3
Inter-gene relations and correlation between the housekeeping genes and the BestKeeper index.

	RPL13A	SHDA	HPRT1	ACTB	TBP	CYPA	HMBS	B2M	GUSB	GADPH
SHDA	0.710	–	–	–	–	–	–	–	–	–
HPRT1	0.600	0.840	–	–	–	–	–	–	–	–
ACTB	0.894	0.721	0.566	–	–	–	–	–	–	–
TBP	0.687	0.883	0.787	0.656	–	–	–	–	–	–
CYPA	0.821	0.836	0.698	0.878	0.727	–	–	–	–	–
HMBS	0.737	0.664	0.444	0.830	0.555	0.829	–	–	–	–
B2M	0.802	0.722	0.601	0.780	0.727	0.789	0.583	–	–	–
GUSB	0.876	0.780	0.567	0.917	0.719	0.892	0.873	0.815	–	–
GADPH	0.668	0.522	0.328	0.824	0.458	0.687	0.869	0.468	0.767	–
BestKeeper	0.900	0.892	0.756	0.928	0.831	0.949	0.845	0.851	0.945	0.744
p-Value	0.001	0.001	0.001	0.001	0.001	0.001	0.001	0.001	0.001	0.001

9. Appendix

be sufficient as a validation combination of housekeeping genes for normalization of real-time RT-PCR data in our study system.

In order to check the value of the validation of endogenous controls, we have used different housekeeping genes selected in this study to normalize the expression of CXCL1, gene which is known to be involved in acute pulmonary inflammation in response to CNP exposure. We have observed differences in the results obtained when suitable and unsuitable housekeeping genes are used.

5. Conclusion

Our current results showed that ACTB, GUSB and RPL13A were the most stably expressed genes in lung tissues from CNP-induced acute lung inflammation mice, regardless of genotype and treatment. Thus, these are appropriate housekeeping genes for quantitative real-time PCR studies. Since the current study also observed fluctuations in expression in frequently used housekeeping genes, including 18S rRNA, B2M, CYPA, GAPDH, HMBS, HPRT1, SDHA and TBP, it might be rather recommended to use ACTB, GUSB and RPL13A as housekeeping genes for lung tissues in studies of similar design but also to analyze the stability of housekeeping genes prior to expression studies.

Competing interests

The authors declare no competing interests. Non-financial competing interests exist.

Acknowledgments

This study is supported by the National Genome Research Network (NGRN) and by China Scholarship Council (CSC). R.Y. is the recipient of a fellowship of CSC (2008617097).

References

[1] T. Stoeger, S. Takenaka, B. Frankenberger, et al., Deducing in vivo toxicity of combustion-derived nanaoparticles from a cell-free oxidative potency assay and metabolic activation of organic compounds, Environ. Health Perspect. 117 (2009) 54–60.
[2] C. Andrew, C.S. Xie, X.S. Wang, et al., Air pollution particles activate NF-kB on contact with airway epithelial cell surfaces, Toxicol. Appl. Pharmacol. 208 (2005) 37–45.
[3] P. Thorne, S. Hadina, K. Kulhankova, et al., Monitoring of endotoxin-induced pulmonary inflammation in vivo in NF-kB luciferase transgenic mice, J. Allergy Clin. Immunol. 117 (2) (2006) S147.
[4] L.H. Lancaster, J.W. Christman, T.R. Blackwell, et al., Suppression of lung inflammation in Rats by prevention of NF-kB activation in the liver, Inflammation 25 (1) (2001) 25–31.
[5] M.S. Hayden, S. Ghosh, Signaling to NF-kB, Genes Dev. 18 (2) (2004) 2195–2224.
[6] J. Vandesompele, K. De Preter, F. Pattyn, et al., Accurate normalization of real-time quantitative RT-PCR data by geometric averaging of multiple internal control genes, Genome Biol. 3 (2002) (RESEARCH0034).
[7] C.L. Andersen, J.L. Jensen, T.F. Orntoft, Normalization of real-time quantitative reverse transcription-PCR data: a model-based variance estimation approach to identify genes suited for normalization, applied to bladder and colon cancer data sets, Cancer Res. 64 (5) (2004) 5245–5250.
[8] M.W. Pfaffl, A. Tichopad, C. Prgomet, et al., Determination of stable housekeeping genes, differentially regulated target genes and sample integrity: BestKeeper-Excel-based tool using pair-wise correlations, Biotechnol. Lett. 26 (2004) 509–515.
[9] D.T. Coulson, S. Brockbank, J.G. Quinn, et al., Identification of valid reference genes for the normalization of RT-qPCR gene expression data in human brain tissue, BMC Mol. Biol. 9 (2008) 46.
[10] T. Suzuki, P.G. Higgins, D.R. Crawford, Control selection for RNA quantitation, Biotechniques 29 (2000) 332–337.
[11] C. Gubern, O. Hurtado, R. Rodriguez, et al., Validation of housekeeping genes for quantitative real-time PCR in in-vivo and in-vitro models of cerebral ischaemia, BMC Mol. Biol. 10 (2009) 57.
[12] O. Thellin, W. Zorzi, B. Lakaye, et al., Housekeeping genes as internal standards: use and limits, J. Biotechnol. 75 (1999) 291–295.
[13] K. Dheda, J.F. Huggett, S.A. Bustin, et al., Validation of housekeeping genes for normalizing RNA expression in real-time PCR, Biotechniques 37 (2004) 112–119.
[14] M.B. VanHiel, P.V. Wielendaele, L. Temmerman, et al., Identification and validation of housekeeping genes in brains of the desert locust schistocerca gregaria under different developmental conditions, BMC Mol. Biol. 10 (2009) 56.
[15] K.I. Inoue, H. Takano, R. Yangisawa, et al., Effects of diesel exhaust on lung inflammation related to bacterial endotoxin in mice, Basic Clin. Pharmacol. Toxicol. 99 (5) (2006) 346–352.
[16] M. Dybdahl, L. Risom, J. Bornholdt, et al., Inflammatory and genotoxic effects of diesel particles in vitro and in vivo, Mutat. Res.: Genet. Toxicol. Environ. Mutagen. 562 (1–2) (2004) 119–131.
[17] A.T. Saber, J. Bornholdt, M. Dybdahl, et al., Tumor necrosis factor in not required for particle-induced genotoxicity and pulmonary inflammation, Arch. Toxicol. 79 (3) (2005) 177–182.
[18] S. Huang, J.D. Paulauskis, J.J. Godleski, et al., Expression of macrophage inflammatory protein-2 and KC mRNA in pulmonary inflammation, Am. J. Pathol. 141 (1992) 981–988.
[19] R. Yanagisawa, H. Takano, T. Ichinose, et al., Gene expression analysis of Murine lungs following pulmonary exposure to Asian sand dust particles, Exp. Biol. Med. 232 (2007) 1109–1118.
[20] J. Wilhelm, A. Pingoud, Real-time polymerase chain reaction, ChembioChem 4 (2003) 1120–1128.
[21] W.S. Cho, M. Choi, B.S. Han, et al., Inflammatory mediators induced by intratracheal instillation of ultrafine amorphous silica particles, Toxicology 175 (1–3) (2007) 24–33.
[22] K. Arsalane, F. Broeckaert, B. Knoops, et al., Clara cell specific protein (CC16) expression after acute lung inflammation induced by intratracheal lipopolysaccharide administration, Am. J. Respir. Crit. Care Med. 161 (5) (2000) 1624–1630.
[23] N. Guengoer, A. Haegens, A.M. Knaapen, et al., Lung inflammation is associated with reduced pulmonary nucleotide excision repair *in vivo*, Mutagenesis 25 (1) (2010) 77–82.
[24] P.A. Nieto, P.C. Covarrubias, E. Jedlicki, et al., Selection and evaluation of reference genes for improved interrogation of microbial transcriptomes: case study with the extremophile *Acidithiobacillus ferrooxidans*, BMC Mol. Biol. 10 (2009) 63.
[25] N. Nicot, J.F. Hausman, L. Hoffmann, et al., Housekeeping gene selection for real-time RT-PCR normalization in potato during biotic and abiotic stress, J. Exp. Bot. 56 (412) (2005) 2907–2914.
[26] A. Radonic, S. Thulke, I.M. Mackay, et al., Guideline to reference gene selection for quantitative real-time PCR, Biochem. Biophys. Res. Coummun. 313 (2004) 856–862.
[27] K. Dheda, J.F. Huggett, J.S. Chang, et al., The implications of using an inappropriate reference gene for real-time reverse transcription PCR data normalization, Anal. Biochem. 344 (2005) 141–143.
[28] N.L. Cook, T.J. Kleinig, C. Van den Heuvel, et al., Reference genes for normalizing gene expression data in collagenase-induced rat intracerebral haemorrhage. BMC Mol. Biol. 11 (2010) 7.
[29] K. Langnaese, R. John, H. Schweizer, et al., Selection of reference gens for quantitative real-time PCR in a rat asphyxial cardiac arrest model, BMC Mol. Biol. 9 (2008) 53.
[30] H. Rhinn, C. Marchand Leroux, N. Croci, et al., Housekeeping while brain's storming Validation of normalizing factors for gene expression studies in a murine model of traumatic brain injury, BMC Mol. Biol. 9 (2008) 62.
[31] N. Tanic, M. Perovic, A. Mladenovic, et al., Effects of aging, dietary restriction and glucocorticoid treatment on housekeeping gene expression in rat cortex and hippocampus-evaluation by real-time RT-PCR, J. Mol. Neurosci. 32 (2007) 38–46.
[32] B.E. Bonefeld, B. Elfving, G. Wegener, Reference genes for normalization: a study of rat brain tissue, Synapse 62 (2008) 302–309.
[33] R.E. McNeil, N. Miller, M.J. Kerin, Evaluation and validation of candidate endogenous control genes for real-time quantitative PCR studies of breast cancer, BMC Mol. Biol. 8 (2007) 107.
[34] M. Passmore, M. Nataatmadja, J.F. Fraser, Selection of reference genes for normalization of real-time RT-PCR in brain-stem death injury in *Ovis aries*, BMC Mol. Biol. 10 (2009) 72.
[35] T. Stoeger, C. Reinhard, S. Takenaka, et al., Instillation of six different ultrafine carbon particle indicates a surface area threshold dose for acute lung inflammation in mice, Environ. Health Perspect. 114 (2006) 328–333.
[36] T. Nolan, R.E. Hands, S.A. Bustin, Quantification of mRNA using real-time RT-PCR, Nat. Protoc. 1 (3) (2006) 1559–1582.
[37] K.J. Livak, T.D. Schmittgen, Analysis of relative gene expression data using real-time quantitative PCR and the $2^{-\Delta\Delta C_t}$ method, Methods 25 (2001) 402–408.

Appendix 3

R. Yin, Z. Ding, X. Liu, L. Mu, Y. Cong, T. Stoeger, Inhibition of Newcastle disease virus replication by RNA interference targeting the matrix protein gene in chicken embryo fibroblasts, J Virol Methods 167 (2010) 107-111.

Renfu Yin's contributions:

Renfu Yin was involved in the conceiving and designing of the study, was responsible for all experimental parts of the study, performed statistical data analysis and wrote the paper.

Journal of Virological Methods 167 (2010) 107–111

Contents lists available at ScienceDirect

Journal of Virological Methods

journal homepage: www.elsevier.com/locate/jviromet

Short communication

Inhibition of Newcastle disease virus replication by RNA interference targeting the matrix protein gene in chicken embryo fibroblasts

Renfu Yin[a,b], Zhuang Ding[a,*], Xinxin Liu[a,c], Lianzhi Mu[a], Yanlong Cong[a], Tobias Stoeger[b]

[a] Department of Veterinary Preventive Medicine, College of Animal Science and Veterinary Medicine, Jilin University, Xi'an Road 5333, Changchun, Jilin 130062, China
[b] Comprehensive Pneumology Center, Institute of Lung Biology and Disease (iLBD), Helmholtz Zentrum München, Ingolstädter Landstraße 1, D-85764 Neuherberg/Munich, Germany
[c] College of Quartermaster Technology, Jilin University, Xi'an Road 5333, Changchun, Jilin 130062, China

Article history:
Received 7 May 2009
Received in revised form 8 February 2010
Accepted 11 February 2010
Available online 18 February 2010

Keywords:
Newcastle disease virus
RNA interference
Short hairpin RNA
Inhibition

A B S T R A C T

Newcastle disease (ND) is an infectious viral disease of birds caused by the Newcastle disease virus (NDV), also known as avian paramyxovirus type 1 (AMPV-1), which leads to severe economic losses in the poultry industry worldwide. In this study, the application of RNA interference (RNAi) for inhibiting the replication of NDV in cell culture by targeting the viral matrix protein gene (M) is described. Two M-specific shRNA-expressing plasmid constructs, named pS_{M641} and pS_{M827}, were evaluated for antiviral activity against the NDV strain NA-1 by cytopathic effects (CPE), virus titration and real-time RT-PCR. After 36 h of infection, both pS_{M641} and pS_{M827} reduced virus titers by 79.4- and 31.6-fold, respectively, and they down-regulated mRNA expression levels of the matrix protein gene M by 94.6% and 84.8%, respectively, in chicken embryo fibroblast (CEF) cells, while only pS_{M641} significantly decreased CPE, compared to the control group. These results indicated that the M gene 641 and 827 sites represent potential antiviral therapy targets, and RNAi targeting of the M gene could not only represent an effective treatment in Newcastle disease but also aid as a method for studying the replication of NDV.

NDV is an enveloped virus containing a non-segmented, single-stranded, negative-sense RNA genome of approximately 15 Kb (Alexander, 1997; De Leeuw and Peeters, 1999), which codes for six major proteins: nucleoprotein (NP), phosphoprotein and V protein (P/V), matrix protein (M), fusion glycoprotein (F), haemagglutinin-neuraminidase glycoprotein (HN) and large polymerase protein (L), in the order '3-NP–P–M–F–HN–L-5' (Millar and Emmerson, 1998). Strains of NDV can be classified as highly virulent (velogenic), intermediate (mesogenic) or non-virulent (lentogenic) on the basis of their pathogenicity for birds (Alexander, 1997).

It has been suggested that the preferred method for controlling the virus is to interfere with replication of the viral genome and the expression of viral genes. RNAi technology has emerged not only as a powerful tool for functional genomic studies but also as a potentially useful method for developing specific gene-silencing treatments, especially for viral diseases (Mallanna et al., 2006; Peng et al., 2005). Previous studies demonstrated the possibility for treating serious viral diseases *in vivo* and *in vitro*, including foot and mouth disease virus (Chen et al., 2004), influenza virus (Ge et al., 2003), SARS (Wu et al., 2005), hepatitis B virus (Giladi et al., 2003; McCaffrey et al., 2003), hepatitis C virus (Krönke et al., 2004), avian leukosis virus (Chen et al., 2007), anatid herpes virus-1 (Mallanna et al., 2006), porcine circovirus (Sun et al., 2007) and avian metapneumovirus (Ferreira et al., 2007).

The matrix (M) protein, the smallest of six structural proteins of NDV, forms an internal viral envelope around the viral nucleocapsid (Rott and Klenk, 1977). Also, recent studies revealed the remarkable genetic stability of the M protein among isolates of different virus types (Rima, 1989; Panshin et al., 1997). The current study investigated the inhibition of replication of NDV by RNA interference targeting the matrix protein gene (M) of the virus in cell culture.

An isolate of the NDV strain NA-1 (velogenic, 10^6 $CCID_{50}$/0.1 mL) from geese (Xu et al., 2008) was replicated in the allantoic cavity of 9–10-day-old embryonated specific pathogen-free (SPF) chicken eggs (Alexander, 1997). The virus was purified directly from the allantoic fluid as described previously (Seal et al., 1995).

Based on previous studies (Elbashir et al., 2002) and web-based criteria (www.ambion.com), the two best target sequences within the Open Reading Frame (ORF) of the M gene (GenBank accession no. DQ659677) and one negative control sequence targeting the green fluorescent protein (GFP, GenBank accession no. YP_002302326.1) were chosen (shown in Table 1) and inserted into the *pSilencer™ 2.1-U6 neo* Vector (Ambion, Austin, USA). The three respective constructs were, according to gene and target site, named pS_{M641}, pS_{M827} and pS_{GFP}.

Primary chicken embryo fibroblast (CEF) cells prepared from 10-day-old, SPF chicken eggs (obtained from the Marival Vital

* Corresponding author. Tel.: +86 431 87836171.
E-mail address: Ding_zhuang@yahoo.com.cn (Z. Ding).

0166-0934/$ – see front matter © 2010 Elsevier B.V. All rights reserved.
doi:10.1016/j.jviromet.2010.02.014

Table 1
List of shRNA sequences in this study.

Target name	Sequences of shRNA[a]
M641 up	5′-gATCC*gTCTTgCgCTCAATgTCACT*TTCAAgAgAAgTgACATTgAgCgCAAgATTTTTTggAAA-3′
M641 down	5′-AgCTTTTCCAAAAAATCTTgCgCTCAATgTCACTCTCTTgAAAgTgACATTgAgCgCAAgACg-3′
M827 up	5′-gATCC*gTCTATCTgTCgggCTCAgT*TTCAAgAgAACTgAgCCCgACAgATAgATTTTTTggAAA-3′
M827 down	5′-AgCTTTTCCAAAAAATCTATCTgTCgggCTCAgTTCTCTTgAAACTgAgCCCgACAgATAgACg-3′
Control up	5′-gATCC*gACTACCgTTgTTATAggTg*TTCAAgAgACACCTATAACAACggTAgTTTTTTggAAA-3′
Control down	5′-AgCTTTCCAAAAAACTACCgTTgTTATAggTgTCTCTTgAACACCTATAACAACggTAgTggATC-3′

[a] For each target gene (up strand as a example), we designed complementary 55–60-mer oligonucleotides with 5′ single-stranded overhangs (gATCC) for ligation into the p*Silencer* vectors. The oligonucleotides should encode 19-mer hairpin sequences specific to the mRNA target, a loop sequence separating the two complementary domains (TTCAAGA), and a polythymidine tract to terminate transcription (TTTTTT).

Laboratory Animal Technology Co., Ltd., Beijing, China) were trypsinised and seeded in 12-well plates (Costar, Bethesda, USA) at 2.0×10^5 cells per well in E-MEM containing 3% foetal calf serum (5% in growth, FBS, Hyclone, Logan, Utah), 2 mM glutamine, 100 U/mL penicillin, 100 μg/mL streptomycin (Invitrogen, CA, USA) 1 day before transfection and maintained in a 5% CO_2 humidified incubator at 37 °C. When the cells reached 70–80% confluence, the cells were washed and overlaid with transfection complexes containing 2 μg of pS_{M641}, 2 μg of pS_{M827}, and 2 μg of pS_{GFP}, respectively, in 100 μL of OPTI-MEM medium (Invitrogen, CA, USA) mixed with Lipofectamine™ 2000 (Invitrogen, CA, USA) according to the manufacturer's instructions. Transfection complexes were completely removed after transfection for 6 h, and 100 μL of virus suspensions, at a multiplicity of infection (MOI) of 10, were added into each well. Non-transfected CEF cells were used as a control.

At 36 h after virus infection, CPE indicated only for pS_{M641} a significant inhibitory effect on virus replication, while the cells transfected with either of the other two or without constructs exhibited no distinct inhibition. The CPE was characterised by syncytium formation, the rounding of refringent cells, the accumulation of detached cells and finally plaque formation (shown in Fig. 1).

To substantiate further the inhibitory effect of pS_{M641} and pS_{M827}, the microtiter method was used for the titration of the NDV stock virus at 36 h post-infection. Briefly, after adding two drops (0.1 mL) of medium to each well, 10-fold dilutions of virus or supernatants prepared previously in glass test tubes were trans-

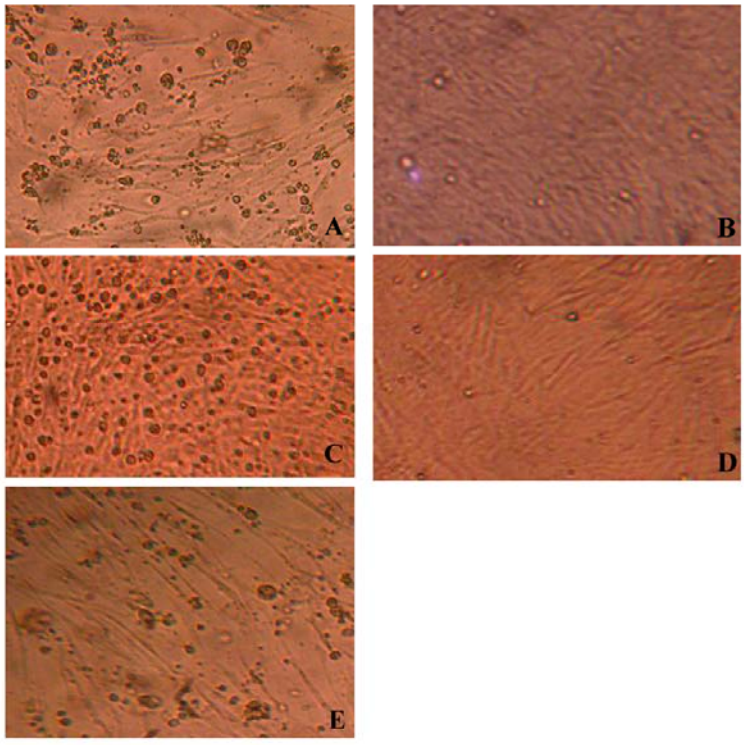

Fig. 1. Cytopathic effect (CPE) of primary CEF cells 36 h after virus infection shows that viral replication is notably inhibited by pS_{M641} and pS_{M827} plasmid transfection. Interestingly, the presence of pS_{M641} obviously alleviates the CPE of CEF cells. CEF cells were transfected with 2 μg of plasmid constructs (pS_{M641}, pS_{M827}, and pS_{GFP}) using Lipofectamine™ 2000 reagent. 6 h later, transfection complexes were completely removed and then 100 μL of virus at a MOI of 10 was added into each well except healthy CEF cells well. Virus-produced CPE was observed by light microscopy (200×) 36 h after virus incubation. (A) Mock; (B) CEF cells transfected with pS_{M641}; (C) CEF cells transfected with pS_{M827}; (D) Healthy CEF cells; (E) CEF cells transfected with pS_{GFP}.

9. Appendix

Table 2
List of primer sequences, sizes of PCR products and GenBank accession no. used in this study.

Gene name	Sequence (5′ → 3′)	Amplicon	GenBank accession no.
NDV NA-1 M	F:TGATTCTGCCCTCCCTTCCA R:TGATGAACACCGAGTCTTCCTTAC	146 bp	DQ659677
Chick β-actin	F:GAGAAATTGTGCGTGACATCA R:CCTGAACCTCTCATTGCCA	152 bp	L08165

ferred to the microplate. Each dilution was distributed to eight wells. Virus and supernatants were transferred in a descending manner, from the highest (10^{-9}) to the lowest (10^{-3}) dilutions using one microplate. One drop of a CEF suspension containing 10^6 cells per mL was then added to appropriate wells and microplates were incubated in a 5% CO_2, 37 °C for 48 h. A cell control, virus control and medium control were also included in every microplate. The virus titer was determined by the HA method using a 0.75% chicken erythrocyte suspension under refrigeration (4 °C) and reading in an almost vertical position after 5–10 min. Fig. 2, shows a 79.4- and 31.6-fold reduction in NDV titer for culture supernatants from pS_{M641}, and pS_{M827} CEF transfected cells, respectively, in comparison to the cells transfected with pS_{GFP} vector ($P < 0.05$). No significant differences in viral titers were seen between the pS_{GFP} group and mock.

To investigate the influence of RNAi on virus M gene transcription, the relative expression level of the M gene was evaluated by real-time quantitative RT-PCR. At 36 h after virus infection, total RNA from transfected and control samples was isolated by Trizol® (Invitrogen, Carlsbad, USA) phenol-chloroform extraction and ethanol precipitation following the manufacturer's instructions. To eliminate traces of DNA, all RNA samples were incubated with RNase-free DNase 1 (Shanghai Sangon Bio Engineering Technology and Services Co. Ltd., Shanghai, China) for 30 min at 37 °C, and then DNase was inactivated by incubation at 65 °C for 10 min. To detect M and β-actin mRNA expression in CEF cells, real-time quantitative RT-PCR using RNA-direct™ SYBR Green Real-time PCR Master Mix (Toyobo Bio Co. Ltd., Tokyo, Japan) was performed in a 20 μL reaction volume, containing 2 μg of RNA extract, 10 μL SYBR Green Real-time PCR Master Mix (2×), 0.6 μM anti-sense and sense primers (information regarding the primers are shown in Table 2). The cycling parameters were set to 90 °C for 30 s, 61 °C for 20 min and 95 °C for 30 s, followed by 40 cycles of 95 °C for 5 s and 60 °C for 15 s, and dissociation curve analysis from 55 to 95 °C. Reactions were done in duplicate. The correlation coefficients (R^2) of the standard curves were 0.999 (β-actin) and 0.992 (M gene), respectively. All PCR amplification efficiencies (E) were >0.96 with only one peak in all dissociation curves. Gene expression levels of NDV M were normalised to β-actin using the $2^{-\Delta\Delta ct}$ method. Results indicated a significant reduction in the relative expression level of M gene transcripts by 94.6% and 84.8%, as compared to the mock group at 36 h post-infection, when pS_{M641} and pS_{M827} were used (shown in Fig. 3). In contrast, there were no significant differences in M gene transcript levels between pS_{GFP} and mock, although there was a trend toward lower levels in the pS_{GFP} group (shown in Fig. 3).

To confirm the specificity of the RNAi effect and the absence of interferon activity in the respective cells, RNAi-expressing plasmid-transfected CEF cells were also challenged with 500 pfu of Marek's disease virus (MDV) RB1B strain (velogenic, provided by Prof. Xubin Wei, Jilin University, China) in a plaque counting assay. No significant difference in plaque number and plaque size between mock and all transfected groups was observed from 0 to 48 h after MDV infection (shown in Fig. 4).

It has been shown that the NDV M protein is found abundantly in the nuclei of infected CEF cells. Early in infection the M protein enters the nucleus, accumulates in discrete regions of the nucleus and remains there throughout infection (Peeples et al., 1992). Because the M protein concentrates in the nucleolus, it may affect ribosome assembly or function, leading to inhibition of host protein synthesis. Moreover, the M protein is directly involved in NDV particle assembly (Pantua et al., 2006). Therefore, the M protein plays a vital role during the life cycle of NDV.

NDV infection is not only a major problem in many avian species worldwide, which leads to substantial economic losses in the poultry industry (Yusoff and Tan, 2001), but there is currently no effective antiviral treatment against NDV infection. One possi-

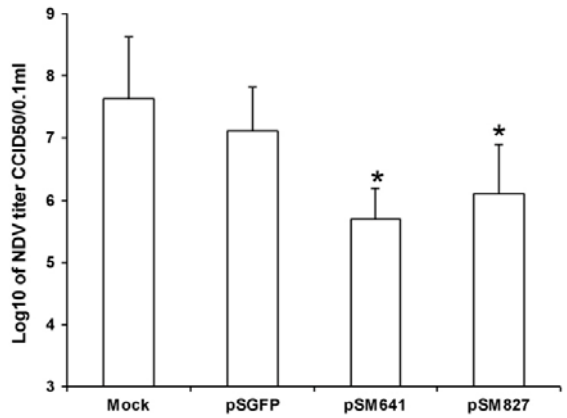

Fig. 2. Transfection with pS_{M641} and pS_{M827} plasmids reduces the viral titer in the CEF cells after 36 h of virus infection. At 36 h after virus infection, cell culture supernatants were collected for viral titration (by microtiter method). All the data were obtained by experiments performed in triplicates and repeated three times. * Significant difference from mock group ($P < 0.05$; Mann–Whitney U-test).

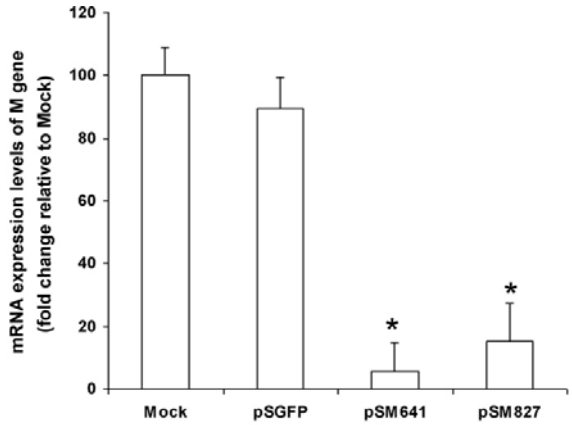

Fig. 3. Real-time quantitative RT-PCR results indicate a significant decrease of M gene mRNA expression level by the pS_{M641} and pS_{M827} plasmids at 36 h after virus infection. The values are shown as means of triplicates and three independent experiments. * Significant difference from mock and pS_{GFP} groups ($P < 0.05$; Mann–Whitney U-test).

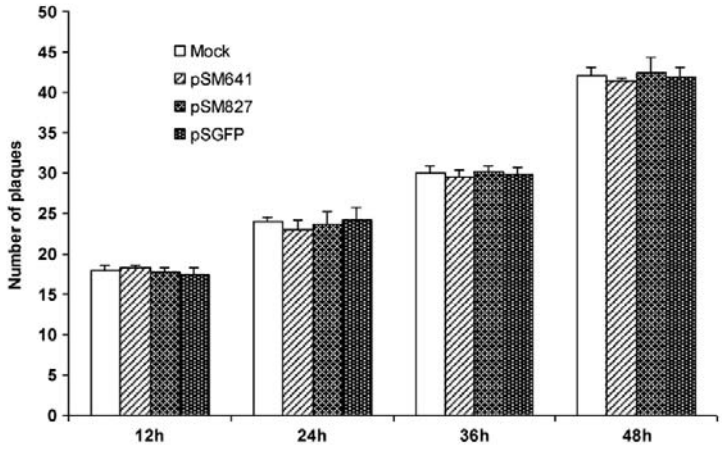

Fig. 4. Three plasmid constructs failed to significantly alter plaque number or size (not shown) from 0 to 48 h after 500 pfu of MDV incubation. At 12, 24, 36 and 48 h after virus infection, respectively, the medium was removed, cells were fixed and stained, and the number of plaques was counted. All data were collected in triplicate wells and in three independent experiments.

ble strategy might be represented by RNAi technology because it can theoretically be directed to cleave any target RNA, providing a single methodology for rational drug design for many different diseases. For this reason, RNAi has generated substantial interest; it has proven to be a powerful tool potent for host protection against viral infection (Wu et al., 2007; Kumar et al., 2008), suppression of viral genome transcription and blocking viral replication (Mungall et al., 2008). However, when using RNAi an efficient delivery method is as mandatory as a strategy to restrict the virus escape from RNAi. Carefully selected viral vectors as well as choosing a genetically stable target sequence are also required for successful RNAi applications (Lambeth et al., 2009).

It is clear from this study that the DNA vector-based shRNA approach, that is, the use of RNAi expression plasmids directed against the NDV M gene, could effectively block expression of the viral target gene and inhibit viral replication. Besides this therapeutic aspect for prevention and treatment of ND, the presented strategy could also be a potential candidate to study further NDV gene functions. Additional studies are necessary to determine the antiviral mechanism of RNAi on NDV replication.

Conflict of interest

The authors report no conflicts of interest.

Acknowledgements

This study is supported by two grants (30972192 and 30771606) from National Natural Science Foundation of China and a grant (2008617097) from China Scholarship Council.

References

Alexander, D., 1997. Newscastle disease and other avian Paramyxoviridae infections. In: Calnek, B.W., et al. (Eds.), Diseases of Poultry, 10th ed. Iowa State University Press, Ames, pp. 541–569.
Chen, M., Granger, A.J., Vanbrocklin, M.W., Payne, W.S., Hunt, H., Zhang, H., Dodgson, J.B., Holmen, S.L., 2007. Inhibition of avian leukosis virus replication by vector-based RNA interference. J. Virol. 365, 464–472.
Chen, W., Yan, W., Du, Q., Fei, L., Liu, M., Ni, Z., Sheng, Z., Zheng, Z., 2004. RNA interference targeting VP1 inhibits foot-and-mouth disease virus replication in BHK-21 cells and suckling mice. J. Virol. 78, 6900–6907.
De Leeuw, O.S., Peeters, B.P.H., 1999. Complete nucleotide sequence of Newcastle disease virus: for the existence of a new genus within the subfamily Paramyxovirinae. J. Gen. Virol. 80, 131–136.
Elbashir, S.M., Harborth, J., Weber, K., Tuschl, T., 2002. Analysis of gene function in somatic mammalian cells using small interfering RNAs. Methods 26, 199–213.
Ferreira, H.L., Spilki, F.R., de Almeida, R.S., Santos, M.M., Arns, C.W., 2007. Inhibition of avian metapneumovirus (AMPV) replication by RNA interference targeting nucleoprotein gene (N) in cultured cells. Antiviral Res. 74, 77–81.
Ge, Q., McManus, M.T., Nguyen, T., Shen, C.H., Sharp, P.A., Eisen, H.N., Chen, J.Z., 2003. RNA interference of influenza virus production by directly targeting mRNA for degradation and indirectly inhibiting all viral RNA transcription. PANS 100, 2718–2723.
Giladi, H., Ketzinel-Gilad, M., Rivkin, L., Felig, Y., Nussbaum, O., Galun, E., 2003. Small interfering RNA inhibits hepatitis B virus replication in mice. Mol. Ther. 8, 769–776.
Krönke, J., Kittler, R., Buchholz, F., Windisch, M.P., Pietschmann, T., Bartenschlager, R., Frese, M., 2004. Alternative approaches for efficient inhibition of Hepatitis C virus RNA replication by small interfering RNAs. J. Virol. 78, 3436–3446.
Kumar, P., Ban, H.S., Kim, S.S., Wu, H., Pearson, T., Greiner, D.L., Laouar, A., Yao, J., Haridas, V., Habiro, K., Yang, Y.G., Jeong, J.H., Lee, K.Y., Kim, Y.H., Kim, S.W., Peipp, M., Fey, G.H., Manjunath, N., Shultz, L.D., Lee, S.K., Shankar, P., 2008. T cell-specific siRNA delivery suppresses HIV-1 infection in humanized mice. Cell 134, 577–586.
Lambeth, L.S., Zhao, Y.G., Smith, L.P., Kgosana, L., Nair, V., 2009. Targeting Marek's disease virus by RNA interference delivered from a herpesvirus vaccine. Vaccine 27, 298–306.
Mallanna, S.K., Rasool, T.J., Sahay, B., Aleyas, A.G., Ram, H., Mondal, B., Nautiyal, B., Premraj, A., Sreekumar, E., Yadav, M.P., 2006. Inhibition of anatid herpes virus-1 replication by small interfering RNAs in cell culture system. Virus Res. 115, 192–197.
McCaffrey, A.P., Nakai, H., Pandey, K., Huang, Z., Salaza, r, F.H., Xu, H., Wieland, S.F., Marion, P.L., Kay, M.A., 2003. Inhibition of hepatitis B virus in mice by RNA interference. Nat. Biotechnol. 21, 639–644.
Millar, N.S., Emmerson, P.T., 1998. Molecular cloning and nucleotide sequencing of Newcastle disease virus. In: Alexander, D.J. (Ed.), Newcastle Disease. Kluwer Academic, Boston, pp. 79–97.
Mungall, B.A., Schopman, N.C., Lambeth, L.S., Doran, T.J., 2008. Inhibition of Henipavirus infection by RNA interference. Antiviral Res. 80, 324–331.
Panshin, A., Shihmanter, E., Weisman, Y., Oervel, L.C., Liokind, M., 1997. Antigenic epitope characterization of matrix protein of Newcastle disease virus using monoclonal antibody approach: contrasting variability amongst NDV strains. Comp. Immun. Microbiol. Infect. Dis. 20, 177–189.
Pantua, H.D., McGinnes, L.W., Peeples, M.E., Morrison, T.G., 2006. Requirements for the assembly and release of Newcastle disease virus-like particles. J. Virol. 80, 11062–11073.
Peeples, M.E., Wang, C., Gupta, K.C., Coleman, N., 1992. Nuclear entry and nucleolar localization of the Newcastle disease virus (NDV) matrix protein occur early in infection and do not require other NDV proteins. J. Virol. 66, 3263–3269.
Peng, J.L., Zhao, Y.G., Mai, J.H., Pang, W.K., Wei, X.H., Zhang, P.Z., Yu, Y.H., 2005. Inhibition of hepatitis B virus replication by various RNAi constructs and their pharmacodynamic properties. J. Gen. Virol. 86, 3227–3234.
Rima, B., 1989. Comparison of amino acid sequences of the major structural proteins of the paramyxo- and morbilliviruses. In: Kolakofsky, D., Mahy, B.M.J. (Eds.), Genetics and Pathogenicity of Negative Strand Viruses, pp. 254–263.
Rott, R., Klenk, H.D., 1977. Structure and assembly of viral envelopes. In: Poste, G., Nicolson, G.L. (Eds.), Virus Injection and the Cell SurJace. Elsevier, North-Holland Biomedical Press, Amsterdam, pp. 47–81.
Seal, B.R., King, D.J., Bennet, J.D., 1995. Characterisation of Newcastle disease virus isolates by reverse transcription PCR coupled to direct nucleotide sequencing

9. Appendix

and development of sequence database for pathotype prediction and molecular epidemiological analysis. J. Clin. Microbiol. 33, 2624–2630.
Sun, M.X., Liu, X.Q., Cao, S.B., He, Q.G., Zhou, Q., Ye, J., Li, Y.M., Chen, H.C., 2007. Inhibition of porcine circovirus type 1 and type 2 production in PK-15 cells by small interfering RNAs targeting the Rep gene. Vet Microbiol. 123, 203–209.
Wu, C.J., Huang, H.W., Liu, C.Y., Hong, C.F., Chan, Y.L., 2005. Inhibition of SARS-CoV replication by siRNA. Antiviral Res. 65, 45–48.
Wu, Y., Lü, L., Yang, L.S., Weng, S.P., Chan, S.M., He, J.G., 2007. Inhibition of white spot syndrome virus in Litopenaeus vannamei shrimp by sequence-specific siRNA. Aquaculture 271, 21–30.
Xu, M., Chang, S., Ding, Z., Gao, H.W., Wan, J.Y., Liu, W.S., Liu, L.N., Gao, Y., Xu, J., 2008. Genomic analysis of Newcastle disease virus strain NA-1 isolated from geese in China. Arch. Virol. 153, 1281–1289.
Yusoff, K., Tan, W.S., 2001. Newcastle disease virus: macromolecules and opportunities. Avian Pathol. 30, 439–455.

10. Acknowledgements

Completing a PhD is really one of biggest events in my life so far, and I am much obliged to the many people for their endless and countless aids and supports during the last three and half year, without their helps I may not be able to finish my journey.

First of all, I would like to thank **Prof. Dr. Martin Hrabě de Angelis** and **Prof. Dr. med. Dirk Busch** for supervising me in my PhD thesis committee and supporting me with their knowledge and advice as well as **Prof. Dr. Dieter Langosch** for chairing the thesis committee. I am grateful to **Dr. Tobias Stöger** for providing me the opportunity to perform my doctoral thesis work at the institute of lung biology and disease (iLBD) of Helmholtz Zentrum München, and his continuous encouragement and valuable suggestions during this project.

I also greatly appreciate the aids and helps from my colleagues in the group of Dynamics of Pulmonary Inflammation of institute of lung biology and disease (iLBD): **Dr. Anke-Gabriele Lenz, Dr. Furong Tian, Dr. Ingrid Beck-Speier**, **Dr. Alexander A Götz, Dr. Andrea Beyerle, Shanze Chen, Nunja Habel, Gabriele Schumann, Birgit Frankenberger, Kathrin Kappes, Simon Orth, David Kutschke** and people from institute of lung biology and disease and Comprehensive Pneumology Center: **Prof. Dr. Holger Schulz, Dr. Wolfgang G Kreyling, Dr. Shinji Takenaka, Dr. Ali Önder Yildirim, Dr. Melanie Königshoff, Dr. Matthias Wjst, Dr. Otmar Schmid, Dr. Koustav Ganguly**, **Dr. Oana-Veronica Amarie, Bärbel Ritter, Bernd Lentner, Gunter Eder, Jie Jia, Qiongman Wang, Katrin Kohse.** I am thankful to all the colleagues, who have working in the Institute of lung biology and disease and Comprehensive Pneumology Center, especially to the director, **Prof. Dr. Oliver Eickelberg**, for a dynamic, international, scientific and friendly atmosphere.

I would like to thank **Dr. Daniel Krappmann**, **Dr. Michelle Vincendeau** and **Richard Griesbach** from Institute of Molecular Toxicology and Pharmacology (TOXI) of Helmholtz Zentrum München for their supporting in EMSA. I would like to thank **Dr. Falk Weih** from Leibniz institute for Age research- Fritz Lipmann institute, Jena for the gift of $p50^{-/-}$ mice.

I am particularly grateful to my wife **Xinxin Liu** for her personal support, her motivating words and patience during my PhD period.

10. Acknowledgements

My apologies go to the numerous colleagues, family members and friends who I cannot continue listing who have supported me in one way or another over the past years.

Finally, I would like to acknowledge my family, especially my parents, my elder brother and my wife's parents, for their tremendous supports, for continuously building up my mental health, for financial sponsorships throughout the whole PHD study in Germany.

11. Lebenslauf

Persönliche Daten:

Name	Renfu Yin
Geschlecht	Männlich
Staatsangehörigkeit	Chinesisch
Geburtsdatum/-ort	29.10.1982, Hunan, China
E-mail Adresse	renfu.yin@gmail.com

SCHULBILDUNG:

Nov 2008 - heute **Doktorand**

Fach:	Biologie
Betreuer:	Prof. Martin Hrabé de Angelis und Dr. Tobias Stoeger
Titel der Arbeit:	Role of NFkB subunit p50 in particle induced, aseptic lung inflammation
Adresse:	Institut für Lungenbiologie, HelmholtzZentrum München, Ingolstaedter Landstraße 1, D-85764 München, Germany

Sep 2005 – Oct 2008 **Master in vorbeugender Veterinärmedizin**

Fach:	Mikrobiologie in der Veterinärmedizin und vorbeugende Veterinärmedizin
Betreuer:	Prof. Zhuang Ding
Forschungsthema:	Tier Infektionen, virale Erkrankungen und Zoonosen
Universität:	Jilin University

Sep 2001 - Jul 2005 **Universtätsstudent**

Fach:	Veterinärmedizin
Abschluss:	Bachelor in Agrikultur, Facharzt für Veterinärmedizin
Universität:	Hunan Agricultural University

Vorträge:

1. Acute lung inflammation in response to carbon nanoparticle exposure is augmented in the absence of NFkB
   Herbsttreffen der Sektion Zellbiologie in der DGP,12th-13th November 2010, in Berlin Germany
2. Inhibition of Newcastle disease virus replication by RNA interference targeting the M and P gene in chicken embryo fibroblasts
   Branch of Animal Infectious Diseases of China Animal Science and Veterinary Medicine Society, 2008, in Jingganshan of Jiangxi

Poster:

1. **Poster 1:** NFkB1 Triggers Carbon Nanoparticle Induced Lung Inflammation: - a Common Misconception?

   Poster 2: Difficulties deducing the inflammatory in vivo toxicity of combustion derived nanoparticles from in vitro data

   12th International Congress on Combustion By-Products and their Health Effects: Combustion Engineering and Global Health in the 21st Century - Issues and Challenges. June 5 – 8, 2011. Zhejing University, Hanzhou of China
2. Acute lung inflammation in response to carbon nanoparticle exposure is augmented in the absence of NFkB

   Lung Science Conference of European Respiratory society (ERS). 30 March - 1 April 2010. Estoril of Portugal
3. Unknown roles of NFkB p50 during carbon nanoparticle induce acute lung inflammation

   6th International PhD Student Symposium"Horizons in Molecular Biology". 9-12 September, 2009, University of Gottingen, Gottingen of Germany

Preise (seit 2009):

1. Travel award was provided by Louisiana State University and National Institute of Environmental Health Sciences of USA , June of 2011
2. Travel award was provided by European Respiratory society (ERS), March of 2010
3. Scholarship was provided by China Scholar Council for 48 months (from Nov. 2008 to Nov. 2012)

Publikationen (seit 2009):

1. **R. Yin**, X. Liu, C. Liu, Z. Ding, X. Zhang, F. Tian, W. Liu, J. Yu, L. Li, M.H. de Angelis, T. Stoeger, Systematic selection of housekeeping genes for gene expression normalization in chicken embryo fibroblasts infected with Newcastle disease virus, Biochem Biophys Res Commun 413(2011) 537-540.
2. **R. Yin**, Z. Ding, X. Liu, L. Mu, Y. Cong, T. Stoeger, Inhibition of Newcastle disease virus replication by RNA interference targeting the matrix protein gene in chicken embryo fibroblasts, J Virol Methods 167 (2010) 107-111.
3. **R. Yin**, F. Tian, B. Frankenberger, M.H. de Angelis, T. Stoeger, Selection and evaluation of stable housekeeping genes for gene expression normalization in carbon nanoparticle-induced acute pulmonary inflammation in mice, Biochem Biophys Res Commun 399 (2010) 531-536.
4. L. Mu, Z. Ding, Y. Cong, **R. Yin**, M. Liu, C. Wang, S. Li, M. Qiu, Inhibition of Newcastle disease

virus (NDV) replication by RNA interference targeting phosphoprotein (P) gene in CEF, Chinese Journal of Veterinary Science 07(2009) (auf Chinesisch)

5. M. Liu, L. Mu, K. Meng, Z. Ding, Y. Cong, **R. Yin**, Z. Li, Inhibition of goose paramyxovirus (GPMV) replication by RNA interference targeted to matrix protein NP and L gene in CEF, Chinese Journal of Veterinary Science 06(2009) (auf Chinesisch)
6. C. Wang, Y. Cong, S. Li, Z. Ding, **R. Yin**, H. Wu, M. Liu, M. Qiu, L. Mu, Construction and identification of the full-lenth cDNA clone of GPMV NA-1 strain, Chinese Journal of Veterinary Science 04(2009) (auf Chinesisch)
7. S. Li, Y. Cong, C. Wang, Z. Ding, **R. Yin**, Y. Zhang, M. Liu, Construction of the mini-genome of NA-1 GPMV for rescue, Chinese Journal of Veterinary Science 04(2009) (auf Chinesisch)
8. M. Qiu, Y. Cong, Z. Ding, K. Meng, Z. Li, **R. Yin**, S. Li, C. Wang, M. Liu, H. Wu, L. Mu, Nested PCR to detect nucleic acid of swine hepatitis E virus and sequence analysis, Chinese Journal of Veterinary Science 03(2009) (auf Chinesisch)
9. J. Chang, Z. Wang, **R. Yin**, Anti-viral effect of anti-microbial peptides, Chinese Journal of Traditional Veterinary Science 01 (2009) (auf Chinesisch)
10. H. Wu, K. Meng, Z. Ding, **R. Yin**, Y. Bi, Y. Cong, Z. Li, C. Wang, M. Liu, M. Qiu, S. Li, Genetic variation analysis of porcine paramyxovirus strain JL-1, Chinese Journal of Veterinary Science 02(2009) (auf Chinesisch)